

**DETERMINATION OF FLOW UNITS FOR CARBONATE RESERVOIRS BY  
PETROPHYSICAL - BASED METHODS**

**A THESIS SUBMITTED TO  
THE GRADUATE SCHOOL OF NATURAL AND APPLIED SCIENCES  
OF  
MIDDLE EAST TECHNICAL UNIVERSITY**

**BY**

**CEYLAN YILDIRIM AKBAŞ**

**IN PARTIAL FULFILLMENT OF THE REQUIREMENTS  
FOR  
THE DEGREE OF MASTER OF SCIENCE  
IN  
PETROLEUM AND NATURAL GAS ENGINEERING**

**AUGUST 2005**

Approval of the Graduate School of Natural and Applied Sciences

---

Prof.Dr. Canan Özgen  
Director

I certify that this thesis satisfies all the requirements as a thesis for the degree of Master of Science

---

Prof. Dr. Birol Demiral  
Head of Department

This is to certify that we have read this thesis and that in our opinion it is fully adequate, in scope and quality, as a thesis for the degree of Master of Science

---

Prof. Dr. Suat Bağcı  
Supervisor

**Examining Committee Members**

Prof. Dr. Birol Demiral	(METU,PETE)	_____
Prof. Dr. Suat Bağcı	(METU, PETE)	_____
Prof. Dr. Nurkan Karahanoğlu	(METU,GEOE)	_____
Prof.Dr. Fevzi Gümrah	(METU, PETE)	_____
Yıldız Karakeçe (Msc.)	(TPAO)	_____

**I hereby declare that all information in this document has been obtained and presented in accordance with academic rules and ethical conduct. I also declare that, as required by these rules and conduct, I have fully cited and referenced all material and results that are not original to this work.**

Name, Last name : Ceylan YILDIRIM AKBAŞ

Signature :

## **ABSTRACT**

### **DETERMINATION OF FLOW UNITS FOR CARBONATE RESERVOIRS BY PETROPHYSICAL - BASED METHOD**

**Yıldırım Akbaş, Ceylan**

**M.Sc., Department of Petroleum and Natural Gas Engineering**

**Supervisor : Prof. Dr. A. Suat Bağcı**

**August 2005, 146 pages**

Characterization of carbonate reservoirs by flow units is a practical way of reservoir zonation. This study represents a petrophysical-based method that uses well loggings and core plug data to delineate flow units within the most productive carbonate reservoir of Derdere Formation in Y field, Southeast Turkey.

Derdere Formation is composed of limestones and dolomites. Logs from the 5 wells are the starting point for the reservoir characterization. The general geologic framework obtained from the logs point out for discriminations within the formation. 58 representative core plug data from 4 different wells are utilized to better understand the petrophysical framework of the formation. The plots correlating petrophysical parameters and the frequency histograms suggest the presence of distinctive reservoir trends. These discriminations are also represented in Winland porosity-permeability crossplots resulted in clusters for different pore-sizes that are responsible for different flow characteristics. Although the correlation between core plug porosity and air permeability yields a good correlation coefficient, the formation has to be studied within units due to differences in pore-sizes and reservoir process speed.

Linear regression and multiple regression analyses are used for the study of each unit. The results are performed using STATGRAPH Version Plus 5.1 statistical software. The permeability models are constructed and their reliabilities are compared by the regression coefficients for predictions in un-cored sections.

As a result of this study, 4 different units are determined in the Derdere Formation by using well logging data, and core plug analyses with the help of geostatistical methods. The predicted permeabilities for each unit show good correlations with the calculated ones from core plugs. Highly reliable future estimations can be based on the derived methods.

**Keywords:** Carbonate reservoir characterization, flow unit, Derdere Formation, petrophysics, geostatistics, permeability prediction.

## ÖZ

# KARBONAT REZERVUARLARINDA PETROFİZİKSEL YÖNTEMLERİ KULLANARAK AKIŞ BİRİMLERİNİN BELİRLENMESİ

Yıldırım Akbaş, Ceylan

Yüksek Lisans, Petrol ve Doğal Gaz Mühendisliği Bölümü

Tez Yöneticisi : Prof. Dr. A. Suat Bağcı

Ağustos 2005, 146 sayfa

Karbonat rezervuarlarının karakterizasyonu, rezervuar zonlarının belirlenmesinde pratik bir yöntemdir. Bu çalışma, Güneydoğu Anadolu'daki en üretken karbonat rezervuarlarından biri olan Derdere Formasyonu'nun, Y sahası içinde akış birimlerinin belirlenmesi amacıyla, kuyu logları ve karot tapan verilerinin kullanılmasına yönelik petrofiziksel yöntemlere dayanmaktadır.

Derdere Formasyonu, kireçtaşı ve dolomitlerden oluşmaktadır. 5 kuyudan alınan kuyu logları, rezervuar karakterizasyonu için başlangıç noktasıdır. Loglardan elde edilen genel jeolojik yapı, formasyon içinde farklılıklara işaret etmektedir. 4 ayrı kuyudan alınan 58 adet karot tapan verisi, formasyonun petrofiziksel yapısını daha iyi anlayabilmek için kullanılmıştır. Petrofiziksel parametreleri ilişkilendiren grafikler ve sıklık histogramları farklı rezervuar eğilimlerinin varlığını göstermektedir. Bu farklılıklar Winland gözeneklilik-geçirgenlik kümeleme grafiklerinde, farklı akış karakteristiklerinden sorumlu olan, farklı gözenek boyu dağılımlarının gruplanmasıyla da temsil edilmiştir. Karot tapan gözenekliliği ve hava geçirgenliği yüksek regresyon katsayısı vermiş olmasına rağmen, gözenek boylarındaki ve rezervuar işlem hızlarındaki ayırmalar dolayısıyla, Derdere Formasyonu farklı birimler bakımından incelenmelidir.

Her bir birimin incelenmesi için doğrusal regresyon ve çoklu regresyon analizleri kullanılmıştır. Sonuçlar, STATGRAPH Version Plus 5.1 istatistiksel paket programı kullanılarak ifade edilmiştir.

Geçirgenlik modelleri yapılmış, ve karot alınmamış kısımlarda geçerli tahminlerin yapılması için regresyon katsayıları karşılaştırılmıştır.

Bu çalışma sonucunda, Derdere Formasyonu içinde kuyu logları verisi ve karot tapa analizleri kullanılarak, jeostatiksel yöntemler yardımıyla 4 ayrı birim belirlenmiştir. Her bir birim için tahmin edilen geçirgenlik değerleri, hesaplanmış olan değerlerle geçerli korelasyonlar göstermiştir. Elde edilen metotlarla yüksek güvenilirliğe sahip gelecek tahminleri yapılabilir.

**Anahtar Kelimeler:** Karbonat rezervuar karakterizasyonu, akış birimi, Derdere Formasyonu, petrofizik, jeostatistik, geçirgenlik tahmini.

**To My Family**

## ACKNOWLEDGMENTS

I would like to express my sincere gratitude to my supervisor Prof. Dr. A. Suat Bağcı for his continuous support, guidance and encouragements throughout the thesis study.

My appreciation also goes to Mrs. Yıldız Karakeçe. I have learned a great deal through discussions with her and I greatly thank the valuable contributions she has provided to conduct this study.

I also thank Mr. Alper Karadavut for his suggestions.

I am also very grateful to all of my colleagues for their helps.

Special thanks go to Ms. Berna Haşçakır for her intelligent and outstanding contributions.

Finally, I owe a great deal of thanks to İhsan A. Akbaş for his endless support and patience during this challenging work.

# TABLE OF CONTENTS

PLAGIARISM.....	iii
ABSTRACT .....	iv
ÖZ .....	vi
DEDICATION .....	viii
ACKNOWLEDGMENTS .....	ix
TABLE OF CONTENTS.....	x
LIST OF FIGURES .....	xii
LIST OF TABLES .....	xv
NOMENCLATURE.....	xviii
CHAPTERS	
1. INTRODUCTION .....	1
2. LITERATURE SURVEY.....	3
2.1. Southeast Turkey .....	3
2.2. Carbonate Rocks and Reservoirs .....	4
2.3. Permeability Predictions .....	5
2.4. Hydraulic Flow Unit Concept .....	7
3. GEOLOGICAL BACKGROUND.....	10
3.1. Regional Geologic Setting .....	10
3.2. Stratigraphy of the Study Area.....	10
3.3. Field Background.....	13
3.4. Carbonate Reservoirs.....	14
4. STATEMENT OF THE PROBLEM.....	16
5. METHODS AND APPLICATIONS .....	17
5.1. Available Data .....	17
5.2. Well Logging Data Analysis .....	19
5.2.1. Gamma Ray Analysis.....	20
5.2.2. Sonic Log Analysis .....	22
5.2.3. Caliper Log Analysis.....	23
5.2.4. Density Log Analysis.....	26
5.2.5. Neutron Log Analysis .....	31
5.2.6. Effective Porosity and Shale Content from Density-Neutron Crossplot .....	37
5.2.7. Resistivity Log Analysis .....	42
5.3. Core Data Analysis.....	49

5.3.1. Core Plug Porosity Analysis .....	50
5.3.2. Core Plug Permeability Analysis .....	52
5.3.3. Core Plug Grain Density Analysis .....	55
5.4. Geostatistical Methods .....	57
5.4.1. Linear Regression .....	57
5.4.2. Multiple Regression Analysis (MRA) .....	58
6. RESULTS AND DISCUSSION .....	60
6.1. Well Log Interpretation .....	60
6.1.1. Lithology and Porosity Interpretation .....	60
6.1.2. Resistivity and Saturation Interpretations .....	63
6.2. Core Plug Data Interpretation .....	74
6.2.1. Porosity-Permeability Relations.....	74
6.2.2. Rock-Fabric Classification .....	75
6.2.3. Reservoir Quality.....	78
6.3. Flow Unit Determination & Permeability Prediction.....	80
6.3.1 Limestone L - 1 Unit Analysis .....	87
6.3.2. Limestone L - 2 Unit Analysis .....	90
6.3.3. Dolomite D – 1 Unit .....	93
6.3.4. Dolomite D - 2 Unit.....	99
7. CONCLUSIONS .....	105
REFERENCES .....	107
APPENDICES	
A. CARBONATE ROCKS CLASSIFICATION SCHEMES.....	115
A.1. CLASSIFICATION BASED ON ROCK TEXTURE .....	115
A.2. CLASSIFICATION BASED ON POROSITY AND PORE SYSTEMS.....	116
B. WELL LOGGING DATA .....	118
B.1. WELL A.....	118
B.2. WELL B.....	120
B.3. WELL C.....	121
B.4. WELL D.....	122
B.5. WELL X.....	124
C. CORE PLUG DATA .....	125
D. WELL LOG DERIVED PARAMETERS .....	127
D.1. Lithology Fractions.....	127
D.2. Well-Log Derived Porosities.....	132
D.3. Depth vs. Porosity Plots.....	137
D.4. Saturations.....	140
E. R <sub>35</sub> AND K/Ø.....	145

## LIST OF FIGURES

Figure 3. 1 Petroleum districts of Southeast Turkey and location map showing the study area.....	11
Figure 3. 2 The generalized stratigraphic columnar section observed in the study area..	12
Figure 5. 1 Well Locations .....	18
Figure 5. 2 Gamma Ray Correlation.....	24
Figure 5. 3 Sonic Log Correlation .....	25
Figure 5. 4 Frequency histogram plots for sonic travel times.....	27
Figure 5. 5 Frequency histogram of density recordings - Well A.....	29
Figure 5. 6 Frequency histogram of density recordings - Well B.....	29
Figure 5. 7 Frequency histogram of density recordings - Well C.....	30
Figure 5. 8 Frequency histogram of density recordings - Well D.....	30
Figure 5. 9 Neutron Porosity Equivalence Chart.....	32
Figure 5. 10 Crossplot for Porosity and Lithology Determination from density log and compensated neutron log .....	34
Figure 5. 11 Frequency histogram of neutron porosity recordings - Well A.....	35
Figure 5. 12 Frequency histogram of neutron porosity recordings - Well B.....	35
Figure 5. 13 Frequency histogram of neutron porosity recordings - Well C .....	36
Figure 5. 14 Frequency histogram of neutron porosity recordings - Well D .....	36
Figure 5. 15 Determination of shale point and porosity in shaly formations .....	38
Figure 5. 16 Lithology fractions - Well A .....	40
Figure 5. 17 Lithology fractions - Well B .....	40
Figure 5. 18 Lithology fractions - Well C.....	41
Figure 5. 19 Lithology fractions - Well D.....	41
Figure 5. 21 Resistivity of NaCl solutions .....	45
Figure 5. 22 Resistivity Log Correlation .....	47
Figure 5. 23 Frequency histogram of Rt recordings - Well A .....	48
Figure 5. 24 Frequency histogram of Rt recordings - Well B .....	48
Figure 5. 25 Frequency histogram of Rt recordings - Well C .....	48
Figure 5. 26 Frequency histogram of Rt recordings - Well D .....	49
Figure 5. 27 Frequency histogram of core plug porosity.....	51
Figure 5. 28 Relative cumulative curve of core plug porosity.....	51
Figure 5. 29 Frequency histogram of coreplug air permeability .....	53
Figure 5. 30 Frequency histogram of coreplug liquid permeability.....	53

Figure 5. 31 Relative cumulative curve of coreplug air permeability .....	54
Figure 5. 32 Relative cumulative curve of coreplug liquid permeability .....	54
Figure 5. 33 Relationship between measured air and liquid permeabilities .....	55
Figure 5. 34 Frequency histogram of grain density .....	56
Figure 5. 35 Relative cumulative curve of grain density .....	57
Figure 6. 1 Density & Neutron Logs Correlations .....	64
Figure 6. 2 Density-Neutron Crossplot - Well A .....	65
Figure 6. 3 Density-Neutron Crossplot - Well B .....	66
Figure 6. 4 Density-Neutron Crossplot - Well C .....	67
Figure 6. 5 Density-Neutron Crossplot - Well D .....	68
Figure 6. 6 Density and Neutron Porosity Recordings Plot .....	69
Figure 6. 7 $R_t$ vs. $R_{xo}$ plot .....	69
Figure 6. 8 $R_t$ vs. Density-Neutron porosity .....	70
Figure 6. 9 Depth vs. $S_w$ – Well A .....	70
Figure 6. 10 Depth vs. $S_w$ – Well B .....	71
Figure 6. 11 Depth vs. $S_w$ – Well C .....	71
Figure 6. 12 Depth vs. $S_w$ – Well D .....	72
Figure 6. 13 $S_w$ vs. Density-Neutron Porosity .....	72
Figure 6. 14 $R_o$ - $R_t$ curves for 100 % $S_w$ .....	73
Figure 6. 15 Core plug porosity vs. logarithm of air permeability for all data set .....	75
Figure 6. 16 Comparison between Archie & Lucia classifications .....	76
Figure 6. 17 Porosity-permeability cross plot of Lucia classification .....	78
Figure 6. 18 Winland $R_{35}$ Plot for Derdere Formation .....	81
Figure 6. 19 Porosity-Permeability plot of $k/\phi$ for Derdere Formation .....	81
Figure 6. 20 Distinctive units in Derdere Formation .....	83
Figure 6. 21 Stratigraphic flow profile - Well X .....	85
Figure 6. 22 Stratigraphic flow profile - Well B .....	86
Figure 6. 23 Linear regression between whole limestone data set .....	87
Figure 6. 24 Linear regression for core plug porosity and logarithm of air permeability for L-1 .....	87
Figure 6. 25 Relation between calculated permeability & measured permeability for L-1 .....	89
Figure 6. 26 Linear regression for core plug porosity and logarithm of air permeability for L-2 .....	91
Figure 6. 27 Relation of core plug porosity and well log derived porosities for L-2 .....	91
Figure 6. 28 Relation between calculated values of permeability and core plug permeability for L-2 .....	93
Figure 6. 29 Linear regression for core plug porosity and logarithm of air permeability for dolomites .....	94

Figure 6. 30 Relation between log derived porosities and core plug porosity for D-1.....	95
Figure 6. 31 Linear regression for core plug porosity and logarithm of air permeability for D-1 .....	96
Figure 6. 32 Relation between calculated permeability and measured permeability .....	98
Figure 6. 33 Relation between core plug porosity and well log derived porosities .....	100
Figure 6. 34 Linear regression for core plug porosity and logarithm of air permeability for D-2 .....	101
Figure 6. 35 Stratigraphic Flow Profile – Well C .....	104
Figure A. 1 Dunham Classification according to depositional texture .....	115
Figure A. 2 Geological classification of pores and pore systems in carbonate rocks .....	116
Figure A. 3 Classification of carbonates by interparticle pore space (Lucia, 1995) .....	117
Figure A. 4 Classification of carbonates by vuggy pore space (Lucia, 1995) .....	117
Figure D. 1 Depth vs. Well log derived porosities – Well A .....	137
Figure D. 2 Depth vs. Well log derived porosities – Well B .....	137
Figure D. 3 Depth vs. Well log derived porosities – Well C .....	138
Figure D. 4 Depth vs. Well log derived porosities – Well D .....	138
Figure D. 5 Depth vs. Well log derived sonic porosities – Well X .....	139

## LIST OF TABLES

Table 3. 1 Summarized reservoir parameters for field Y .....	13
Table 3. 2 Summarized oil properties .....	14
Table 5. 1 Available well log data for the studied wells .....	20
Table 5. 2 Matrix velocities used in Wyllie's Equation.....	22
Table 5. 3 Summary statistics of GR recordings.....	23
Table 5. 4 Summary statistics of sonic travel time recordings .....	23
Table 5. 5 Matrix values for common types of rocks.....	28
Table 5. 6 Fluid densities according to the mud type.....	28
Table 5. 7 Summary statistics of density recordings for all wells .....	30
Table 5. 8 Summary statistics of neutron porosity recordings.....	33
Table 5. 9 Calculated $R_w$ and salinity values for each well.....	44
Table 5. 10 Summary statistics of $R_t$ recordings for all wells .....	46
Table 5. 11 Summary statistics of $R_{xo}$ recordings for all wells .....	46
Table 5. 12 Summary statistics of core plug porosity (%) .....	50
Table 5. 13 Summary statistics of air permeability.....	52
Table 5. 14 Summary statistics of liquid permeability .....	53
Table 6. 1 Porosity Comparisons.....	61
Table 6. 2 Linear regression results for core plug porosity and logarithm of air permeability-whole data set.....	75
Table 6. 3 Correlation coefficients for well log parameters .....	84
Table 6. 4 Average values for each unit .....	84
Table 6. 5 Linear regression results for core plug porosity and logarithm of air permeability for L-1.....	88
Table 6. 6 Linear regression results for core plug porosity and sonic porosity for L-1.....	88
Table 6. 7 Linear regression results for permeability and sonic porosity for L-1 .....	88
Table 6. 8 Multiple regression results for logarithm of air permeability .....	89
Table 6. 9 Predicted $k_a$ values for Well C, L - 1 Unit .....	90
Table 6. 10 Linear regression results for core plug porosity and well log derived porosities for L-2.....	92
Table 6. 11 MRA coefficients between logarithm of air permeability and log derived parameters .....	92
Table 6. 12 The predicted $k_a$ values for L - 2 unit in Well C.....	93

Table 6. 13 Linear regression results for core plug porosity and logarithm of air permeability for dolomites .....	94
Table 6. 14 Linear regression results of log derived porosities and core plug porosity for D-1 unit.....	95
Table 6. 15 Linear regression results of core plug porosity and logarithm of air permeability for D-1 .....	96
Table 6. 16 Correlation coefficient between logarithm of air permeability and log derived porosity, D-1 .....	96
Table 6. 17 Correlation coefficients between logarithm of permeability and log derived parameters .....	97
Table 6. 18 The change in $R^2$ with the number of parameters in the MRA equation .....	97
Table 6. 19 The predicted ka values for of D-1 unit in Well C .....	99
Table 6. 20 Linear regression results of core plug porosity and log derived porosities for D-2 .....	100
Table 6. 21 Linear regression results for core plug porosity and logarithm of air permeability for D-2 .....	101
Table 6. 22 Correlation between logarithm of air permeability and log derived porosities for D-2 .....	101
Table 6. 23 Correlation coefficients of logarithm of permeability and log derived parameters for D-2 .....	102
Table 6. 24 The change in $R^2$ with the number of parameters in the MRA equation .....	102
Table 6. 25 The change in $R^2$ between predicted and calculated values of air permeability with decreasing number of variables .....	102
Table 6. 26 The predicted ka values for of D-2 unit in Well C .....	103
Table 6. 27 Average values for each unit – Well C .....	103
Table B. 1 Well Log Data -Well A .....	118
Table B. 2 Well Log Data - Well B .....	120
Table B. 3 Well Log Data - Well C .....	121
Table B. 4 Well Log Data - Well D .....	122
Table B. 5 Well Log Data - Well X .....	124
Table C. 1 Core plug data for the studied wells .....	125
Table D. 1 Lithology Fractions - Well A.....	127
Table D. 2 Lithology Fractions - Well B.....	128
Table D. 3 Lithology Fractions - Well C .....	129
Table D. 4 Lithology Fractions - Well D .....	130
Table D. 5 Porosities – Well A.....	132
Table D. 6 Porosities – Well B.....	133
Table D. 7 Porosities – Well C.....	134
Table D. 8 Porosities – Well D.....	135

Table D. 9 Saturations - Well A .....	140
Table D. 10 Saturations – Well B.....	141
Table D. 11 Saturations – Well C .....	142
Table D. 12 Saturations – Well D .....	143
Table E. 1 Calculated R35 and k/Ø values from core data .....	145

## NOMENCLATURE

RHOB	Bulk Density Log
CAL-X	Caliper Log
R-LLD	Deep Resistivity Log
D – 1	Dolomite D – 1 Unit
D – 2	Dolomite D – 2 Unit
S <sub>xo</sub>	Flushed Zone Saturation (%)
F	Formation Factor
k <sub>a</sub>	Air Permeability (mD)
k <sub>liquid</sub>	Liquid Permeability (mD)
L – 1	Limestone L – 1 Unit
L – 2	Limestone L – 2 Unit
R-MSFL	Micro-Spherically Focused Log (Ω.m)
PHIN	Neutron Log
R-LLS	Shallow Resistivity Log
ppm	Parts per million
k	Permeability (mD)
p.u.	Porosity unit
R <sub>35</sub>	Port size (μ)
R <sup>2</sup>	Regression Coefficient
k/∅	Reservoir process speed
R <sub>xo</sub>	Resistivity of flushed zone (Ω.m)
R <sub>o</sub>	Resistivity of a formation with 100% S <sub>w</sub> (Ω.m)
R <sub>mf</sub>	Resistivity of mud filtrate (Ω.m)
R <sub>w</sub>	Resistivity of water (Ω.m)
STB	Stock-tank Barrel
V <sub>sh</sub>	Shale Volume (%)
R <sub>t</sub>	True Resistivity (Ω.m)
S <sub>w</sub>	Water Saturation (%)

### Greek Symbols

ρ <sub>b</sub>	Bulk Density (g/cc)
ρ <sub>f</sub>	Density of fluid (g/cc)
ρ <sub>ma</sub>	Density of matrix (g/cc)
∅ <sub>D</sub>	Density Porosity (%)

$\emptyset_{D-N}$	Density-Neutron Porosity (%)
$\emptyset_{\text{effective}}$	Effective Porosity (%)
$\emptyset_N$	Neutron Porosity (%)
$\emptyset$	Porosity (%)
$\Delta t$	Sonic Travel Time ( $\mu\text{sec}/\text{ft}$ )
$\emptyset_{\text{total}}$	Total Porosity (%)

### **Abbreviations**

Dlt	Dolomite
HFU	Hydraulic Flow Unit
Lst	Limestone
MRA	Multiple Regression Analysis
MOS	Movable Oil Saturation (%)
GR	Gamma Ray Log (API Unit)
ROS	Residual Oil Saturation (%)
SP	Spontaneous Potential Log

# CHAPTER 1

## INTRODUCTION

Reservoir characterization methods are valuable as they provide a better description of the storage and flow capacities of a petroleum reservoir. Carbonate reservoirs show challenges to engineers and geologists to characterize because of their tendency to be tight and generally heterogeneous due to depositional and diagenetic processes. The extreme petrophysical heterogeneity found in carbonate reservoirs is demonstrated by the wide variability observed especially in porosity-permeability crossplots of core data analysis.

Characterization of carbonate reservoirs into hydraulic flow units is a practical way of reservoir zonation. The presence of distinct units with particular petrophysical characteristics such as porosity, permeability, water saturation, pore throat radius, storage and flow capacities help researchers to establish strong reservoir characterization. The earlier in the life of a reservoir the flow unit determination is done, the greater the understanding of the future reservoir performance.

A *hydraulic flow unit (HFU)* is defined as the representative volume of total reservoir rock within which geological properties that control fluid flow are internally consistent and predictably different from properties of other rocks (Ebanks et.al.,1984). A flow unit is a reservoir zone that is continuous laterally and vertically and has similar flow and bedding characteristics.

Knowledge of permeability is essential for developing an effective reservoir description. Formation permeability controls the strategies in involving the well completions, stimulation, and reservoir management. Permeability data can be obtained from well tests, core data analysis and well loggings. Not all the wells are cored, due to problems occurred during coring and higher costs. Generally, the estimation of permeability from well logs is considered to be the lowest cost method, where one can use values of well derived porosities, and water saturations, but the prediction of permeability in heterogeneous carbonates from well log data represents difficult and complex problems. A basic correlation between permeability and porosity can not be established, due to the effect of other well log parameters that are needed to be imbedded into the correlation. Besides all of these challenges for permeability estimation from well logs, using wireline log data provides a continuous permeability profile throughout the particular interval that can be described as a *hydraulic flow unit* (Al-Ajmi et.al, 2000).

The Southeast Turkey covers an area 120,000 km<sup>2</sup>. The oil fields in Southeast Anatolia Basin are the main oil-producing fields in Turkey. The study area is located in the XI. Petroleum District, in Southeastern Anatolia. The studied wells are located in oil field Y, which is close to city of Diyarbakır. The size of the field is about 534 acres, with nearly 16 wells producing a net oil production of 800 bbl/day. The studied field is producing from Derdere Formation belonging to Mardin Group Carbonates, which are one of the most prolific reservoirs of Southeast Anatolia Basin.

The objective of this study is to describe and characterize the Derdere Formation by using available conventional core data, and well log data from 5 different wells. The distribution of distinct reservoir parameters concerning the petrophysical properties are taken into consideration for an effective hydraulic flow unitization. The well logs are analyzed for each well, meter by meter and then the results are correlated with core data information to produce reliable estimates between parameters.

All data obtained from cores and well logs are analyzed to model a petrophysically-based reservoir zonation for the Derdere formation with geostatistical techniques which are frequency histogram diagrams, linear regression methods, and multiple regression.

## CHAPTER 2

### LITERATURE SURVEY

#### 2.1. Southeast Turkey

The studied wells are located in XI. Petroleum District in Southeastern Turkey, where many researches about the stratigraphical, sedimentological, lithological and petrographical properties of the reservoir units including the Mardin Group carbonates are present.

Rigo de Righi and Cortesini, (1964) were first to establish the stratigraphy and structural setting of Southeast Turkey. They also modified the stratigraphic succession of the Southeast Anatolia Basin with Ala and Moss (1979).

The stratigraphy, petrography, general facies properties, reservoir characteristics and the diagenetic properties of the Karaboğaz Formation and Mardin Group carbonates in Southeast Turkey were studied by Cordey and Demirmen (1971), Tuna (1974), Duran (1981), Şengüdüz and Aras (1986) , Duran and Aras (1990), Görür, et. al., (1991), Çelikdemir et al. (1991), Alaygut (1992), Karabulut ,et al. (1992) Duran and Alaygut (1992), İşbilit, et.al., (1992), and Ulu (1996).

Cordey and Demirmen (1971) were the first researchers to point out the stratigraphical position of the Mardin Group Carbonates.

Wagner et al. (1986) studied the geological evolution of the Derdere, Karababa, Karaboğaz, and Sayındere formations. These researchers investigated the depositional characteristics and the paleogeographical framework of these formations.

Görür et al. (1986) studied the facies characteristics, distributions, depositional environments and paleogeographies of the Mardin Group carbonates in X., XI. And XII. Petroleum Districts.

Duran et al. (1988-1989) studied the stratigraphy, sedimentology and reservoir properties of Mardin Group carbonates.

Çelikdemir et al. (1990) enlarged their previous studies on Mardin Group carbonates for the study of Diyarbakır region. They implemented that the Mardin Group carbonates showed micritic and sparitic structures, but the depositional environment is a low-energy environment, which is suitable for the deposition of micritic limestones. For this reason, Mardin Group limestones do not have good porosities.

## 2.2. Carbonate Rocks and Reservoirs

The carbonate rocks, especially the characterization of these reservoirs were studied by many authors and researchers.

Archie, (1952) published a world known paper titled "Classification of carbonate reservoir rocks and petrophysical consideration".

Aufricht, et al., (1957) studied the interpretation of capillary pressure data from carbonate reservoirs.

Folk, (1959) made studies on practical petrographic classification of limestones.

Murray, (1960) studied the origin of porosity in carbonate rocks.

Dunham, (1962) established a classification of carbonate rocks according to their depositional texture. His classification is still in use as "Dunham Classification".

Bertrand, et al., (1967) studied on determination of porosity and lithology from logs in carbonate reservoirs.

Choquette, et al., (1970) studied on geologic nomenclature and classification of porosity in sedimentary carbonates.

Pittman, (1971) studied the microporosity in carbonate rocks.

Wardlaw, (1976) studied pore geometry of carbonate rocks as revealed by pore casts and capillary pressure.

Asquith, (1985) published a handbook of log evaluation techniques for carbonate reservoirs.

Lucia, et al., (1987) studied the rock fabric, permeability and log relationships in vuggy carbonate sequences.

Chilingarian, (1992) studied on carbonate reservoir characterization based on a geologic-engineering analysis. He also worked on oil and gas production from carbonate rocks (1972).

Lucia, et al., (1992) studied a characterization of karsted, high energy, ramp-margin carbonate reservoirs.

Senger, (1993) et al studied the reservoir flow behavior carbonate reservoirs as determined from outcrop studies.

Kerans, et al., (1993) studied the characterization of facies and permeability patterns in carbonate reservoirs as based on outcrop analogs.

Wang, et al., (1994) studied scaling and modeling of shallow-water carbonate reservoirs.

Asquith, (1994) worked on determination of carbonate pore types from petrophysical logs.

Lucia, et al., (1995) studied the characterization of dolomitized carbonate ramp reservoirs.

Lucia ,et. al., (1996) studied diagenetically altered carbonate reservoirs.

Talabani, et. al., (2000) studied the validity of Archie Equation in carbonate rocks.

There are some studies which are done on petrophysical properties of carbonate reservoirs.

Lucia, (1983) investigated petrophysical parameters estimated from visual descriptions of carbonate rocks. He established a field classification of carbonate pore space. He stated that visual descriptions of the pore geometry can play an important role in the evaluation, where permeability estimations are needed.

Davies, et. al., (1997) worked on improved prediction of carbonate reservoir behaviour through integration of quantitative geological and petrophysical data. Their method was based on identifying intervals of unique pore geometry.

Lucia, (1995) established a rock-fabric/petrophysical classification of carbonate pore space for reservoir characterization. His study was a basic for the forthcoming petrophysical studies of carbonates.

### **2.3. Permeability Predictions**

Many empirical models were proposed regarding to correlations between permeability, porosity, and permeability estimations from porosity and other relevant data available.

Amaefule, et. al., (1993) stated that core data provide information on various depositional and diagenetic controls on pore geometry, and the variations in pore geometry attributes lead to the existence of separated zones ( hydraulic flow units ) with similar flow properties. They proposed a method; mainly based on Cozeny-Karmen equation and the concept of hydraulic mean radius, in which core porosity and core permeability values determined from routine core analyses are used. These data are used to determine reservoir quality index (RQI), and flow zone indicator (FZI). The determination of these values can be transformed to hydraulic flow units by means of combination of petrophysical, geologic and statistical analyses. These hydraulic flow units are correlated to well logging responses in order to establish regression models for permeability estimatons in the uncored wells or intervals.

Yao and Holditch, (1993) focused on a different method for estimation of permeability. They used time-lapse log data and history matching production data besides core data in order to predict permeability. The permeability values predicted were well correlated with the estimates done using logging data.

Johnson, (1994) studied methodologies for accurately estimating permeability from well logging responses, with available core and log data. The logging tools which show different responses for each hydraulic flow unit were selected. Permeability and porosity data obtained by means of laboratory tests were used to identify the number of hydraulic flow

units, and these data were linked to logging responses in order to predict permeability for the uncored, but logged wells.

Davies and Vessell, (1996) studied hydraulic flow units in a mature, heterogeneous, shallow shelf carbonate reservoir. They developed a model fundamentally based on measurement of pore geometrical parameters. Depositional and diagenetic model of the reservoir was developed. Pore geometrical attributes were integrated with well logging data in order to establish a log-derived determination of zones of rock with different capillarities and log-derived estimation of permeability.

Saner, et.al., (1997) discussed the experimental relationship between permeability, water saturation and rock resistivity. Rock resistivity and permeability are flow parameters which are controlled by the pore geometry and pore interconnectivity , so if a relation between rock resistivity and water saturation is obtained, estimation of permeability can also be achieved.

Alden, et al., (1997) studied the characterization of petrophysical flow units in carbonate reservoirs. They emphasize on the importance of these units for helping solve some of the key challenges faced in exploration and production of carbonate reservoirs.

Barman, et.al., (1998) implemented Alternating Conditional Expectations (ACE) to use non-parametric transformations and regressions. ACE is an iterative procedure and helped the research by maximizing the correlation between permeability and the well logging responses.

Al-Ajmi and Holditch, (2000) were two of the researchers which implemented Amaefule's hydraulic flow unit concept of reservoir quality index and flow zone indicator. They extended the method of hydraulic flow unitization to uncored wells by implementing the "Alternating Conditional Expectation " (ACE) algorithm, which provides a data-driven approach for identifying the functional forms for the well log variables involved in the correlation. They developed a computer program to determine the optimal number of hydraulic flow units and the analysis done by the program was based on this optimal number. This program also included a regression analysis for the prediction of permeability values.

Akatsuka, et. al., (2000) conducted a study for a reservoir characterization based on lithofacies in order to build a numerical 3-dimensional geologic model including permeability prediction and rock typing for reservoir flow simulation.

Mathisen, et. al., (2001) focused on electrofacies characterization. They first classified the well log data into electrofacies type which is based on the unique characteristics of well log measurements reflecting minerals and lithofacies within the logged interval by the help of statistical methods. Secondly, they applied non-parametric regression techniques in order to estimate permeability using logs within each electrofacies.

Antelo, et. al., (2001) used clustering electrofacies technique for more accurate prediction of permeability.

Electrofacies analysis is a system for identifying rock types with similar properties out from wireline logs and then define the reservoir rocks from the non reservoir rocks. Their technique uses the clustering K-Means algorithm which is based on log responses to identify electrofacies. This is an iterative statistical technique.

Soto, et.al., (2001) used multivariate statistical analysis for prediction of permeability and fuzzy logic model to predict the rock types in order to develop a rock type model. This model was used with combination of Gamma Ray log responses and core porosity to establish a neural network model for estimation of the flow zone indicator (FZI) value accurately in Amaefule's method. These neural network estimated FZI values were then used for permeability predictions.

Jennings, et.al., (2001) focused on geologic rock-fabric descriptions and petrophysical measurements for permeability estimations and modeling. They started their study with carbonate rock-fabric petrophysical classification which was proposed by Lucia, F.J (1995). Permeability modeling was done by using exponential and power law porosity-permeability models. Their model was then compared to Winland-Pittman model, and Kozeny-Carman model. Well logs were used to predict the permeability in uncored sections. They introduced a new term called " rock-fabric number" that shows the correlation between porosity, water saturation, capillary pressure derived from mercury injection.

Babadağlı and Al-Salmi, (2002) reviewed the existing correlations between porosity and permeability which are in literature. They discussed the importance of petrophysical properties of the rock, especially the porosity for permeability prediction.

## **2.4. Hydraulic Flow Unit Concept**

Various methods were proposed for subdividing carbonate reservoirs into layers (these layers are mentioned as lithofacies, petrofacies, electrofacies, hydraulic flow units or also called flow units).

Lucia, et. al., (1992) defined flow units in dolomitized carbonate-ramp reservoirs. They focused on averaging petrophysical properties within geological constraints and tried to describe the three-dimensional spatial distribution of petrophysical properties within a reservoir.

Abbaszadeh, et. al., (1995) also studied permeability prediction by hydraulic flow units using Amaefule's method. After calculating pore-throat related parameters of reservoir quality index and flow zone indicator from core data, they used clustering analysis techniques in order to find the optimal number of hydraulic flow units. These techniques include histogram analysis, probability plot and the Ward's analytical algorithm. These methods provide a general visual image of flow zone indicator distribution to determine the optimal number of hydraulic flow units. A combination of these graphical approaches with analytical clustering methods give a better result for delineation of hydraulic flow units.

Klimentos, (1995) combined petrophysics and seismic wave technology in order to make contributions for explorations, formation evaluations and characterizations of carbonate reservoirs within the concept of hydraulic flow unit.

Gunter, et.al., (1997) emphasized the importance of early determination of hydraulic flow units, because such kind of an earlier study will contribute a lot to understanding the future reservoir performance. Their study was based on graphical tools to determine these units. These tools are Winland porosity-permeability cross plots, Stratigraphic Flow Profile (SFP), Stratigraphic Modified Lorenz Plot (SMLP), and Modified Lorenz Plot (MLP). Their methodology is feasible and easy for any kind of reservoir.

Wang, et. al., (1998) studied on carbonate ramp reservoirs and characterized them by the help of rock-fabric and petrophysical property relationships. They stated the necessity of defining a geological framework which is fundamental for defining flow units, interpolating well log data and modeling a fluid flow.

Ratchkovski, et. al., (1999) used geostatistics and conventional methods in order to derive hydraulic flow units for improved reservoir characterization. They combined geostatistical applications of conditional simulation with conventional methods of deriving hydraulic flow units to characterize a carbonate reservoir. They constructed variogram modeling of porosity and permeability.

Lee and Datta-Gupta, (1999) studied electrofacies characterization using multivariate analysis and non-parametric regression techniques. For electrofacies classification and identification, they used principal component analysis, model-based cluster analysis, and discriminant analysis. Non-parametric regression techniques were applied to estimate permeability from well logs regarding to each electrofacies. Regression models were analysed by means of Alternating Conditional Expectations (ACE) and neural networks (NNET).

Porras, et. al., (1999) tried to establish a comparison between three different models of reservoir flow units; which are hydraulic units, petrofacies and lithofacies. These three reservoir unit zonations differ from one another, where hydraulic flow unit is defined as a continuous zone with similar average rock properties that affect flow of fluid, petrofacies are defined as intervals with similar average pore-throat radius, and lithofacies are defined as mappable stratigraphic units that are distinguishable from adjacent intervals by mineralogy, petrography and paleontology.

Rincones, et. al., (2000) studied flow unit concept in order to define an effective petrophysical fracture characterization. They used porosity and permeability relations, flow zone indicator, reservoir quality index concepts to delineate flow units. They then trained the well logs to recognize the flow units or to calculate the flow zone indicator, FZI.

Aguilera and Aguilera, (2001) introduced a different methodology for flow unit determination.

They used Pickett crossplots of effective porosity versus true resistivity in order to obtain reservoir process speed, which is equal to  $k/\phi$ . Capillary pressure data, pore-throat apertures and Winland  $R_{35}$  values analysis are also included in their study to define hydraulic flow units.

Shedid and Almehaideb, (2003) developed a new technique for improved reservoir description of carbonate reservoirs. This technique is called the Characterization Number (CN) technique and it is based upon considering fluid, rock-fluid properties, and flow mechanisms of oil reservoirs, since description and/or characterization of porous media, especially a heterogeneous one have to consider all types of fluid and rock properties. The Characterization Number combines the comprehensive set of variables which are considered the most relevant and representative of porous media and its contained fluids. These are the rock data permeability, porosity, pore diameter, the dynamic flow data, (velocity of oil and water, respectively), the fluid properties data ( viscosity of oil and water, respectively ), and the rock-fluid data ( contact angle between rock and fluid ).

## CHAPTER 3

### GEOLOGICAL BACKGROUND

#### 3.1. Regional Geologic Setting

The study area is located in the XI. Petroleum District, in Southeastern Anatolia (Figure 3.1). The Southeast Anatolia is situated at the northernmost part of the Arabian Platform which formed a part of the north facing, passive Gondwanian margin of the southern branch of Neo-Tethys ocean during Cretaceous (Şengör and Yılmaz, 1981, Harris et.al. ,1984). The main structural framework of the Southeast Turkey Basin is dominated by broad faulted uplifts and by large anticlinal features. The region is bounded by the Late Cretaceous to Tertiary Taurus orogenic belt through the north (Cater and Tunbridge, 1992). Southeast Turkey Basin includes rock units, varying from Cambrian to Miocene. These rock units are divided into two major groups: (1) autochthonous rock units which include the Palaeozoic and Mesozoic sequences representing the Arabian Plate, and (2) allochthonous rock units which include the Late Cretaceous and Early Tertiary sequences belonging to Anatolian Plate and suture zone. Five main depositional cycles can be recognized in the sedimentary sequence of the basin. (1) Late Precambrian, (2) Cambrian-Devonian, (3) Permo-Carboniferous to Upper Jurassic, (4) Lower Cretaceous to Lower Eocene, (5) Middle Eocene to Recent in age (Ala and Moss, 1979). Cretaceous carbonate section overlies unconformably a Lower Palaeozoic succession and contains significant source beds. Although the accumulations are smaller than the Middle East oil plays, about 70% of the petroleum in Southeast Turkey is produced from these carbonates (Çelikdemir, Dülger, Görür, Wagner, & Uygur, 1991). In this study, the chosen Y Field also produces mainly from the Upper Cretaceous carbonates of the Mardin Group.

#### 3.2. Stratigraphy of the Study Area

The shallow marine conditions in Southeast Turkey at the end of Aptian resulted in the deposition of a thick sequence of carbonates known as the *Mardin Group Carbonates*.

The Mardin Group carbonates which are the main reservoirs in the study area lie unconformably on Palaeozoic clastics and is overlain conformably by Şirnak Group Formations. In the study area Kayaköy Formation of Paleocene age is observed over the Mardin Group.

The generalized stratigraphic columnar section observed in the study area is given in Figure 3.2.

The Mardin Group carbonates are Turonian-Aptian in age and thickness differs from 350 to 750 meters.

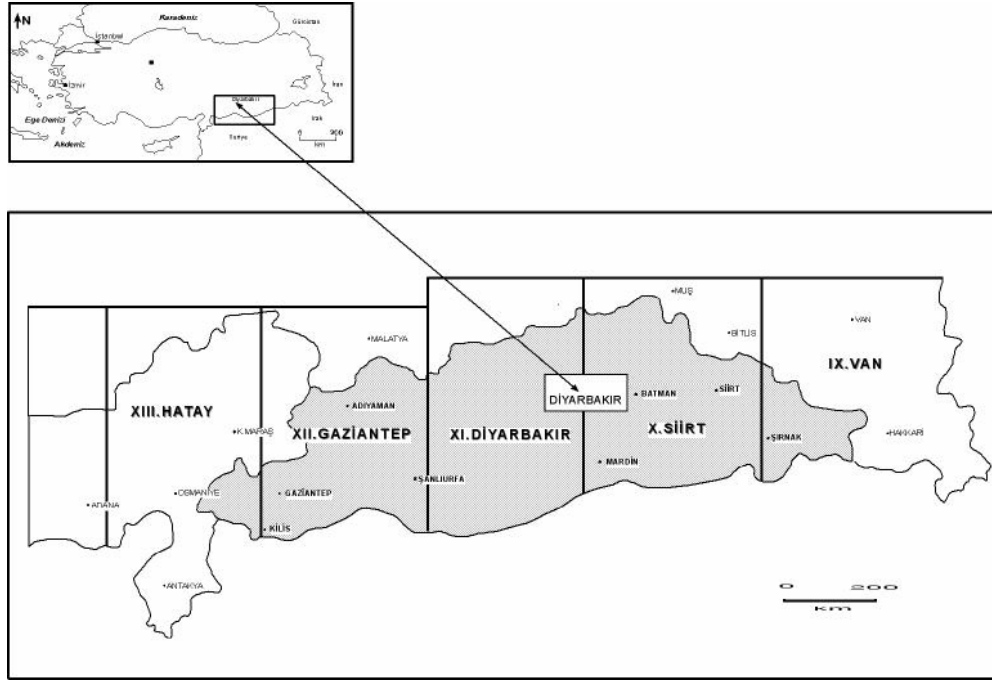


Figure 3. 1 Petroleum districts of Southeast Turkey and location map showing the study area.

During the formation of these units, the Southeast Anatolia was one of the major carbonate platform developing on the Arabian shelf (Görür, et. al., 1991).

These carbonates are characterized by successive depositional sequences that differ in age, and regional disconformities separate each other. These sequences are named *Sabunsuyu Formation* and *Derdere Formation*, from bottom to top of the group as observed in the studied petrolum district.

*Sabunsuyu Formation*; located at the bottom of this sequence, overlies the Derdere formation conformably and its dominant rock type is dolomites with minor amount of limestone at the top especially around Adıyaman and Diyarbakır oil fields (Çelikdemir et. al., 1991, Görür et. al., 1991). Dolomites may contain evaporites and sandy horizons in some sections.

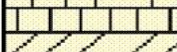
AGE	FORMATION	LITHOLOGY	DESCRIPTION
Miocene	Şelmo		Conglomerate
	Germik		Limestone
Eocene	Midyat		Massive limestone
			Dolomite
Eocene	Gercüş		Evaporites
			Conglomerate Sandstone
Paleocene	Kayaköy		Marn
			Evaporites
Paleocene	Kayaköy		Shale
			Shale
Cretaceous	Kastel		Shale
			Sandstone
			Conglomerate
	Karadut		Shale
			Marn
	Cretaceous	Kastel	
Sayındere			Conglomerate
Derdere			Marn
			Limestone
Cretaceous	Sabunsuyu		Dolomite
			Dolomite

Figure 3. 2 The generalized stratigraphic columnar section observed in the study area

At the base of Sabunsuyu formation, Areban formation is located, where basal clastics of Mardin Group can be observed.

*Derdere formation*; Cenomanian-early Turonian in age, overlies the Sabunsuyu formation conformably. The units were deposited in a partly closed basin or carbonate platform under reducing conditions (Şengündüz, et. al., 1986). Its thickness ranges from 50 to 250 meters and the formation displays an upward change in facies from deep water carbonates to shallow water carbonates of dolomites. Since the Derdere formation (especially the dolomite section of the formation) is one of the most important reservoirs in the study area, (also throughout the Southeast Anatolia Basin), and they are the scope of this study, the formation characteristics will be explained extendedly here.

In the uppermost section of the formation, bioclastic mudstones and wackestones are observed. This is the limestone dominant part of the formation. The limestones of the formation are generally massive and do not have good porosities, but they have intense fracture systems in some sections. The porosity is dominated by primary intergranular porosity (Duran and Alaygut, 1992). Through the bottom parts of the limestones, pooree porosity values are observed. This the tight limestone section which is generally in combination with minor dolomite percentages. Overlain by these limestones, dolomites are seen. The dolomites are generally light brown. The dolomites are characterized by dolosparites, and packstones with intraclasts and pellets (İşbilir, et. al.,1992). The dolomites of the formation have better porosities compared to limestones, due to secondary porosity generation as a result of dolomitization. The original texture was changed to dolomitic texture because of early diagenetic periods. The changed texture is characterized by dolosparites, which show medium - high intercrystalline porosity. The porosity values range from 5 % to 12 % ( Karabulut, et. al. 1992). In addition to dolomitization, due to early diagenesis, there exist cavernous porosity types that contributes an increase in the amount of touching-vug pores. Derdere dolomites show optimum characteristics for a good reservoir as a result of these diagenetic processes.

### 3.3. Field Background

The Y field has approximately 38 wells, 16 of there are operating. The drilled 22 wells were abandoned. Daily oil production is 800 STB. The total reserve was estimated as 53,500,000 bbls, whereas only 11,800,000 bbls is recoverable. The summarized reservoir and produced oil properties are given in Tables 3.1, and 3.2, respectively.

Table 3. 1 Summarized reservoir parameters for field Y

<b>Reservoir Pressure (psia)</b>	<b>Reservoir Temperature (°F)</b>	<b>Water/Oil Contact (m)</b>	<b>Porosity (%)</b>	<b>Permeability (md)</b>
2675	148	-1240	15	100

Table 3. 2 Summarized oil properties

API Gravity	Viscosity (cp)	Pbubble (psia)	GOR (scf/stb)	Bo (bbl/stb)	Sulfur Content (%)	Calorific Value (cal/gr)
32	4.7	30	7	1.028	0.5	10492

### 3.4. Carbonate Reservoirs

The carbonate rocks mainly constitute of *calcite* ( $\text{CaCO}_3$ ), *aragonite* ( $\text{CaCO}_3$ ) (a polymorph of calcite; same chemistry, but different structure) and *dolomite* ( $\text{CaMg}(\text{CO}_3)_2$ ). Classifications of carbonate rocks may be analogous with those of sandstones, and the schemes proposed by Folk, (1959) and Dunham, (1962) show this tendency. They are based on relative amounts of grains and mud (carbonate mud ) and the types of grains (fossils, rock fragments and minerals ). Several classification schemes for carbonates were proposed. The main differences between these classifications are the lithology, grain size, rock texture, and porosity. Some of the important carbonate classification schemes, which are also mentioned within this study are given in Appendix A.

About 40% of all oil and gas produced is found in carbonate rocks. The greatest oil fields in the world are found in Jurassic limestones in Saudi Arabia. The methods exploring carbonate petroleum reservoirs are described and illustrated by case histories in Reeckmann and Friedman (1982) and Roehl and Choquette (1985). Bathurst (1975) and Moore (1989) summarize data on carbonate rock diagenesis.

Carbonate reservoirs distinguish themselves from sandstone reservoirs in a number of important respects; (1) carbonate minerals are more soluble than silicate minerals , and solution and formation of secondary porosity is even more important than in sandstones, (2) carbonate rocks, which otherwise have low porosity and permeability often form fracture reservoirs, (3) carbonate minerals have essentially different surface properties from silicate minerals, and generally tend to be more oil wetting than sandstones.

Carbonate reservoirs can only be understood against a background of general carbonate sedimentology and diagenesis. Primary porosity in carbonate rocks consists of ; (1) interparticle porosity in grainstones, e.g. between ooids, pellets, and fossils , (2) interparticle porosity in fossils e.g. snails , (3) protected cavities under fossils ( shelter porosity ), (4) cavities formed in carbonate mud due to gas bubbles (fenestral porosity ), (5) primary cavities in reefs (growth framework porosity ). Secondary porosity can be formed through; (1) biological breakdown-cavities formed by boring organisms, e.g. living mussels, (2) chemical breakdown of minerals which are unstable in relation to the composition of pore water. The most important type of secondary porosity is dolomitisation. During dolomitisation, the amount of dolomite precipitated is often less than that the corresponding to the dissolved calcite, the result being a net increase in porosity.

About 30% of the world's carbonate reservoirs are found in dolomite. Dolomite rocks, essentially composed of the mineral dolomite and also called dolostone, are important as potential carbonate reservoirs, because dolomites may be coarse and their intercrystalline porosity as well as their permeability may be more uniform and, thus, more predictable than in limestones. Dolomitization can play a dual role; it can improve a reservoir by increasing pore size or it can destroy porosity by advanced dolomitization, creating a dense, interlocking crystal fabric.

The most important cause of reduction of both primary and secondary porosity in carbonate rocks is pressure solution. Carbonate minerals are more soluble than silicate minerals under pressure. When carbonates are dissolved, silicates and other minerals with low solubility remain behind and form a membrane consisting of largely of clay minerals, and may almost be impermeable to water and especially oil.

Fracturing plays an important role in carbonate reservoirs. It can create permeability in carbonate rocks where none existed before and form additional pathways for leaching or cementing solutions. The permeability of fractures are very high. It increases as the square of the fracture width (a fracture only 0,1 mm width has a permeability of 833 md). On the contrary, the permeability of a limestone matrix may be 0,001 darcies or less. Fractured carbonate reservoirs are characterized by high initial production rates. Fractures are essential for oil production from carbonate rocks with low matrix permeability, (e.g. Middle East Carbonate Reservoirs ).

## **CHAPTER 4**

### **STATEMENT OF THE PROBLEM**

The main aim of this study is to determine the flow units in the Derdere Formation, which is the most oil productive carbonate reservoir in Y Field. The flow unit delineation concept is mainly based on the available core plug data measurements and the conventional well logging data. The basic geologic framework of the studied wells should be constructed by well log attributes. The study is followed by the core plug analysis for the determination of the petrophysical framework. The core data will be fitted within the methods and classifications available in the literature. A profile of different units should be achieved after the combination of these studies.

To reach the goal, geostatistical methods will be utilized for discrimination of similar data and groups. Since, not all the wells in the field are cored, for the continuity of a defined unit delineation, a non-cored well will be chosen and permeability predictions will be tried to be applied within the geostatistical applications. The derived estimations will be mainly based on regression models.

## CHAPTER 5

### METHODS AND APPLICATIONS

In order to define a petrophysically based reservoir characterization and zonation, the best representative data of the studied reservoir must be obtained. The methods for obtaining such data can be listed as (1) well logging , (2) conventional core plug tests. In this chapter, the methods and their applications; which are employed to construct a hydraulic flow unit zonation within the reservoir of scope (Derdere carbonates of Y field), will be described that utilizes the available data. The technique tried to be applied in this research includes the basic geologic framework of the study area, the petrophysical properties of Derdere carbonates, analyses of core-plug data, interpretation of well logging data, combination of all these studies to obtain a hydraulic flow unit zonation with the help of permeability estimation in the logged but uncored well.

#### 5.1. Available Data

5 oil producing wells, named Well A, Well B, Well C, Well D, and Well X, from Y field are the scope of this study, in order to characterize the Derdere Formation carbonates into units.

The location map for the wells is given in Figure 5.1.

The conventional open-hole well logging data are utilized. Well A, B, C, and D have conventional Gamma Ray (GR) , Caliper (CAL-X), Sonic Transit Time ( $\Delta T$ ), Neutron Porosity (PHIN), Bulk Density (RHOB), Resistivity ( R-LLD, R-LLS and R-MSFL ), and Spontaneous Potential (SP) log data. Well X has only Gamma Ray and Sonic log data. The available well logging data within for the studied wells are shown in Table 5.1.

Well logs for the 5 wells were available in conventional forms. The logs were read by 1 meter increments. The interpretations included only the Derdere formation. The log data for each well as read by 1 meter increments is given in Appendix B.

Lithology discriminations were the first interpretations. Shale volume calculations, porosity determinations from sonic logs, neutron logs and density logs followed shale calculations. Necessary cross-plots for porosity determinations and corrections were constructed.

LESA, (Log Evaluation System Analysis - Version 4.2) trial software was used to generate these crossplots.

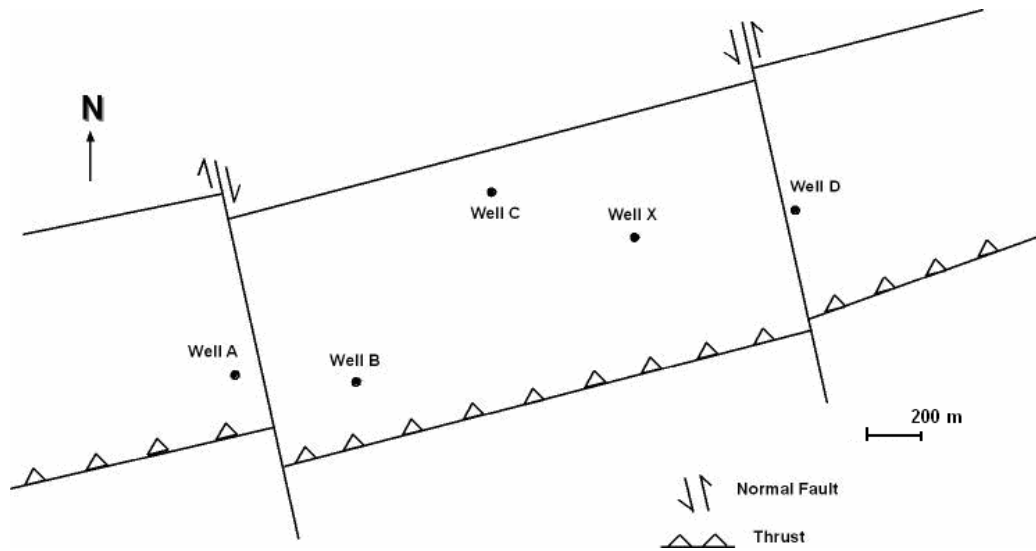


Figure 5. 1 Well Locations

Formation factors were calculated. Lithology fractions were calculated using appropriate cross-plots. The resistivity logs were utilized in order to obtain water saturations, movable and residual oil saturations.

For geostatistical study, *StatGraph Plus Version 5.1* software was utilized. Summary statistics for each parameter were done. Frequency histogram plots were constructed for lithology and porosity type discriminations. Cumulative curves of the parameters were plotted. Necessary plots, mainly depth versus obtained values were constructed in order to investigate the change of parameters with depth. Correlations were tried to be established between well-log derived parameters.

Conventional core analyses were also utilized. These analyses include coreplug porosities (in %), air and liquid permeabilities (in mD) , and grain densities ( in g/cc ) within related depth intervals. Well A has 2 core plug data, Well B has 8, Well D has 23, and Well X has 25 core plug data. Well C has no recorded and analysed core plug data. The raw coreplug data is given in Appendix C.

58 coreplug measurements are available for the studied 5 wells, only Well C has no core plug data. The conventional porosity-permeability relationships were constructed at the very early stage of the study. Corrections for the air and liquid permeability were established. Lithology descriptions were done by the help of available log data. Various statistical methods and applications were held in order to make exact correlations between porosity and permeability that will lead the study to the estimation of permeability in logged, but uncored well. For the petrophysical study of the studied wells, pore-size ( $r_{35}$ ) and reservoir process speed ( $k/\phi$ ) values were calculated by using the available core plug data.

Lack of capillary pressure data forced this study to use calculated values of the conventional core plug data in order to obtain these petrophysical parameters. All the necessary calculations, tables, graphs and plots were constructed.

Reservoir units were defined which have continuous and similar porosity and permeability data within the general similar petrophysical characteristics as obtained by coreplug data analysis. The geological framework, the established petrophysical parameters, the correlations between porosity and permeability were combined with the interpretation of well logging data in order to delineate flow units within the studied wells.

## **5.2. Well Logging Data Analysis**

Surface geological methods help to identify interesting surface structures which could possibly bear fluids, but they are unable to predict whether these fluids are hydrocarbons. So far, there is no other solution than to drill a well to exactly determine the presence of hydrocarbons below the surface. But drilling is a time and money consuming process, which possibly end with a result of none-hydrocarbon bearing formations in the drilled sections. One can use the formation evaluation tests in order to analyse the interested subsurface sections, rather than drill a well.

Formation evaluation is the process of using borehole measurements to evaluate the characteristics of the subsurface reservoirs, such as determining the physical properties of reservoirs and their contained fluids.

Four categories are available for formation evaluation: (1) mud logging, (2) coring and core analysis, (3) drillstem testing, (4) well logging. The easiest way of getting reservoir data at the very beginning of the study can be considered as well logging, which mainly contributes to formation evaluation. The main objectives of the well logging is to identify the reservoirs, estimate the hydrocarbons in place, and estimate the recoverable hydrocarbons, but the data provided from well logs also help so many studies besides their main objectives.

In Y field, the conventional open-hole well logs are available as mentioned before (Figure 5.1). These logs are used to examine the lithological-mineralogical composition and the petrophysical properties such as porosity and water saturations. Besides the use of raw log data, some crossplots are utilized based on log parameters are used to understand the nature of porosity. Obtained well log parameters are also run as input for the geostatistical methods, in order to correlate with core data for permeability estimations. The evaluation methods on well logs and the applications of these methods to the studied wells will be described in this part.

Table 5. 1 Available well log data for the studied wells

R-LLS	R-LLD	R-MSFL	SP	PHI	RHOB	Sonic	Caliper	Gamma Ray	Log Type Well Name
X	X	X	X	X	X	X	X	X	Well A
X	X	X	X	X	X	X	X	X	Well B
X	X	X	X	X	X	X	X	X	Well C
X	X	X	X	X	X	X	X	X	Well D
						X	X	X	Well X

### 5.2.1. Gamma Ray Analysis

The evaluation of shaly formations (formations containing clay minerals) can be done by mainly using Gamma Ray (GR) Log. Spontaneous Potential (SP) Log can also be utilized. Two radioactive elements, potassium (K) and Thorium (Th) tend to concentrate in shales. Shale-free sandstones and carbonates (generally named as *clean zones*) contain very little K and Th, because the chemical environment that prevails during their deposition is not favorable for the accumulation of radioactive minerals. In GR logs, the significant abundance of unstable elements, exhibit a certain level of natural radioactivity. The GR log is a measurement of the total gamma ray intensity in the wellbore, that helps to distinguish potential hydrocarbon-bearing formations and shales.

Shale content can be described as shale volume ( $V_{sh}$ ). Qualitatively,  $V_{sh}$  indicates whether the formation is clean or shaly. Quantitatively,  $V_{sh}$  is used to estimate the shale effect on log responses and, if needed, to correct them to clean formation responses by means of crossplots.

The shale volume from GR log can be calculated as,

$$V_{sh} = \frac{GR_{log} - GR_{clean}}{GR_{shale} - G_{clean}} \quad (5.1)$$

where,

$GR_{log}$  = gamma ray response in the zone of interest

$GR_{clean}$  = average gamma ray response in the cleanest formations

$GR_{shale}$  = average gamma ray response in shale

*Well A ;*

The GR log for well A is available for 1900 -1991 (-1121.04 m. -1215.04 m. ) meters. For this interval, the zone of interest; Derdere Formation, is penetrated at 1949 (-1173.04 m.) meter. The limestones of Derdere is between 1949–1971 (-1173.04 m. -1195.04 m.) meters. After 1971 meter to 1977 meter, (-1201.04 m.) there is a thin section of shale occurrence which shows high GR responses, resulting in high  $V_{sh}$  calculations. This section can be named as *dolomitic shale* or *marn*. The section is observed in all the available logs, which can be described as a key level at the boundary of the dolomite reservoir. Overlaid by this thin section of shale , dolomites can be distinguished through the logged bottom lithology.

For the limestone section of Derdere Formation, GR responses are a little higher compared to dolomite section. This may be because of the organic-rich character of these limestones, These limestones are bioclastic mudstones and wackestones. The observed fractures may also result in comparatively higher GR responses in this section. In each log set, at the entry of the limestones, a section of high GR responses are observed indicating a boundary for the Derdere Formation

*Well B;*

The GR log for well B is available for 1900 -1965 (-1138.04 m. - 1203.04 m.) meters. Derdere Formation, is being penetrated at 1932 (-1170.04 m.) meter. The limestones of Derdere is between 1932- 1957 (-1170.04 m. -1195.04 m.) meters. A section of dolomitic shale that shows high GR responses is between 1957-1960 (-1195.04 m.-1198.04 m.) meters. The reservoir dolomites are followed by the dolomitic shale after 1960 meter.

*Well C;*

The GR log for well C is available for 1850-1942 (-1120.95 m. -1212.95 m.) meters. Derdere Formation, is being penetrated at 1908 (-1178.95 m.) meter. The limestones of Derdere is between 1908 – 1931 (-1178.95 m. -1201.95 m.) meters. The dolomitic shale section is observed between 1931-1934 (-1201.95 m. -1204.95 m.) meters. The dolomites are observed below 1934 m.

*Well D;*

The GR log for well D is available for 1800 -1905 (1054.2 m.-1150 m.) meters. Derdere Formation, is being penetrated at 1829 (-1074.2 m.) meter. The limestones of Derdere is between 1829 – 1854 (-1074.2 m. -1099.2 m.) meters. A section of dolomitic shale is between 1854-1858 (-1099.2 m. -1103.2 m.) meters. The dolomites are below 1858 m. In dolomite section, between 1887 – 1898 meters, GR responses are also high, as seen in other wells.

*Well X;*

The GR log for well X is available for 1835 -1868 (-1113 m. -1146 m.) meters. Since the lithology identification well logs such as neutron porosity and bulk density are absent, the lithology discrimination in Derdere is done, based on the GR log, sonic log and the core plug analysis.

Derdere Formation, is being penetrated at 1840 (-1118 m.) meter. The limestones of Derdere is between 1840–1868 (-1118 m. -1146 m.) meters. A section of dolomitic shale shale formation is between 1868 -1872 (-1146 m. -1150 m.) meters. The reservoir dolomites are observed below 1872 meter.

The raw GR responses are given in Appendix B.

The Gamma Ray log correlations for the studied wells are shown in Figure 5.2.

### 5.2.2. Sonic Log Analysis

Sonic logging is an important part of formation evaluation. This type of logging utilizes the propagation of acoustic waves within and around the borehole. As sonic log readings are not affected from secondary porosity, they can be used to make correlations within wells. Sonic logs are mainly used for porosity calculations. Two methods are described for porosity determination from sonic logs; *Wyllie Method* and *experimental method*.

Conventional sonic tools measure the reciprocal of the velocity of the compressional wave. This parameter is called *interval transit time*,  $\Delta t$ , or *slowness*, and it is expressed in microseconds per foot ( $\mu\text{sec/ft}$ ). Porosity of consolidated formations is related to  $\Delta t$  by Wyllie's equation.

$$\phi = \frac{\Delta t - \Delta t_{ma}}{\Delta t_f - \Delta t_{ma}} \quad (5.2)$$

where;

$\Delta t_{ma}$  and  $\Delta t_f$  are the slowness of the matrix and pore fluid respectively, and  $\Delta t$  is the slowness of the zone of interest.

The average values of matrix used in Wyllie's equation is given in Table 5.2.

Table 5. 2 Matrix velocities used in Wyllie's Equation

Matrix type	$\Delta t_{ma}$ ( $\mu\text{sec/ft}$ )
Sandstone	55,5
Limestone	47,5
Dolomite	43,5
Fluid	189

The sonic porosities of the studied wells are obtained by using Wyllie's equation.

The porosities obtained from sonic log are the primary porosities, since the sonic waves are not recorded within the fractures and vugs of the formation in consider.

The raw data for the sonic log values of the wells are given in Appendix B. Sonic porosities are given in Appendix D.2. The correlation of the formations due to sonic log recordings is given in Figure 5.3.

The summary statistics of the recorded GR and sonic travel time recordings are given in Table 5.3, and Table 5.4.

The frequency histogram plots for the recorded sonic travel times of the studied wells are shown in Figure 5.4.

Table 5. 3 Summary statistics of GR recordings

Well Name	Sample Size	Mean	Median	Variance	Standard Deviation	Minimum	Maximum
A	43	30.26	25.00	247.90	15.75	15	100
B	34	33.21	20.00	782.65	27.98	14	140
C	34	27.03	21.50	213.85	14.62	10	70
D	58	28.24	25.50	239.84	15.49	11	120
X	39	24.49	20.00	137.47	11.72	12	62

Table 5. 4 Summary statistics of sonic travel time recordings

Well Name	Sample Size	Mean	Median	Variance	Standard Deviation	Minimum	Maximum
A	46	60.59	60.25	37.90	6.15	49	72
B	37	60.00	60.00	40.26	6.35	50	73.5
C	37	58.70	64.00	40.16	6.33	49	70
D	58	62.47	61.00	41.32	6.43	50	82
X	39	62.72	63.00	78.21	8.84	50	85

### 5.2.3. Caliper Log Analysis

Measurements of borehole diameter with caliper logging has indicated clearly that the actual borehole diameter often differs from the bit size used to drill it.

The difference is considerable in some cases. Sometimes, the drilled hole is far from being a regular cylinder with uniform diameter.

The borehole's actual diameter and shape depend on the formation drilled. Borehole enlargements are most commonly observed in shales and shaly formations. (Bassiouni, 1994). Because of their electrochemical properties, clay minerals absorb water, causing the shale formation to swell. Enlargements also occur in water-soluble formations, such as salts.

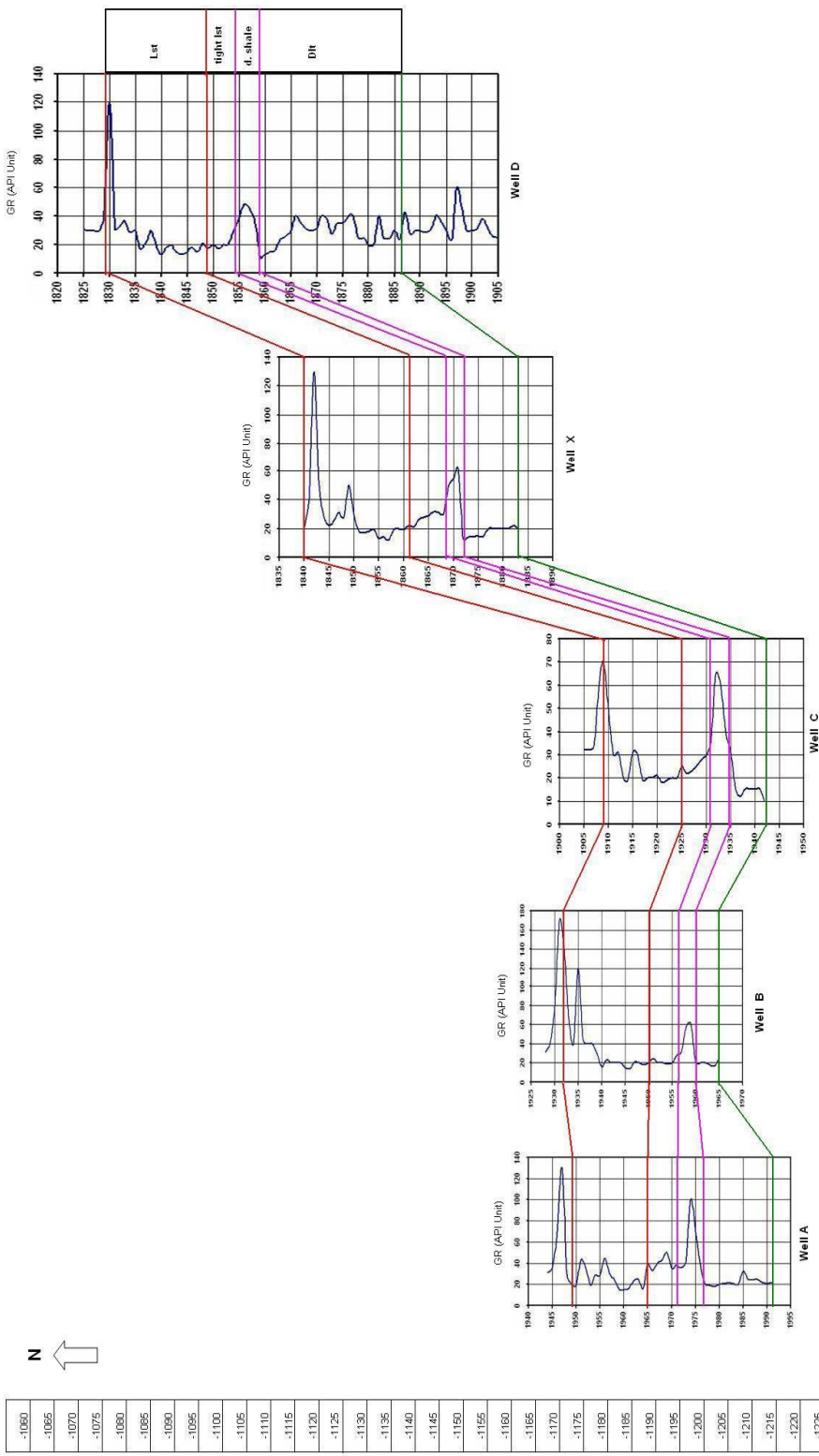


Figure 5. 2 Gamma Ray Correlation

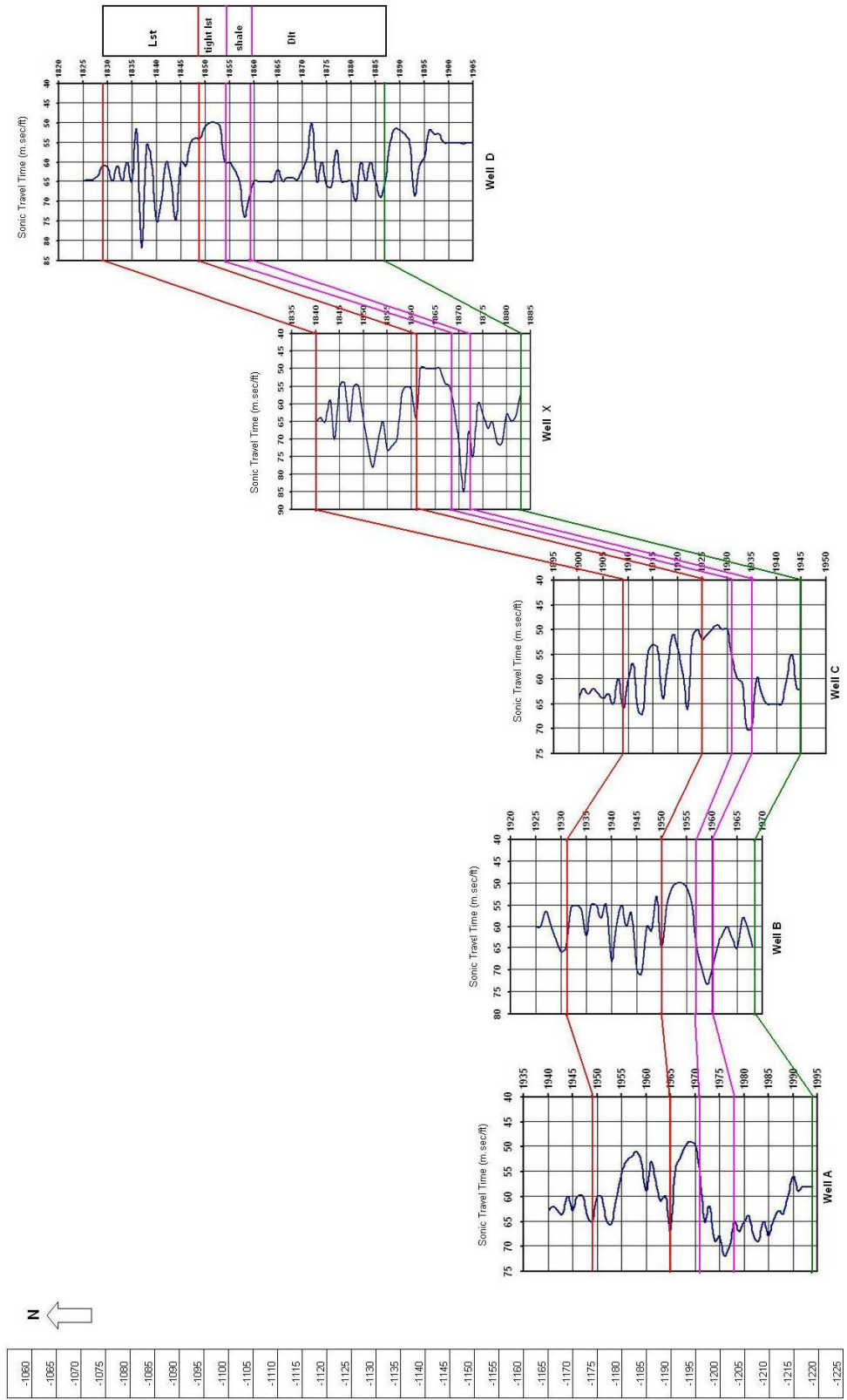


Figure 5. 3 Sonic Log Correlation

Such enlargements are due to soft, unconsolidated formations that the drilling mud has souring effects. In some cases, the hole is seemed as it is being drilled smaller than its actual bit size. This is usually the case in permeable formations drilled with mud that contains solids. Mud cakes are formed in this sections causing smaller diameters.

Adequate analyses of certain log measurements require knowledge of borehole size and shape. To determine the borehole geometry, caliper log is run with microresistivity, density, sidewall neutron, sonic, and dipmeter logs. Besides giving information about the borehole geometry, calipers can help us to determine the permeable zones of the drilled formation.

It must be kept in mind that if there are borehole enlargements or other anomalies within the caliper recordings, some of the well derived parameters may not be reliable. In the studied wells, sections for the borehole enlargements and mud cake occurrences are detected.

In *Well A*, no significant enlargement was seen, but in limestone sections, mud cake developments are seen irregularly.

A continuous mud cake occurrence is detected in the dolomite section in all wells. In *Well B*, mud cake occurrences are generally located in limestones. In *Well C*, there are abnormalities within the density logs, that are caused by the borehole effects, also observed by the caliper logs. In the following chapters, where lithology identifications will be described, the borehole effects will be destructive parameters in determination of lithologies and their percentages for *Well C*.

The most continuous and the thickest mud cake occurrence is observed throughout the dolomite section of *Well D*.

These observations help us to define permeable zones of the formations and the sections where we can not rely on some calculations.

#### 5.2.4. Density Log Analysis

The density log represents the density of the formation rock. If the matrix densities are known, the recorded  $\rho_b$  values can be used to determine the porosity.

The bulk density, ( $\rho_b$ ) is the overall gross or weight-average density of a unit of the formation.

Solving for porosity yields,

$$\phi = \frac{\rho_{ma} - \rho_b}{\rho_{ma} - \rho_f} \quad (5.3)$$

where;  $\rho_f$  is the average density of the fluids in pore spaces. Common values of  $\rho_{ma}$  are given below.

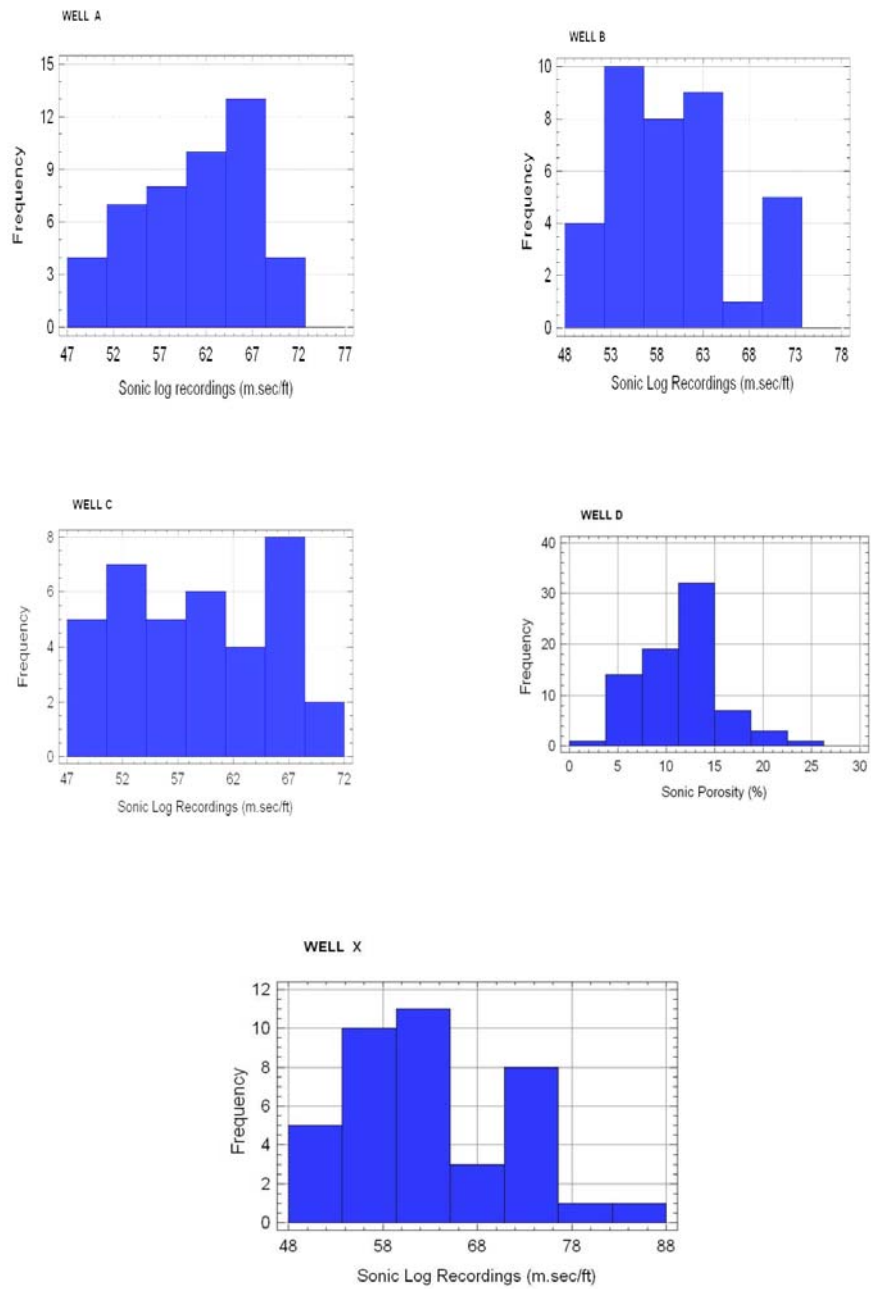


Figure 5. 4 Frequency histogram plots for sonic travel times

Table 5. 5 Matrix values for common types of rocks

Rock type	$\rho_{ma}$ (g/cc)
Sandstone	2.65
Limestone	2.71
Dolomite	2.87
Anhydrite	2.98

The values for  $\rho_f$  are listed in Table 5.6.

Table 5. 6 Fluid densities according to the mud type

Rock type	$\rho_{ma}$ (g/cc)
Oil	0.9
Fresh water	1.0
Brine	1.1

The determination of porosity from density log applies only to relatively simple environments. In complex environments, such as shaly sands, gas-bearing formations, and complex lithology, the density log is combined with other porosity logs. Porosity determination becomes more complex when the lithology is not known or when it consists of two or more minerals of unknown proportions. The most common mixtures associated with carbonate rocks are limestone-dolomite, limestone-sandstone, dolomite-sandstone and dolomite-anhydrite. In the studied wells, limestone-dolomite combinations are observed.

Density logs are generally run with neutron log tools and the interpretations are based upon both of them. If it is used alone, it is utilized to understand the identification of the formation rock porosity and its bulk density. Bulk density is the sum of matrix density and fluid density. Density log recordings can be used as quick-look interpretation methods by the help of frequency diagrams. The dominant lithology within the studied formations can be detected.

In the studied wells such frequency plots were constructed by the help of histograms. The frequency histograms for the recorded density values of the studied wells are given in Figures 5.5, 5.6, 5.7, 5.8 for each well.

For a histogram plot study, consider *Well A*. As seen in all other wells, there are two types of carbonates, limestones and dolomites. In the frequency histogram distribution, recordings are widely scattered between 2.35 and 2.80. For limestones, the density recordings are generally below 2.71 g/cc. These low values (2.40-2.60 g/cc) can be attributed to high porosity zones, whereas the extremely low values (2.40-2.30 g/cc) may be due to the borehole unstabilities causing collapses.

In *Well C* and *D*, some values of 2.30 g/cc are recorded, but this recordings are due to borehole enlargements. In dolomite section, this trend can also be seen. The lower recordings indicate that the dolomite sections are in combination with limestones. The presence of limestones, reduce the density. Also, increases in porosity reduces the density values, since the log recordings are bulk density values. At the entry of the dolomite section, the recorded density values are higher, then the values get smaller indicating more porous zonations. This trend is similar within all the wells.

The raw data for density log are also in Appendix B. The summary statistics of the recorded density values for all wells are given in Table 5.7.

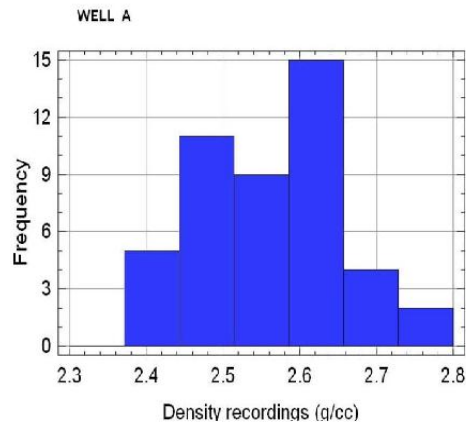


Figure 5. 5 Frequency histogram of density recordings - Well A

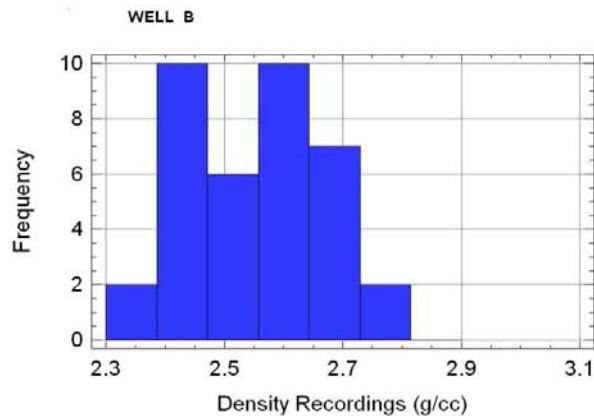


Figure 5. 6 Frequency histogram of density recordings - Well B

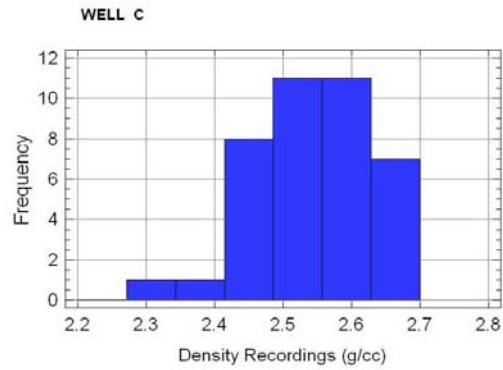


Figure 5. 7 Frequency histogram of density recordings - Well C

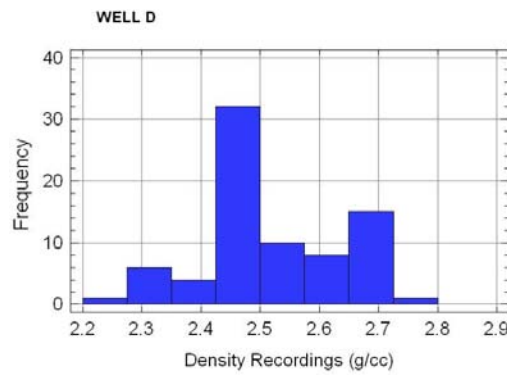


Figure 5. 8 Frequency histogram of density recordings - Well D

Table 5. 7 Summary statistics of density recordings for all wells

Well Name	Sample Size	Mean	Median	Variance	Standard Deviation	Minimum	Maximum
A	46	2.56	2.56	0.0084	0.090	2.40	2.74
B	37	2.55	2.56	0.0130	0.110	2.35	2.78
C	39	2.54	2.55	0.0076	0.087	2.30	2.68
D	58	2.50	2.46	0.0080	0.091	2.30	2.70

### 5.2.5. Neutron Log Analysis

The neutron porosity log is based on the elastic scattering of neutrons as they collide with the nuclei in the formation. Formations with high hydrogen content display low concentrations of neutrons, and inversely, formations with low hydrogen content display high concentrations of neutrons. Because most of the hydrogen is part of the fluids located in the pore space, this concentration is inversely related to porosity.

The borehole diameter, temperature, mud salinity, mud cake, formation pressure, and formation water salinity affects the neutron log recordings, but the effects can be eliminated by using several correlation charts. The presence of shale and gas in the formation also affect the neutron logs. The shale content may result in higher values of neutron porosity. Neutron logs are generally run with density logs as mentioned before. Together, they are the most efficient lithology and porosity identification logs besides determination of gas-bearing formations.

The scale on the log paper may differ for neutron recordings. It may be calibrated for sandstone lithology or for limestone lithology. For the formations other than these calibrations, the recorded values should be corrected using *Neutron Porosity Equivalence Curves*. In this study, the neutron logs were recorded in limestone porosity units, and a correction chart was used for the porosity determination of dolomite sections. The utilized chart is given in Figure 5.9.

The lithology discrimination is generally based on neutron-density logs. The location of neutron and  $\rho_b$  curves, the separation between them give lithology informations.

In this study, the lithology identifications are based on these logs. According to this, two basic types of lithologies were detected in the Derdere Formation, limestone and dolomite from top to bottom.

Neutron logs are used to determine porosity, in fact the actual recordings of the neutron gives porosity values, but when the density recordings are added into the porosity calculations, such as in the density-neutron crossplot technique, the results are more efficient than the neutron and density porosities alone.

The porosity obtained by means of density-neutron can be shown as  $\emptyset_{D-N}$ . This value can be considered to be very close to the core porosity determined by laboratory tests.

The  $\emptyset_{D-N}$  porosity is the total porosity of the section in consider. This total porosity contains the uneffective porosity that are already in the pores.

Since the irreducible water saturation can not be included in the production, as saturation calculations are done, this total porosity can be accepted as an effective porosity as accepting the error that may occur, or instead Magnetic Resonance (MR) can be used, if available.

The  $\emptyset_{D-N}$  value can be calculated as follows,

- The bulk density values are read from the log. These values are used to obtain density porosity ( $\phi_D$ ) by using the Equation 5.3 .
- The neutron porosity values are read from the log. Necessary corrections are done for lithology using the chart in Figure 5.9, to obtain corrected values of neutron porosity ( $\phi_N$ )
- Using below equation, the  $\phi_{D-N}$  porosity is calculated.

$$\phi_{D-N} = \frac{\phi_D + \phi_N}{2} \quad (5.4)$$

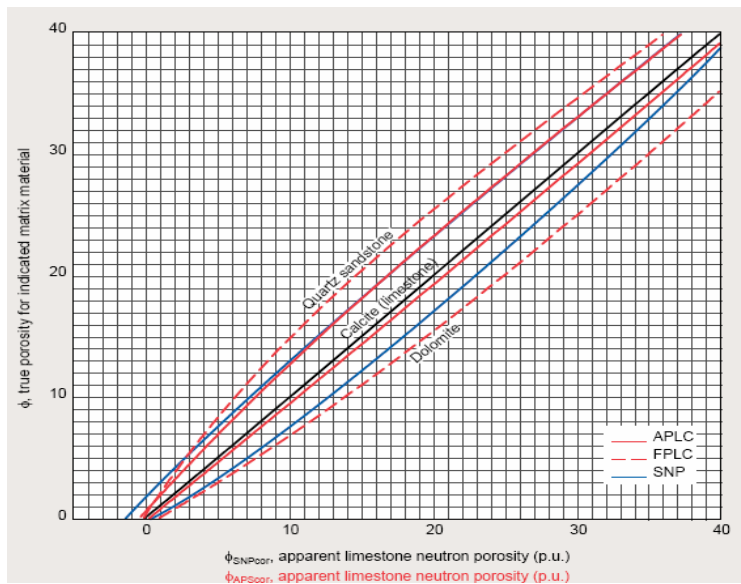


Figure 5. 9 Neutron Porosity Equivalence Chart

(Schlumberger, Log Interpretation Charts, 1988)

The  $\phi_{D-N}$  porosity can also be obtained by means of density-neutron crossplots. The crossplot used in this study is given in Figure 5.10. This crossplot is mainly used for porosity determination. The second aim is to define the lithology types in percentages. A limestone formation is not generally purely and totally composed of  $\text{CaCO}_3$ , it may contain some minor amounts of  $\text{Ca-MgCO}_3$ , or  $\text{SiO}_2$  which are dolomite and silica respectively. In order to determine the exact values of these constituents this crossplot is used.

In this study, the  $\emptyset_{D-N}$  porosity values are obtained by means of the density-neutron crossplot, which is given in Figure 5.10. By the help of this crossplot, corrections based on shale can also be applied. In this study, for the zones of interests, there are some intervals with high GR responses indicating clay minerals. These are the dolomitic shale intervals overlying the dolomite reservoir section. The presence of shale effects the response in the porosity tools. The necessary corrections based on shale presences will be explained in the following chapter. As the corrections are done, lithology fractions are determined from the same crossplot.

The raw data for neutron recordings are given in Appendix B.

The  $\emptyset_{D-N}$  values obtained by means of the density-neutron crossplot are given in Appendix D.2.

The summary statistics for neutron porosity recordings are given in Table 5.8.

The frequency histogram plots were also constructed for the neutron porosity readings from each well.

The histograms are given in Figure 5.11, 5.12, 5.13, 5.14 for each well.

Table 5. 8 Summary statistics of neutron porosity recordings

Well Name	Sample Size	Mean	Median	Variance	Standard Deviation	Minimum	Maximum
A	46	13.86	15	63.67	7.98	2	30
B	37	14.58	15	53.52	7.31	3	27
C	39	10.76	12	59.73	7.73	0	25
D	58	20.04	21	55.40	7.44	3	33

The neutron porosity values vary a lot. Generally, the recorded values for limestones are lower than the ones in dolomites. Most of the lower values seen in the recordings and the frequency plots count for limestones.

Some of these values are also seen for dolomite sections, but generally dolomites give high values of porosity. The porosity values for porous parts of dolomites may reach up to 27 %. Same trends are seen in the  $\emptyset_{D-N}$  calculations, but due to the effect of density porosity addition, values lower

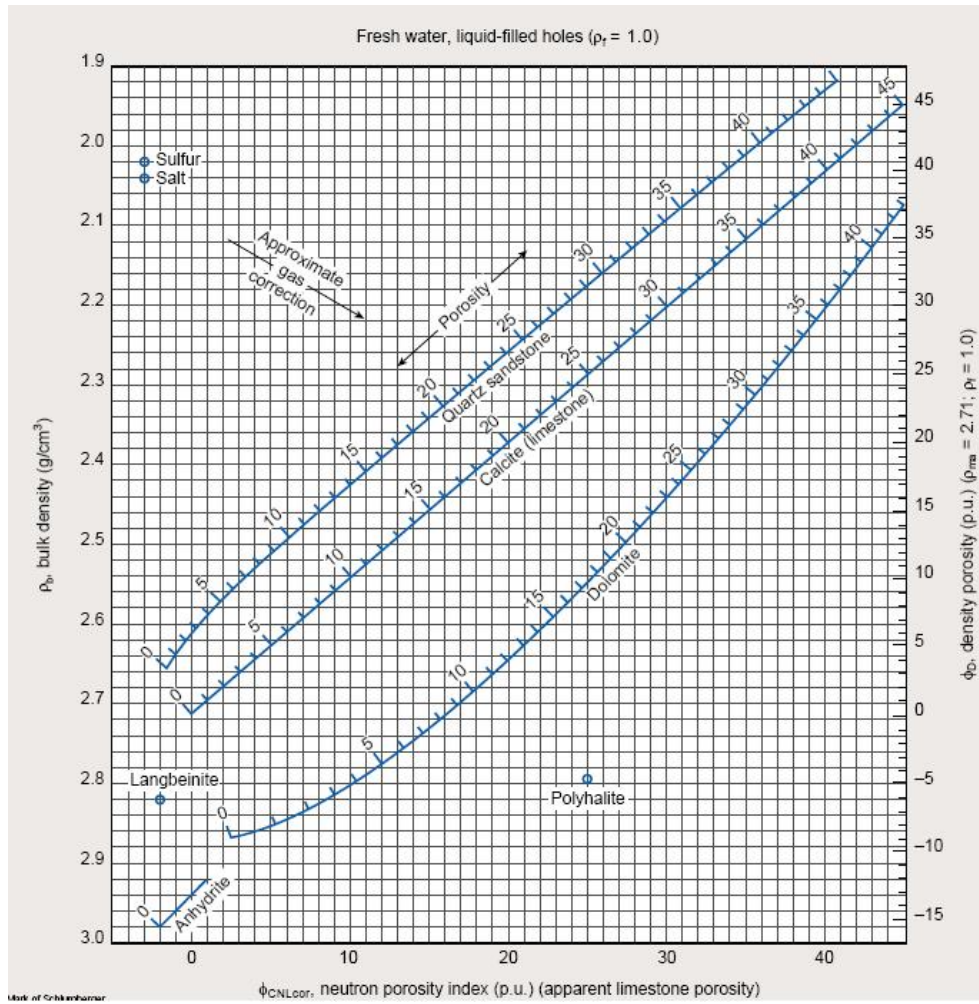


Figure 5. 10 Crossplot for Porosity and Lithology Determination from density log and compensated neutron log  
(Schlumberger, Log Interpretation Charts, 1988)

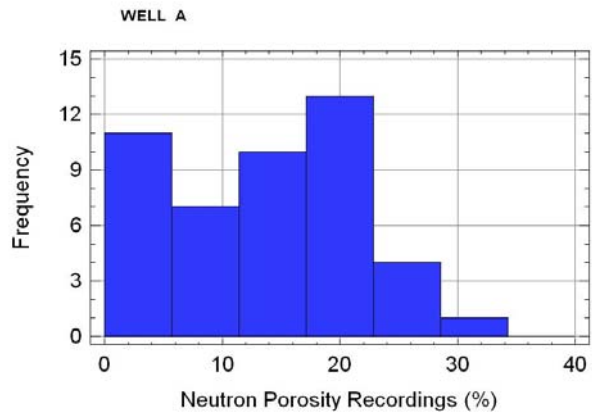


Figure 5. 11 Frequency histogram of neutron porosity recordings - Well A

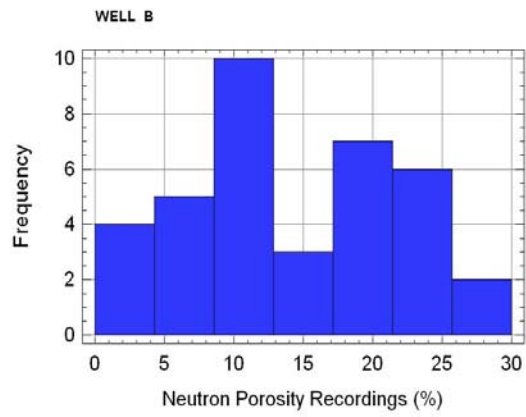


Figure 5. 12 Frequency histogram of neutron porosity recordings - Well B

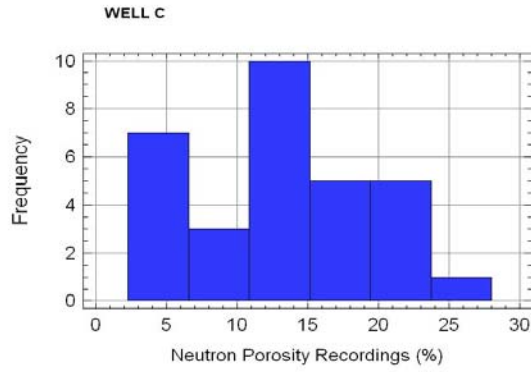


Figure 5. 13 Frequency histogram of neutron porosity recordings - Well C

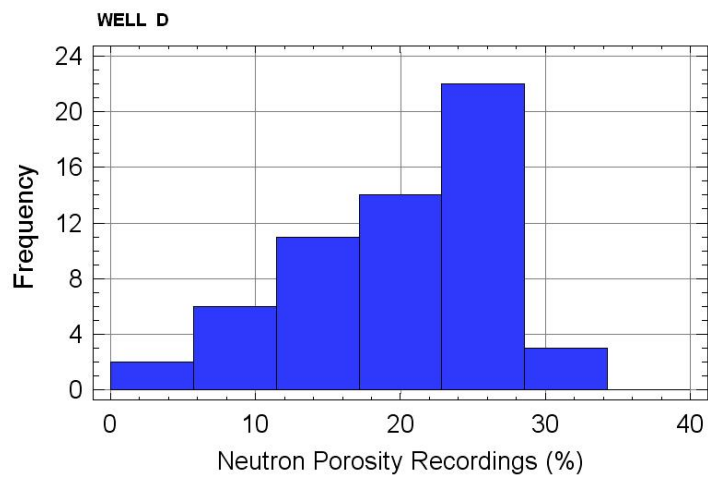


Figure 5. 14 Frequency histogram of neutron porosity recordings - Well D

### 5.2.6. Effective Porosity and Shale Content from Density-Neutron Crossplot

The evaluation of shaly formations can be sometimes a difficult task. Clay minerals affect all well-logging measurements to some degree. The shale effects have to be considered during evaluation of such reservoir parameters as porosity and water saturation. The interpretation problem in shaly formations is in calculating porosity and saturation values free from the shale effect ( Bassiouni, 1994). Because the shale effect depends on the shale content, the estimation of  $V_{sh}$  is of prime importance. Qualitatively,  $V_{sh}$  indicates whether the formation is clean or shaly. This determines the model or approach to use in the interpretation. Quantitatively,  $V_{sh}$  is used to estimate the shale effect on log responses and, if needed, to correct them to clean formation responses.

Because shale affects every logging tool to some degree, numerous methods have been developed to indicate the presence and to estimate the content of shale (Bassiouni, 1994). The most often used methods are SP, GR, and porosity logs.

For the studied wells, as it is mentioned in the GR log analysis section, there exist shale intervals within the zones of interests. The GR recordings reach up to 100 and more API units in some intervals. When conventional shale content calculation models are used, the shale volumes are determined as 100 % . For these high values of shale volumes, porosity values may be higher, but this porosity is not the effective porosity. This gives the total porosity, including the ineffective porosity of the zone of interest. For a better understanding of shale volumes and the effect of shale on porosity, density-neutron crossplot is used in this study.

The steps of the used method is listed below;

- An appropriate density-neutron crossplot is chosen. (For this case, the utilized crossplot is given in Figure 5.10)
- In the full log set, a recording of a maximum shale interval is determined with the values of bulk density and neutron porosity
- This point is put on the density-neutron crossplot and it is named as “ *shale point*”
- The lines indicated as sandstone, limestone and dolomites are named as the clean formation lines, where the formation is free from clay minerals. A straight line combining the shale point and the starting point ( where  $\emptyset = 0$ ) of each clean formation lines is drawn . This line is divided into equal sections of shale volumes. The shale point indicates the 100 % shale.
- Straight lines parallel to the clean formation lines are drawn. Each line can be called as “*isoshale content lines*”
- Straight lines, parallel to the shale line, passing through each porosity values on the clean formation line are drawn. These lines are named as “ *isoporosity lines*”

- A log recording is placed on this new crossplot and shale volume, total porosity, effective porosity and lithology percentages are determined.  
An example study of the explained method above is given in Figure 5.15.

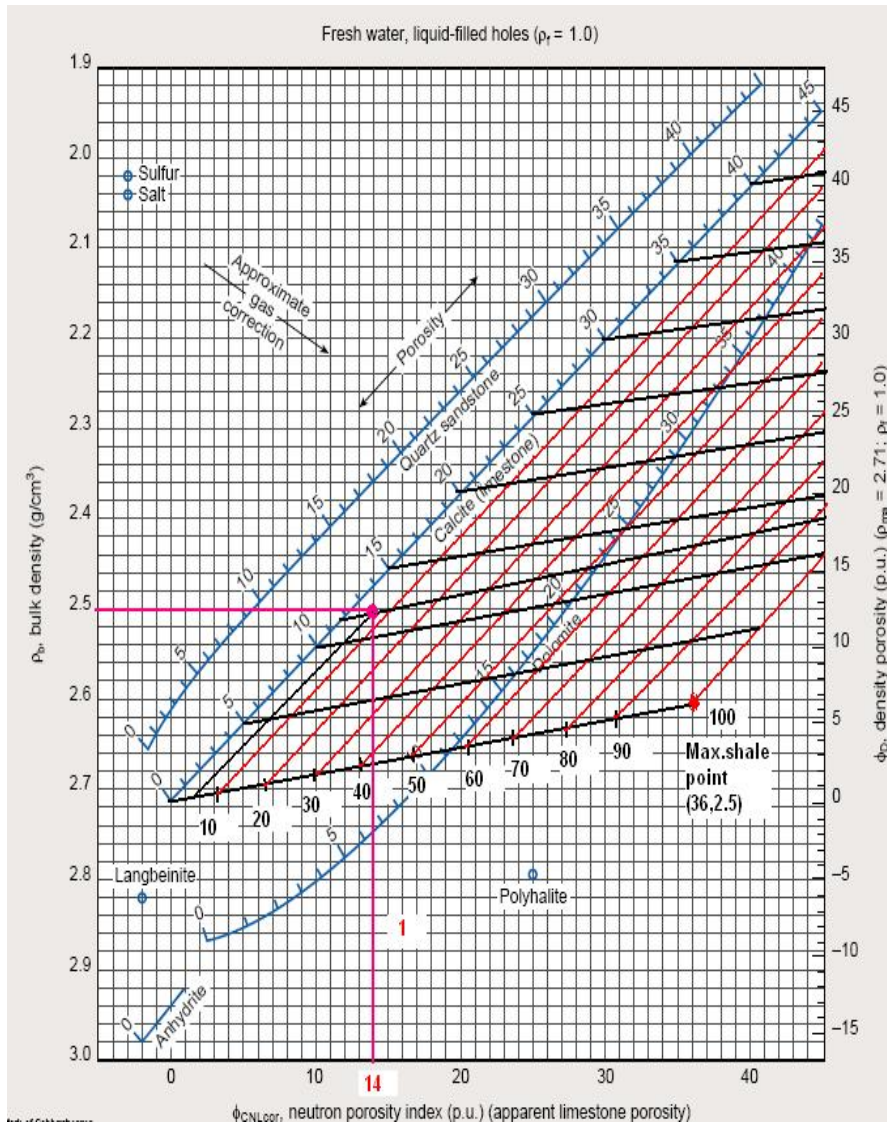


Figure 5. 15 Determination of shale point and porosity in shaly formations

This method is applied in Well D, in order to understand the effect of shale content on porosity. Maximum shale values for the studied well is given as below,

$$\varnothing_N = 36 \text{ p.u.}$$

$$\rho_b = 2.5 \text{ g/cc}$$

These values are plotted on the crossplot which is indicated as “*maximum shale point*”. The studied lithology is limestone, so a line binding this point to clean limestone lithology is drawn starting from 0 porosity. The resulting line is divided into equal shale volumes. These *isoshale content lines* are represented in red. The *isoporosity lines* are in black. A zone of interest is chosen for a study, with  $\varnothing_N = 14 \text{ p.u}$  and  $\rho_b = 2.5 \text{ g/cc}$ . The result is followed by the marked path 1. The resulting point reads as;

$$V_{sh} = 5 \%$$

$$\varnothing_{total} = 12 \%$$

$$\varnothing_{effective} = 11.7 \%$$

The percentages of other lithologies are also derived from the result. Here, the percentage of limestone can be determined as 92 % and dolomite as 3 %.

All the recordings obtained from Well D are plotted on such a crossplot and for each recording, shale content, total and effective porosities are derived. The results are listed in Appendix D.1 for lithology fractions and Appendix D.2 for obtained effective porosities from the crossplot. For the boundary of the Derdere Formation, shale contents show relatively high values as 25 – 30 %. This section is a high shale section, observed at each boundary of each well log. For the limestones, the shale contents lower and give nearly 0 values. The values range 0-15 % for these intervals. An increase in shale content is also observed at the top of dolomites, since this is the dolomitic shale interval observed at each well log. For the reservoir section of dolomites, the shale contents are declining to near 0 values. The range is 0-10 % for the dolomites.

By looking at the results, a statement can be derived for the following studies of other wells. Since we obtain low shale content values by using the density-neutron crossplot method, we can conclude as that the lithologies are “*clean lithologies*” and the porosities obtained from the density-neutron crossplot can be used as effective porosities. The effective porosity values for the other studied wells are given in Appendix D.2.

As mentioned previously, the crossplot is also used for the determination of lithology percentages. Lithology fractions support the distinctions of limestones and dolomites in the formation. The lithology fraction plots are given in Figures 5.16, 5.17, 5.18, and 5.19.

As seen from the lithology fraction plots, there are two types of carbonates which are dominant in the formation. The limestone sections are more dominant than the dolomites. The dolomites are not pure and they can be considered as limy dolomites especially at the top and bottom of the dolomites. These trends effect the porosity distribution. Lithology fractions for all the wells are given in Appendix D.1.

There exist some intervals where there are no percentages are calculated. These are the intervals where the porosity recordings are affected from the borehole. The porosity tools are generally affected from the borehole enlargements. For these cases, the recordings are not reliable. For this reason, the lithology percentages plot represent blank values for these intervals.

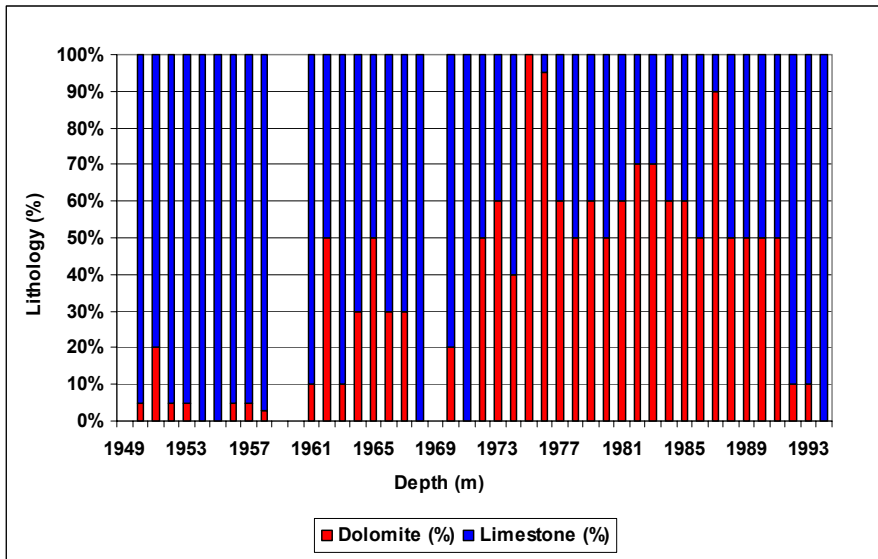


Figure 5. 16 Lithology fractions - Well A

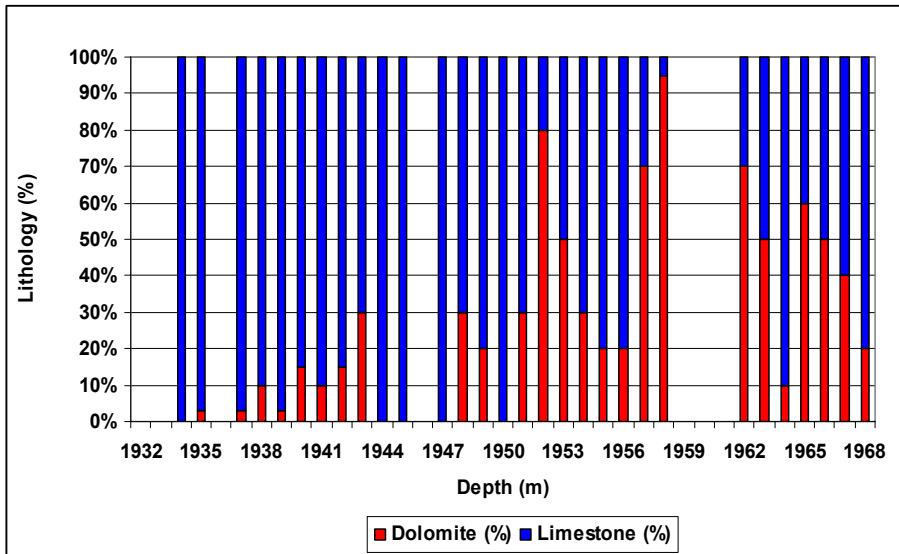


Figure 5. 17 Lithology fractions - Well B

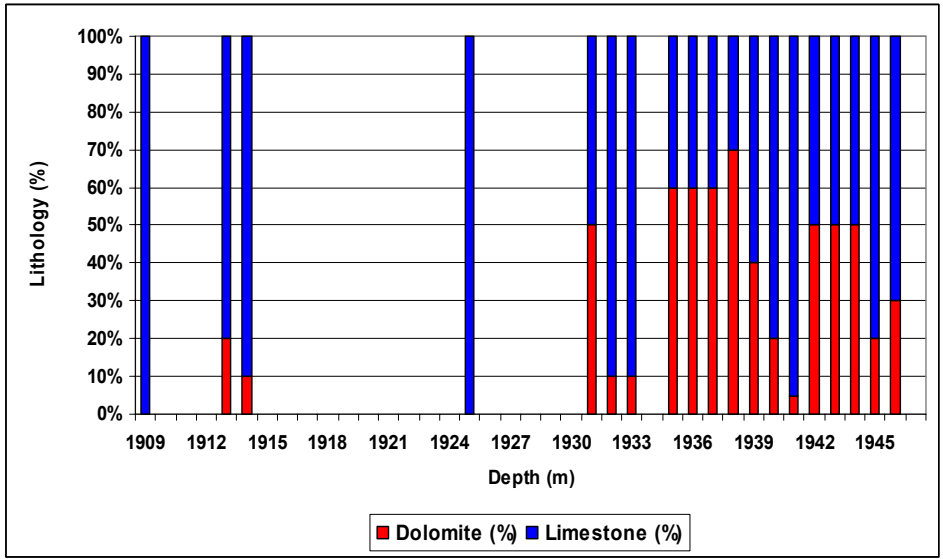


Figure 5. 18 Lithology fractions - Well C

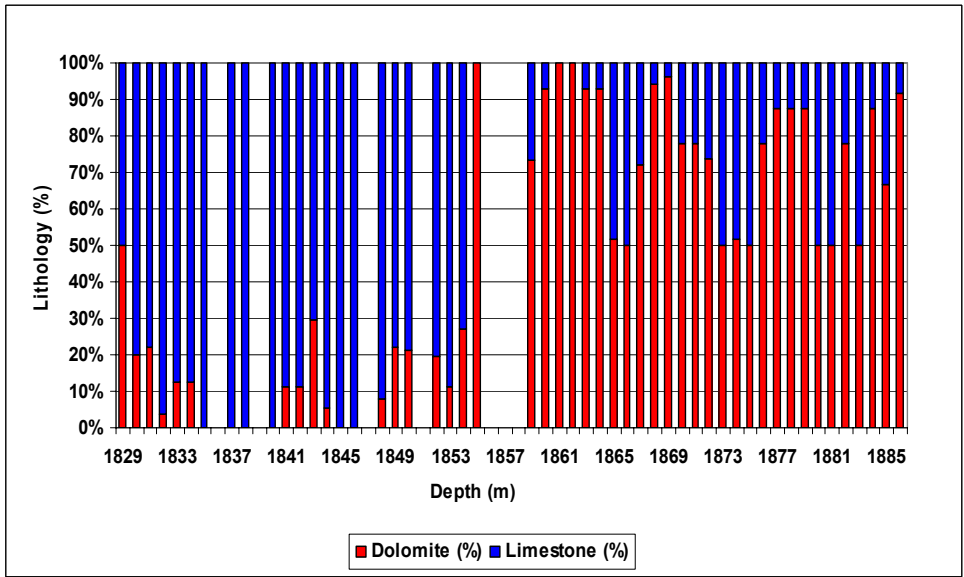


Figure 5. 19 Lithology fractions - Well D

### 5.2.7. Resistivity Log Analysis

In order to determine the saturations of hydrocarbons within the formations, first saturations of water should be calculated. A resistivity of a formation is the ability of its constituents to transmit electricity. The tools used for resistivity logging are classified within depth of investigation as follows;

- Deep resistivity tools for uninvaded zones
- Shallow resistivity tools for transition zones
- Microresistivity tools for flushed zones

The most common resistivity tools in use can be classified as;

- Dual Laterolog Tool
- Dual Induction Tool
- Micro Spherically Focused Log
- Microlog

The resistivity of a formation with its matrix and fluid (water and hydrocarbon) and in the pores is true resistivity ( $R_t$ ) of the formation. A porous and a permeable formation has always water, even it contains hydrocarbon. The water in the pores of formation before it drilled is the formation water saturation ( $R_w$ ) of the formation. After a drilling operation, drilling mud invades and this effects the vicinity of the borehole forming different zones with different resistivities. This zonation is shown in Figure 5.20.

The original water saturation,  $S_w$  is only valid for the uninvaded zone of the formation. The flushed zone is totally invaded with mud with a resistivity of  $R_{mf}$ , and the saturation of this zone is shown as  $S_{xo}$ .

A resistivity of a formation that is saturated 100% with water ( $S_w = 1$ ) can be called as  $R_o$  and the resistivity of the water that saturates the formation is  $R_w$ , then there is a ratio between them. This ratio is called "formation resistivity factor" or "formation factor" ( $F$ ).

$$F = \frac{R_o}{R_w} \quad (5.5)$$

$F$  is mainly controlled by porosity and tortuosity. However, the rock tortuosity is difficult to measure. On the basis of laboratory measurements of  $F$  and porosity, Archie suggested the following equation in 1949.

$$F = \frac{1}{\phi^m} \quad (5.6)$$

where,  $m$  is the cementation exponent.

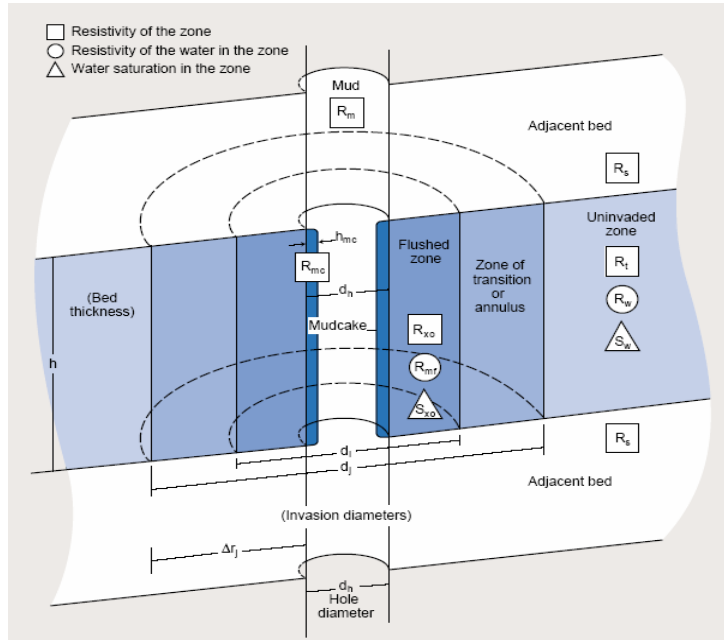


Figure 5. 20 The zones around borehole due to mud invasion  
(Schlumberger, Log Interpretation Charts, 1988)

Another empirical equation relating  $F$  and porosity was also suggested by the results of the experiments conducted by Winsauer in 1952. This equation is in the form of ;

$$F = \frac{a}{\phi^m} \quad (5.7)$$

where  $a$  is the tortuosity constant. The values of  $a$  and  $m$  vary mainly with pore geometry. The  $m$  varies mainly with the degree of consolidation of the rock. In this study,  $a$  was taken as 1 and  $m$  was taken as 2 for carbonates.

After the computation of  $F$  value, water saturations can be computed by using Archie's Equation as below;

$$S_w = \sqrt{\frac{F \cdot R_w}{R_t}} \quad (5.8)$$

$R_w$  is the water saturation in uninvaded zone, and  $R_t$  is the true resistivity of the formation which can be read from deep resistivity logs (R-LLD).

Using the same equation, the water saturation in the flushed zone can also be computed.

$$S_{xo} = \sqrt{\frac{F \cdot R_{mf}}{R_{xo}}} \quad (5.9)$$

where  $R_{mf}$  is the resistivity of the mud filtrate, and  $R_{xo}$  is the resistivity of the flushed zone.  $R_{xo}$  can be computed by Micro Spherically Focused Log (MSFL).

The hydrocarbon saturation in the uninvaded zone, which is the oil saturation ( $S_o$ ) is then,

$$S_o = 1 - S_w \quad (5.10)$$

and the hydrocarbon saturation in the flushed zone, which is the residual oil saturation (ROS) is calculated as;

$$ROS = 1 - S_{xo} \quad (5.11)$$

The difference between the saturations of invaded zone and uninvaded zones result in movable oil saturation (MOS).

$$MOS = S_{xo} - S_w \quad (5.12)$$

In order to find saturations,  $R_w$  should be computed.

$R_w$  is obtained by using the temperature data on log headings. In order to find  $S_{xo}$ ,  $R_{mf}$  should be computed. Also salinity of the field should be known. The salinity of Y field is given as 20,000 ppm. To make the necessary calculations, a chart is used. This chart is called the *Resistivity of NaCl solutions*, which is given in Figure 5.21. On this chart, an example  $R_w$  determination is seen for Well A, with a bottomhole temperature of 148°F, and field salinity of 20,000 ppm, the  $R_w$  is determined as 0.158 Ω.m.

Table 5.9 shows the  $R_w$  and salinity calculations for each well.

Table 5.9 Calculated  $R_w$  and salinity values for each well

Well	BHT (°F)	Measured Rmf (Ω.m)	Rw (Ω.m)	Rmf salinity (ppm)	Rmf at BHT
A	148	0.40 at 68 °F	0.158	17,000	0.18
B	146	0.55 at 76 °F	0.160	10,500	0.29
C	148	0.60 at 74 °F	0.158	10,000	0.30
D	144	0.34 at 70 °F	0.160	19,700	0.16

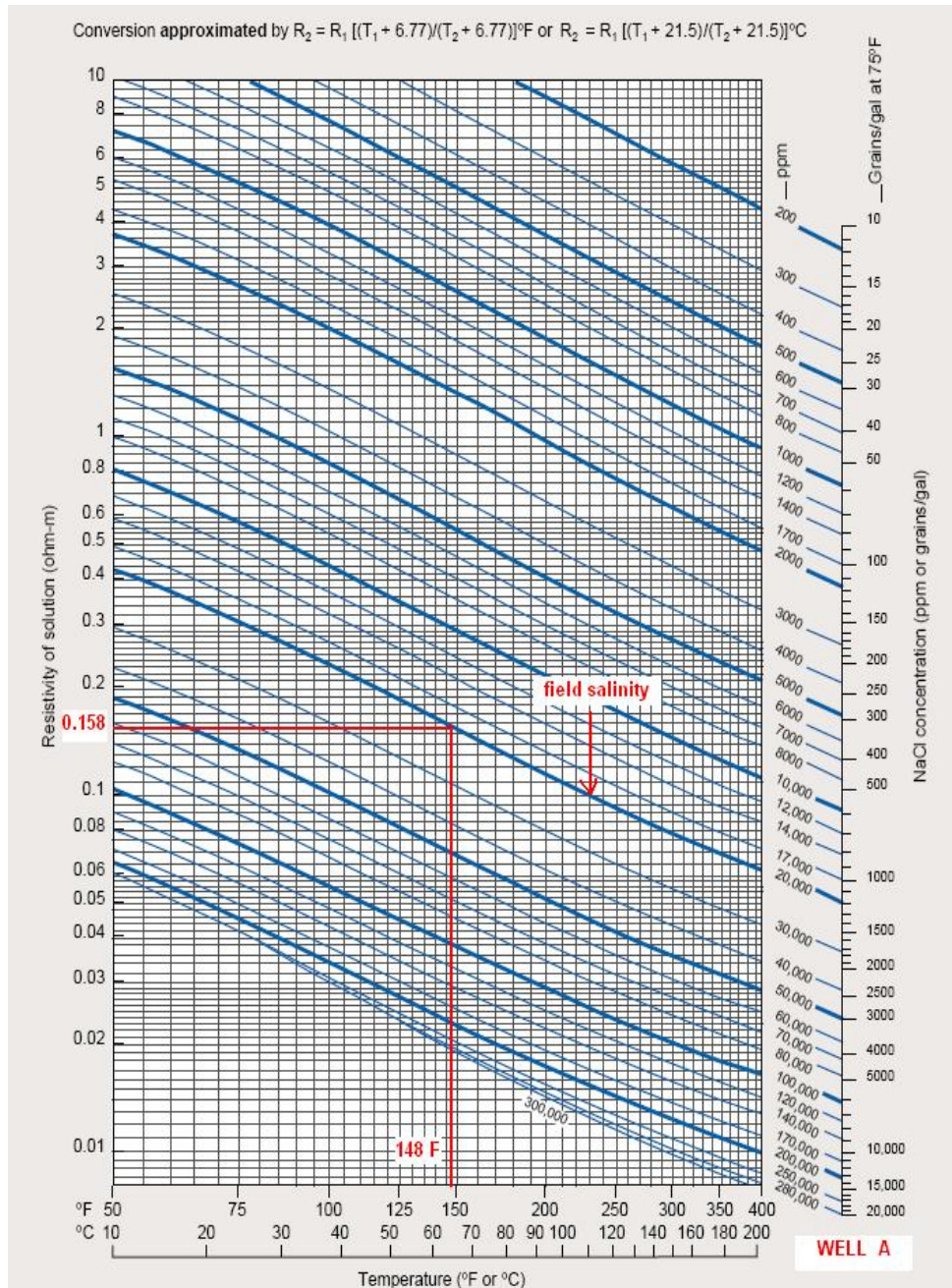


Figure 5. 21 Resistivity of NaCl solutions  
 (Schlumberger Log Interpretation Charts, 1988)

In this study, all the explained steps above were conducted for each well. The raw data for the resistivity recordings of the studied wells are given in Appendix B. The calculated values of formation factors and saturations are given in Appendix D.4. The resistivity log correlations for the wells in Y field in shown in Figure 5.22.

The frequency diagrams of the recorded  $R_t$  values from deep resistivity logs (R-LLD) are shown in Figure 5.23, 5.24, 5.25, and 5.26 for each well.

The  $R_t$  values are generally clustered around low values, indicating water bearing zones. In the calculations of water saturations, there occurred 100% water saturations in some intervals of the wells. These intervals are mainly resulted from the shale intervals, which are observed at the top layer of dolomites. The water in these dolomitic shale intervals are the “bound water”. Bound water is the water within the clay lattice or near the surface within the electrical double layer. This water does not move when fluid is flowed through the rock. Bound water is not part of the effective porosity and is the difference between total and effective porosity. Bound water is understood to include the interlayer water, although the contribution of the latter to the electrical properties of the clay may be different from the water in the electrical double layer (Schlumberger, Oilfield Glossary).

The summary statistics for the recorded resistivity values of the wells are given in Table 5.10, and Table 5.11.

Table 5. 10 Summary statistics of  $R_t$  recordings for all wells

Well Name	Sample Size	Mean	Median	Variance	Standard Deviation	Minimum	Maximum
A	45	314.73	200	87743.4	296.21	11	1100
B	37	353.98	150	224576	473.88	7	1900
C	15	472.20	200	355838	596.52	20	2000
D	58	262.93	240	32796.9	181.10	14	800

Table 5. 11 Summary statistics of  $R_{xo}$  recordings for all wells

Well Name	Sample Size	Mean	Median	Variance	Standard Deviation	Minimum	Maximum
A	45	76.76	50	8560.55	92.52	2	500
B	37	145.02	70	104994	324.02	4	2000
C	15	49.27	40	2029.92	45.05	8	180
D	58	43.61	35	1699.08	41.22	1.5	200

-1060
-1065
-1070
-1075
-1080
-1085
-1090
-1095
-1100
-1105
-1110
-1115
-1120
-1125
-1130
-1135
-1140
-1145
-1150
-1155
-1160
-1165
-1170
-1175
-1180
-1185
-1190
-1195
-1200
-1205
-1210
-1215
-1220
-1225

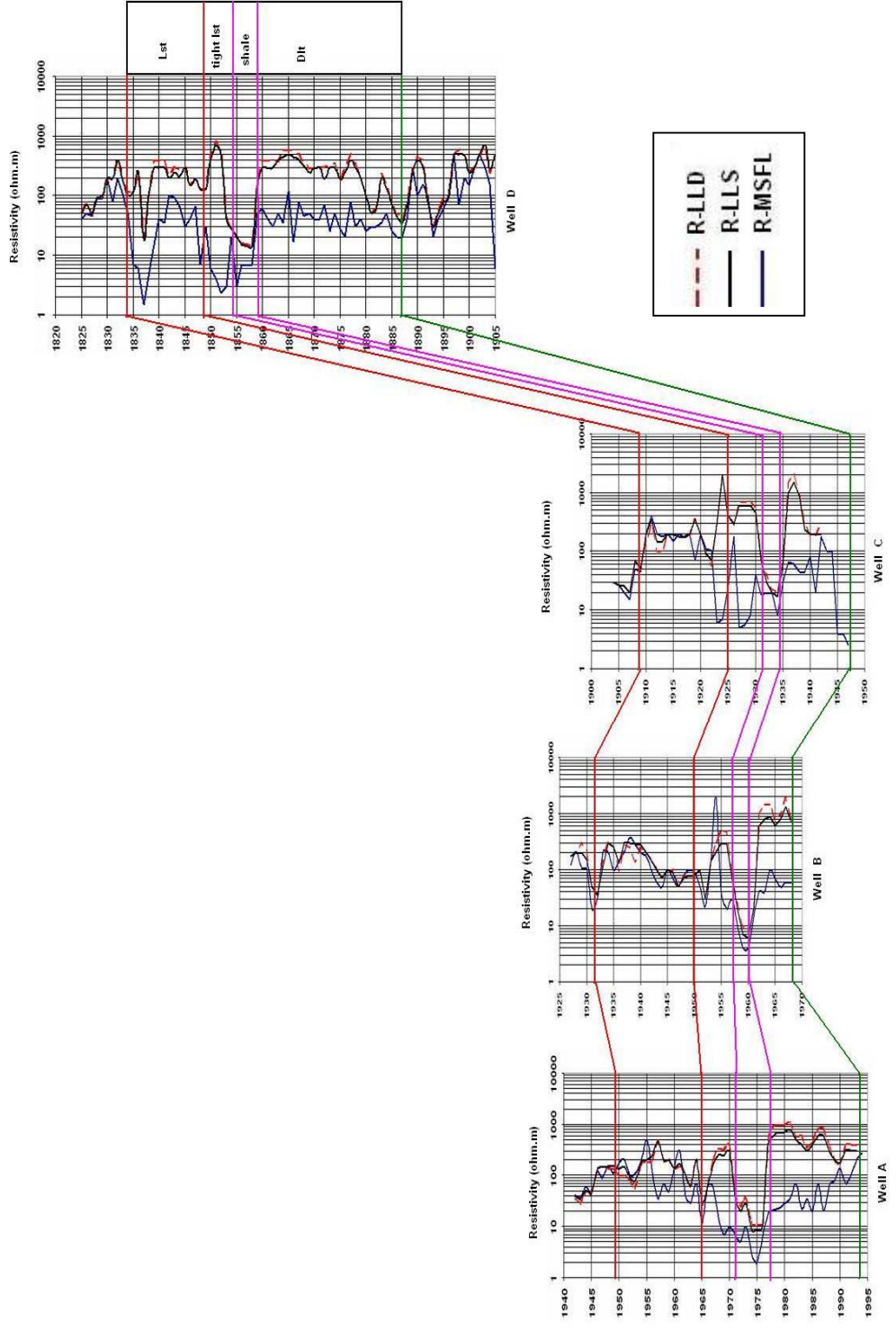


Figure 5.22 Resistivity Log Correlation

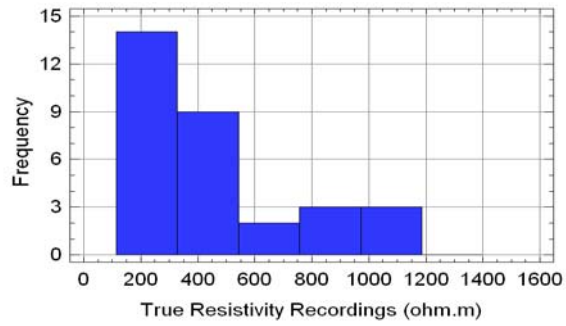


Figure 5. 23 Frequency histogram of Rt recordings - Well A

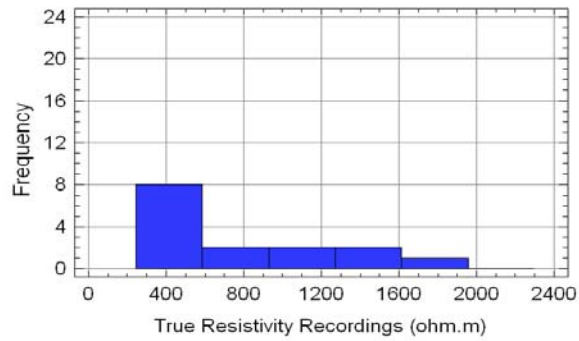


Figure 5. 24 Frequency histogram of Rt recordings - Well B

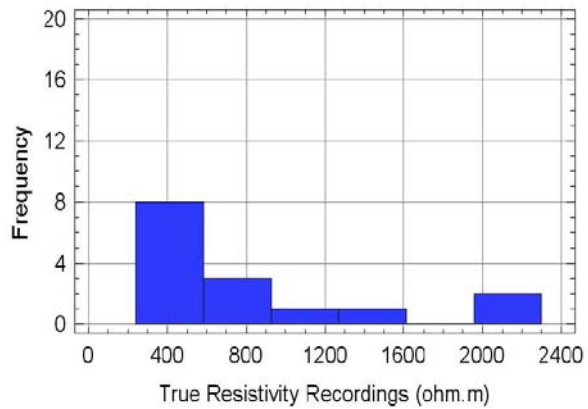


Figure 5. 25 Frequency histogram of Rt recordings - Well C

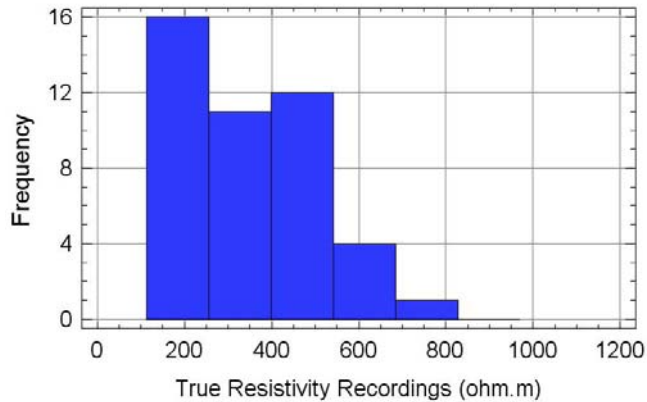


Figure 5. 26 Frequency histogram of Rt recordings - Well D

### 5.3. Core Data Analysis

The reservoir characterization should include core analyses that help researchers to understand the reservoir parameters such as porosity type, porosity distribution, and permeability. All data gained from the core data analyses must be observed carefully and comparisons should be made with other available data. For an efficient reservoir characterization, all available data of core analyses, well logging, and production tests are combined. But sometimes, not all the wells are cored, because coring is an expensive procedure, so with the available data in hand, the other parameters are tried to be compared with one another and estimations are made.

Three types of core analyses are commonly used; (1) conventional or core plug analysis, (2) whole core analysis, (3) sidewall core analysis (Helander, 1983). The most recent technology of Core Tomography (CT) is also used for core analysis.

Core plug method is used commonly. A small plug sample is cut from the core and rock properties such as porosity and permeability are determined.

If there exist heterogeneities such as fractures and vugs, the coreplug analysis is invalid and whole-core analysis is applied.

In sidewall coring, a sidewall core is taken from the wall of a drilled well.

In Y field, there are 58 conventional core analyses are available. These analyses include coreplug porosities (in %), air and liquid permeabilities (in mD) , and grain densities (in g/cc) within related depth intervals. Well A has 2, Well B has 8, Well D 23, and Well X has 25 coreplug data. Well C has no recorded and analysed core plug data. The raw coreplug data is given in Appendix B.

The provided core plug data were first investigated individually; basic statistics were applied to core data, correlation between the parameters were established.

After a wide study on coreplug data, the measurements were correlated with the results from well logging data to construct estimation models and to understand which parameters are dominant over these models.

### 5.3.1. Core Plug Porosity Analysis

From the reservoir engineering standpoint, one of the most important rock properties is porosity, a measure of the space available for storage of petroleum hydrocarbon (Amyx, et al., 1960). Porosity is classified according to its origin, (1) original (primary), (2) induced (secondary). Original porosity is developed in the deposition of the material, and induced porosity is that developed by some geological processes after the deposition of rock (Amyx, et.al, 1960). Carbonate rocks are more heterogeneous than sandstones, as a result induced porosity can be characterized by fractures, vugs and solution cavities as seen in most of the carbonates.

Core plugs sometimes do not yield porosity values that include the effects of vugs and solution cavities. The methods used for the determination of pore volume and bulk volume are unsatisfactory, because drainage may occur from larger pores (Amyx, et.al, 1960). It is necessary to use longer and larger core samples, as in whole core analysis, to determine the bulk volume. But this is not always possible, so the results obtained from the core plug should be relied on.

The basic statistical parameters of the core plug porosity are given in Table 5.12.

Table 5. 12 Summary statistics of core plug porosity (%)

Sample Size	Mean	Median	Variance	Standard Deviation	Minimum	Maximum
58	17.62	19.57	65.65	8.1	0.97	32.19

The frequency histogram for core plug porosity is given in Figure 5.27.

The relative curve of core plug porosity is shown in Figure 5.28.

Both the dolomite and limestone porosities are taken into consider for frequency histogram plot, so there is not a homogeneous distribution. Besides the porosity discrimination between limestone and dolomite, there also exists a porosity difference in dolomite. This trend was observed in the porosity logs at first, and it is detected in the core analysis as the coreplug depth data is matched with the well logging data depth. As mentioned in the well logging part, the porosity values obtained from the porosity logs for limestone are relatively lower than the dolomites. But a unique section of dolomite has some low porosity values and some of these values are even lower than the limestone porosity.

The values clustered around 5-15% contribute for limestone porosity and low porosity sections of dolomites. Besides these low values, there are high and even higher values of porosity. These values are clustered around 20-35%. The histogram plots of coreplug porosity display a similar character with the plots constructed for neutron porosity values.

The relative cumulative curve of coreplug porosity indicates that 60% of the samples have porosity below 20%. 20% of this values count for low porosity values. 40% of the total coreplug porosity data set has relatively higher values of porosity.

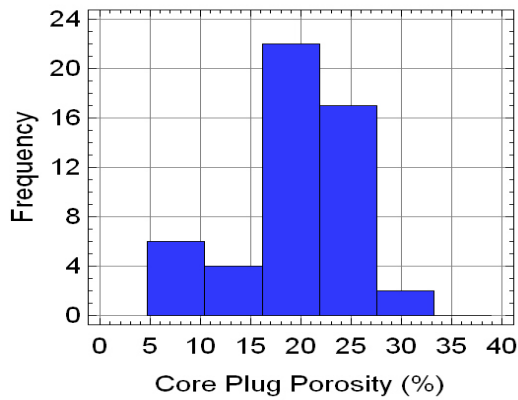


Figure 5. 27 Frequency histogram of core plug porosity

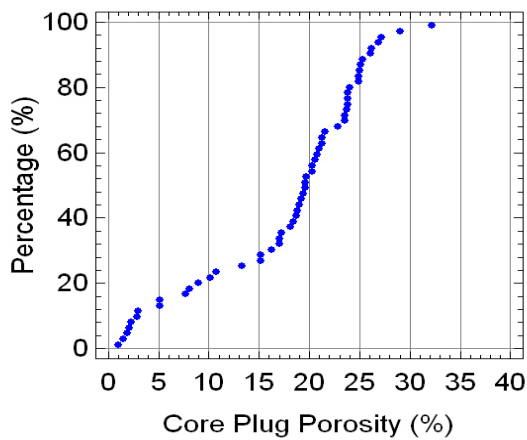


Figure 5. 28 Relative cumulative curve of core plug porosity

The reason for the values for showing different porosity intervals is that, there exists two types of porosity in the formation. As we look at the raw coreplug data, it is clear that some porosity values refer to high permeability values, and some other porosity values refer to another group of permeability. Since permeability is one of the most important driving factors for production, porosity is somehow related to production, so the separation between porosity values contribute to production in the formation. This will be reinforced with other studies following this chapter.

### 5.3.2. Core Plug Permeability Analysis

The ability of the formation to conduct fluids is known as *permeability*. The measurement of *permeability* is a measure of the fluid conductivity of the particular material (Amyx, et.al,1960).

Darcy's equation is used to define fluid flow in porous media.

$$k = \frac{Q}{A} \cdot \frac{\mu \cdot L}{\Delta P} \quad (5.13)$$

where, Q is the flow rate in (cc/sec), A is the cross-sectional area in (cm<sup>2</sup>), L is the length (cm), ΔP pressure difference in (atm), and μ is viscosity of the fluid in (cp).

Permeability measurements must be held in care in order to obtain exact results that represent the reservoir. Permeability can be determined by means of liquid permeability tests or gas permeability tests. In each case, the determined permeability is called as *liquid permeability* and *air permeability* (if air is used). When gas is used as measuring fluid, gas slippage may occur and corrections must be done. When liquid is being used, the fluid should not react with the solids in the core sample. As gas is used, gas slippage occurs known as Klinkenberg effect. As an example of reaction that occurs between liquids and solids can be given as clay swelling in the presence of water.

It must also be kept in mind that, when the core is taken out from the reservoir, all of the confining pressures which attributes to overburden pressures are removed. Compaction of the core due to overburden pressure may cause as much as a 60 percent reduction in the permeability of various formations (Amyx, et.al, 1960).

For Y field, air and liquid permeability values are available.

The basic statistical parameters of the core plug permeabilites are given in Table 5.13, and 5.14.

Table 5. 13 Summary statistics of air permeability

Sample Size	Mean	Median	Variance	Standard Deviation	Minimum	Maximum
58	69.13	7.68	13372.9	115.64	0.01	595.56

Table 5. 14 Summary statistics of liquid permeability

Sample Size	Mean	Median	Variance	Standard Deviation	Minimum	Maximum
58	63	6	11669.2	108.02	0.01	565.56

The frequency histogram for core plug permeabilites are given in Figure 5.29, and Figure 5.30.

The relative curve of coreplug porosity is shown in Figure 5.31, and Figure 5.32.

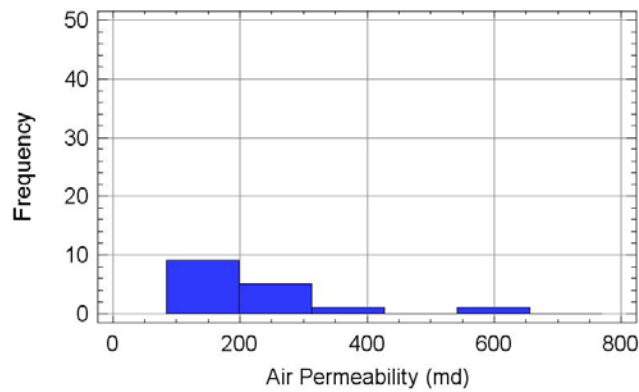


Figure 5. 29 Frequency histogram of coreplug air permeability

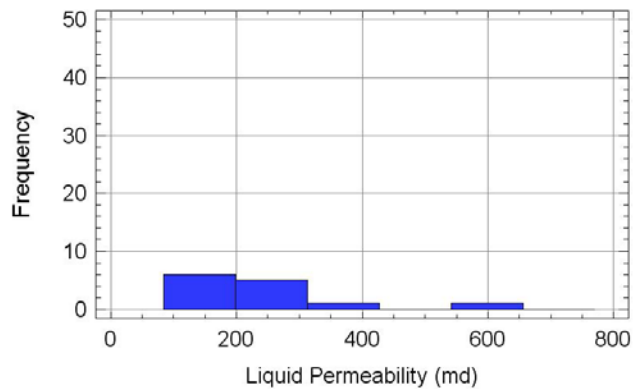


Figure 5. 30 Frequency histogram of coreplug liquid permeability

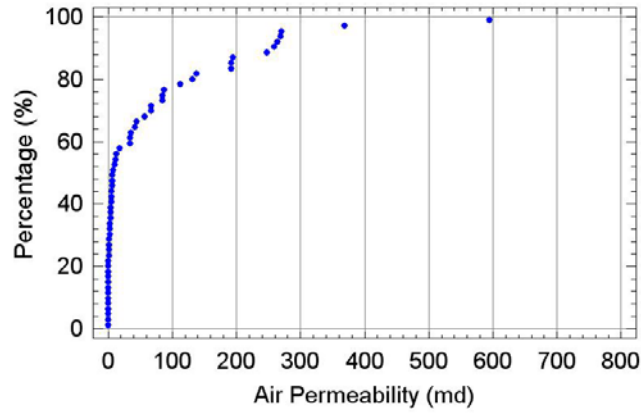


Figure 5. 31 Relative cumulative curve of coreplug air permeability

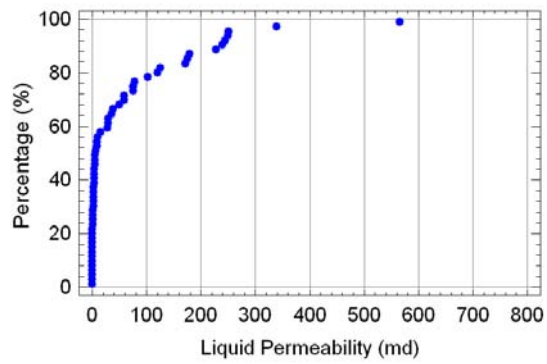


Figure 5. 32 Relative cumulative curve of coreplug liquid permeability

The measured gas permeability values must be corrected to measured liquid permeability values. Figure 5.33 shows the relation between these values. There exists a relatively strong relationship between air and liquid permeabilities. In the calculations where permeability data is needed, air permeability values are utilized in this study.

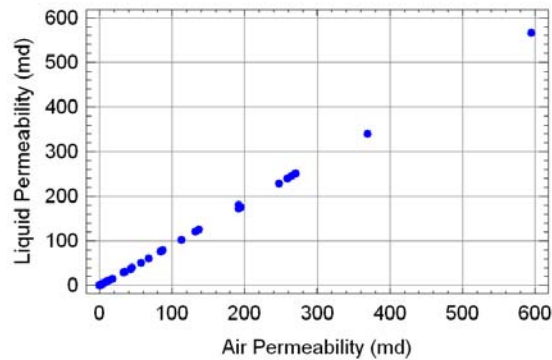


Figure 5.33 Relationship between measured air and liquid permeabilities

The most of the air permeability measurements relatively low, because there are also very high permeability values with high porosity values. The extremely low values of permeability come from *Well B* as seen from the core plug data on Appendix B. This values refer to the low porosity-low permeability part of the limestones. The low values of permeability also count for the limestone samples, these values are generally lower than the dolomites. As it was observed in the porosity derivations from well log analysis, for limestones, low porosity values were detected.

The low values may be resulted from the matrix permeability of dolomites. The matrix permeability may not contribute a lot to production. The dolomites of the *Derdere* formation may have different petrographical features. The reservoir part of the dolomites are dolosparites; which are common dolomites. The other type of dolomites may have poorer pore spaces and poorer porosity values that decrease the reservoir quality. The bimodal porosity distribution and related permeability may be because of these features. Besides, the more permeable parts may come from fractured parts of dolomites, resulting in higher permeability. The presence of limestones in the formation also lower the porosity and permeability. The low values attribute to the tight limestone sections in the formation.

### 5.3.3. Core Plug Grain Density Analysis

The raw data for the grain density results are given in Appendix B.

The summary statistics table for grain density measurements is given in Table 5.15.

The frequency histogram for grain density values is shown in Figure 5.34.

The distribution curve for grain density measurements is seen in Figure 5.35.

Table 5. 15 Summary statistics of grain density

Sample Size	Mean	Median	Variance	Standard Deviation	Minimum	Maximum
58	2.78	2.81	0.0044	0.066	2.42	2.85

Since the lithologies in the formation are limestone and dolomite, the data set should cluster around 2.71 g/cc and 2.87 g/cc respectively. The data set is grouping between 2.65 - 2.9 g/cc. For limestone measurements, the data set fits to the 2.71 g/cc., but for dolomites, there are some lower values.

There only exists one value for limestone that is 2.8 g/cc, which can be due to some components in the sample that have different mineralogies. The values which are close to dolomite density have good reservoir qualities as these values also have moderate-high porosity and permeability measurements. The low values are not as permeable and porous as the higher ones.

The cumulative curve of the grain density data indicates that nearly 10% of the values are smaller than 2.7 g/cc.

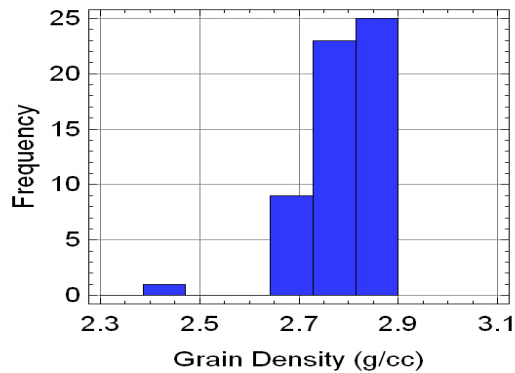


Figure 5. 34 Frequency histogram of grain density

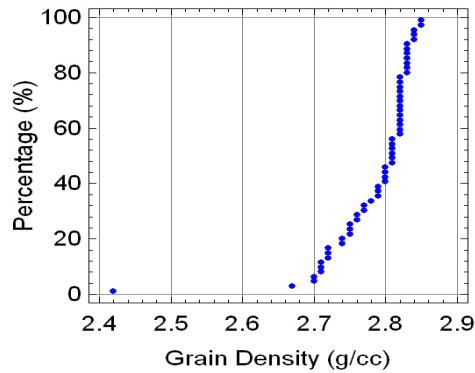


Figure 5. 35 Relative cumulative curve of grain density

#### 5.4. Geostatistical Methods

Mathematical methods have been employed by the earth sciences since the earliest times. Since the observations in earth sciences are based on visual investigations, and the lack of data sampling is a great problem, it is a very straight-forward way to establish models on geostatistics.

Engineering relies on mathematical expressions to understand and solve problems. The more these expressions relate to fluid flow, to the physics, and to the geology of the rocks, the better the ability to describe real flow characteristics and permeability predictions ( Haro C., 2004)

In this study, the flow units are determined by the help of several frequency plots and cross plots. Permeability predictions can only be achieved by using geostatistics. In either case, there is a gap between correlations and prediction, since the data sets are exhaustive. The derived correlations and equations should describe the problem, be simple and practical and this can be achieved by use of geostatistic methods

##### 5.4.1. Linear Regression

In various engineering problems, the values of two (or more) random variables taken in an observation are not statistically independent of each other, thus there is a relation between them. The existence of such a relation shows either that one variable is effected by the other or that both variables are effected by other variables.

However, these relations are not of a deterministic (functional) character, but still the determination of the existence and the form of a non-functional relations between the variables has a great importance in practice, because by using the derived relationship, it is possible to estimate a future value of a variable depending on known value(s) of another.

The mathematical expression showing a relation of the mentioned type is called the *regression*. The aim of the regression analysis is to check whether there is a significant relation between the variables under consideration, and if there is one, then to obtain the *regression equation* expressing this relation and to evaluate the confidence interval of the estimates by using this equation.

Linear regression is mostly used to analyse any bivariate data set. A regression line represented by the regression equation is obtained that shows the statistical relation between the selected variables. A correlation coefficient is also obtained in order to see how the variables are correlated.

In reservoir studies, especially, in characterization, regression is the most useful analysis, because most of the petrophysical parameters derived from well logs and cores are generally tend to be correlated within each other, which help researchers to make future estimates.

A regression analysis was performed among the parameters derived from logs within the studied wells. As many parameters were tried to be included for future permeability estimations.

#### **5.4.2. Multiple Regression Analysis (MRA)**

Multiple regression is used to account for (predict) the variance in an interval dependent, based on linear combinations of interval or independent variables. MRA can establish that a set of independent variables explains a portion of the variance in a dependent variable at a significant level, and can establish relative predictive importance of the independent variables. One can test the significance of difference of two  $R^2$ 's to determine if adding and extracting an independent variable to the model helps significantly.

The multiple regression equation takes the form of ;

$$y = b_1x_1 + b_2x_2 + \dots + b_nx_n + c \quad (5.14)$$

where,  $b$ 's are the regression coefficients, representing the amount the dependent variable  $y$  changes when the independent changes 1 unit. The  $c$  is the constant, where the regression line intercepts the  $y$  axis, representing the amount the dependent  $y$  will be when all the independent variables are 0.  $R^2$ , is called the *multiple correlation* or the *coefficient of multiple determination*, which is the percent of variance in the dependent explained uniquely or jointly by the independents.

Generally, the derived transforms of porosity and permeability can be sufficient, but permeability is a parameter which is affected by many variables. In this study, the data set

obtained from core plug data and logs are put in MRA method to obtain an reasonable model.

In the following geostatistical studies, *stepwise multiple regression method* (also called statistical regression) will be used.

This method is a way of computing ordinary least squares regression in stages. The variables are extracted and included in the model.

## CHAPTER 6

### RESULTS AND DISCUSSION

In previous chapter, general information on the studied field and the available data were described with the procedure of the required methods and applications. Basic background of the study was introduced.

In this chapter, the results obtained by means of described methods will be explained individually, but an effective reservoir characterization and hydraulic flow unit zonation require a combination of many methods and applications. Thus, the results will be gained together for a better explanation of the field and the final discussions of the objectives will be held.

The study requires mainly two categories; the well logging data interpretation, and the core plug data analysis. As mentioned before, all the necessary methods were tried on both available data.

#### 6.1. Well Log Interpretation

There exists 5 wells in the field, and each well were studied individually by the common interpretation methods.

##### 6.1.1. Lithology and Porosity Interpretation

Lithology discriminations are done based on porosity logs. As mentioned previously, necessary shale volume calculations were done based on the density-neutron crossplot for Well D, and the yielding results concluded that the lithologies can be described as clean lithologies. The high shale content part of each well observed at the top of the limestones is the boundary for the Derdere Formation. A typical increase in GR content is also tracked in the very beginning sections of dolomites which is the dolomitic shale, which may again count for a seal.

Below this section of high shale content, dolomites show comparatively high neutron porosities and the resistivity logs indicate presence of hydrocarbons. These porous and permeable zones are also indicated by the formation of mud cake.

The calculations for porosity and especially the saturations (Appendix D.3, and D.4.) point out for reservoir sections.

The dolomites can be considered as clean lithology.

As seen in the lithology fractions, some parts of the dolomites contains limestones, but generally the dominant lithology is dolomite. The shale correction was applied as it was mentioned previously, and the formation was stated to be free from shale.

Porosity of the formations were determined by many methods, sonic porosity, neutron porosity, density porosity, and density-neutron porosity. In all wells, the most reliable porosity values are taken as density-neutron porosities, but only for Well X, since the unavailability of other logs, sonic recordings should be relied on. Generally, the porosity values for limestones give lower values than the dolomites. This may be because of so many reasons concerning the pore-sizes, grain-sorting, secondary porosity formations due to dolomitizations, which also affect the fluid flow in the formation. Porosity is the main effect for such delineations in fluid flow, because it obviously effects the permeability. For having lower porosity values, and also permeability values as determined from the core data, these limestones have poorer characteristics than the dolomites as being the reservoir rock.

The porosity comparison table is shown in Table 6.1.

As seen in the table, except for the Well D, porosity values for limestones in all cases are lower than dolomites.

The maximum porosity for dolomites is observed in Well D, with an average porosity of 20.9 %, and 14.13 % for limestones in Well D. Generally the porosity range for dolomites is 11-24 %.

Table 6. 1 Porosity Comparisons

Well	Lithology	$\emptyset_s$	$\emptyset_D$	$\emptyset_N$	$\emptyset_{D-N}$	Thickness (m)
<b>A</b>	<b>Lst</b>	8.52	8.20	11.90	8.36	22.00
	<b>Dlt</b>	12.68	13.98	18.08	14.15	16.00
<b>B</b>	<b>Lst</b>	8.08	10.72	11.76	10.86	25.00
	<b>Dlt</b>	11.21	18.75	23.75	19.21	12.00
<b>C</b>	<b>Lst</b>	7.77	7.67	6.85	7.45	23.00
	<b>Dlt</b>	11.99	15.63	17.77	15.28	13.00
<b>D</b>	<b>Lst</b>	14.16	13.55	15.80	13.01	25.00
	<b>Dlt</b>	17.05	21.66	24.91	20.27	28.00
<b>X</b>	<b>Lst</b>	9.05	n.a.(* )	n.a.	n.a.	28.00
	<b>Dlt</b>	15.59	n.a.	n.a.	n.a.	13.00

n.a. (\* ) not available

Generally, the sonic porosity gives low values as seen in above table. The second log which is used for porosity is the density log. The density porosities are relatively higher compared to the sonic porosities, because; the density log exactly defines the lithology and its matrix properties.

In both of the plots, the data points are widely scattered showing no obvious relations and correlations, but in the following parts, the change of porosities within depth will be discussed in the statistical method applications.

The porosity values greater than 15% generally counts for the dolomites, and the values grouped around 25% and higher are the representatives of the reservoir section of the dolomites. There exists few values for limestones that reach 20% of porosity.

In order to see the change in porosity, generally, obtained porosity values are plotted against depth, and also many variables derived from logs. Generally, with increasing depth, the porosity values lower due to the overburden pressure of the overlying formations. The change in well-log derived porosities within depth for each well are given in the plots in Appendix D.3. Among all of these four derived porosities, density-neutron porosities are considered to be most efficient and reliable values.

At this point, it necessary to show a log-set of density and neutron recordings in order to see the lithology discriminations. The recorded values for porosity logs are shown in Figure 6.1., as plotted by means of Log Evaluation System Analysis (LESA) Version 4.2. The lithologies are easily observed within the locations of density and neutron log tracks. The yellow filled parts are the sections where the recordings are affected by the borehole enlargements. The density-neutron crossplots as determined by LESA are also shown in Figures 6.2, 6.3, 6.4., and 6.5. On these crossplots, the values that are above the pure limestone line are the values that correspond to those yellow filled parts in the log set. These recordings are affected by the borehole.

In the crossplots, besides the separation of lithologies, some distinctions are seen. If we chose Well D as a type well for this study (since it has a full log set, which may be a good representative of the formation), there exists 4 different clusters, one around the limestones, others are among the dolomites. The clustering of limestone values are also scattered among themselves, because they contain mudstone, wackestone with fossils, grainstones, and packstones as described by previous researchers (Tandircioğlu, A., 2002). Some data points for the limestones fall between low neutron porosity and high bulk density regions. These data points may group one unit, indicating tight limestones. The other data points for the limestones seem to have better reservoir characteristics. A group of dolomites cluster around high porosity-high dolomite content region, whereas there exists another groups within comparable low porosity and limy dolomite section.

The dolomitization in the Derdere formation may preclude the identification of these clusters, and the dolomitization process is the main reason for reservoir development.

Density recordings and neutron porosity from well logs are also plotted against each other. As it was mentioned previously, there are very low values due to borehole instabilities. Most of the low values are represented by high porosity, but as seen in the core data, permeability is low pointing out for a isolated pore system. Vuggy-moldic type of porosity may be the reason for this trend. Limestones should be separately studied for the following petrophysical analysis due to their facies characteristics. Therefore, they form a one flow unit.

The plot of density and neutron readings is shown in Figure 6.6.

For dolomites, as it was calculated in the lithology fractions, the calcite amount is reducing the density recordings.

### **6.1.2. Resistivity and Saturation Interpretations**

In well log interpretation techniques, resistivity logs are the main materials for the study. Since the aim is to detect hydrocarbons, the final conclusions are generally based on these logs. Several methods were proposed in literature for study of resistivity logs. The main aim is to determine saturations of the fluid content in the formation.

There are some correlations for estimation of permeability, utilizing resistivity values, but care must be taken in their usage, because saturations should be relied on. The effect of irreducible water saturation ( $S_{wi}$ ) is the challenging part of such methods.  $S_{wi}$  can be derived from logs of Magnetic Resonance (MR), by a method called free fluid index (FFI), but the values determined from the cores are more certain. For a starting point of the resistivity analysis,  $R_t$  and  $R_{xo}$  values as obtained from R-LLD and MSFL logs are plotted against each other. The resulting plot is given in Figure 6.7.

Such a plot is useful tool for better understanding of pore types and fractures in the formation. Limestones are generally characterized by the low  $R_t$  and high  $R_{xo}$  values, indicating that the pores are compacted and tight.

There are also some values for high  $R_t$  - low  $R_{xo}$  for limestones. This is the indicator for fractures.

For dolomites, again the data is scattered and clustered around some values. The near values of  $R_t$  and  $R_{xo}$  indicate the impermeable zones. The reservoir section is represented by high  $R_t$  values of 500- 1000  $\Omega$ .m.

$R_t$  can also be plotted against  $\emptyset_{D-N}$  values which may result in clustering of different rock type/electrofacies. The resulting plot is given in Figure 6.8.

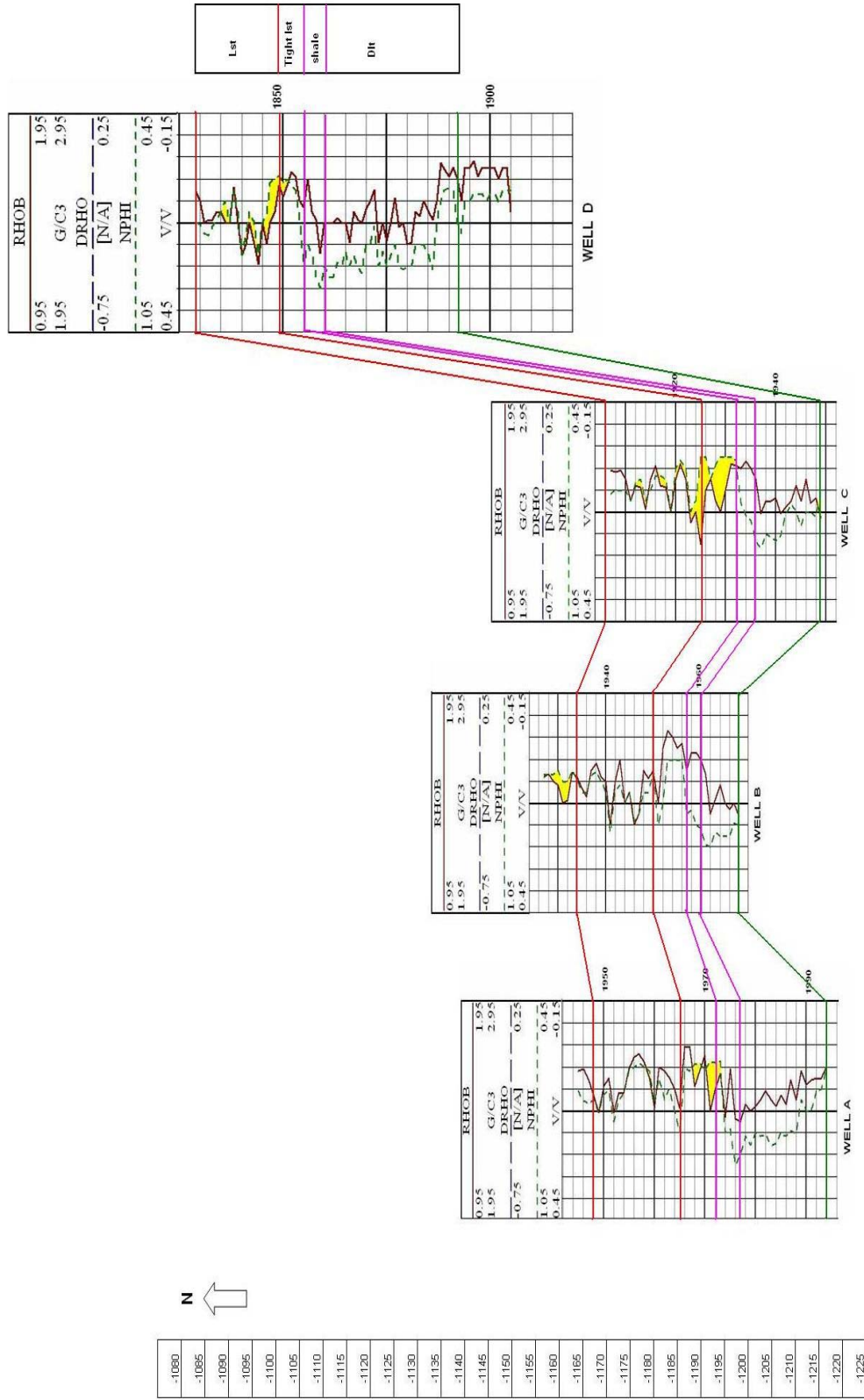


Figure 6. 1 Density & Neutron Logs Correlations

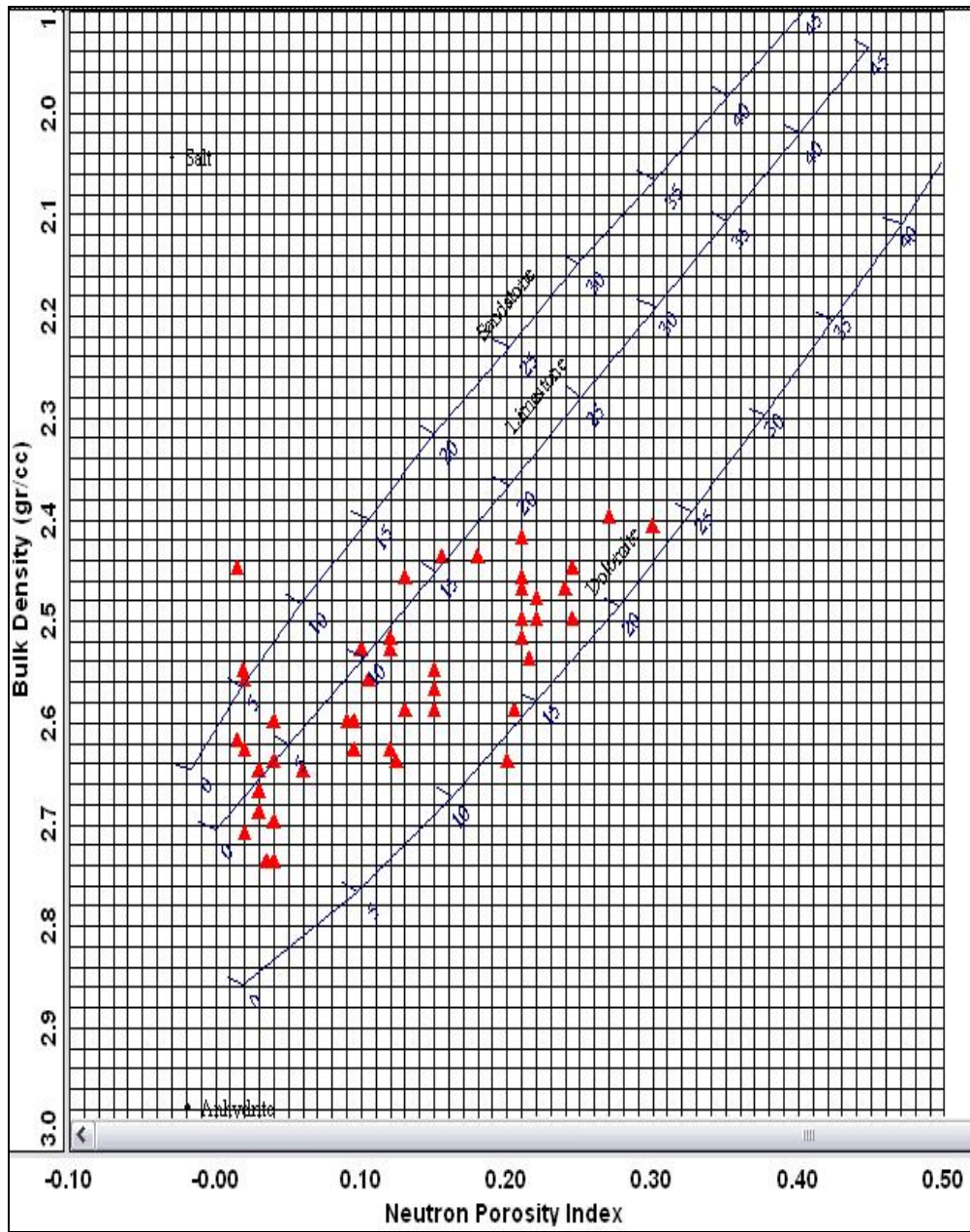


Figure 6. 2 Density-Neutron Crossplot - Well A

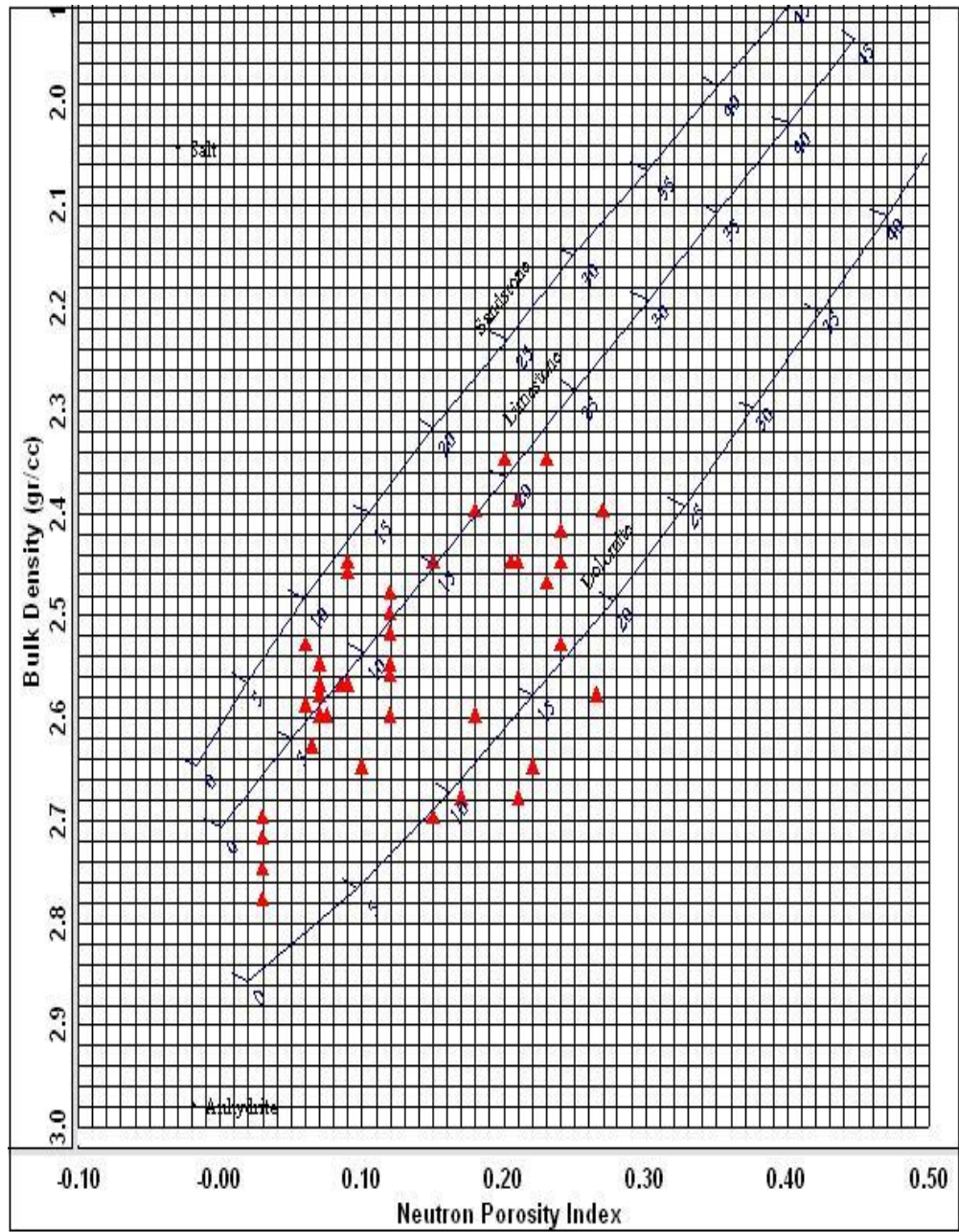


Figure 6. 3 Density-Neutron Crossplot - Well B

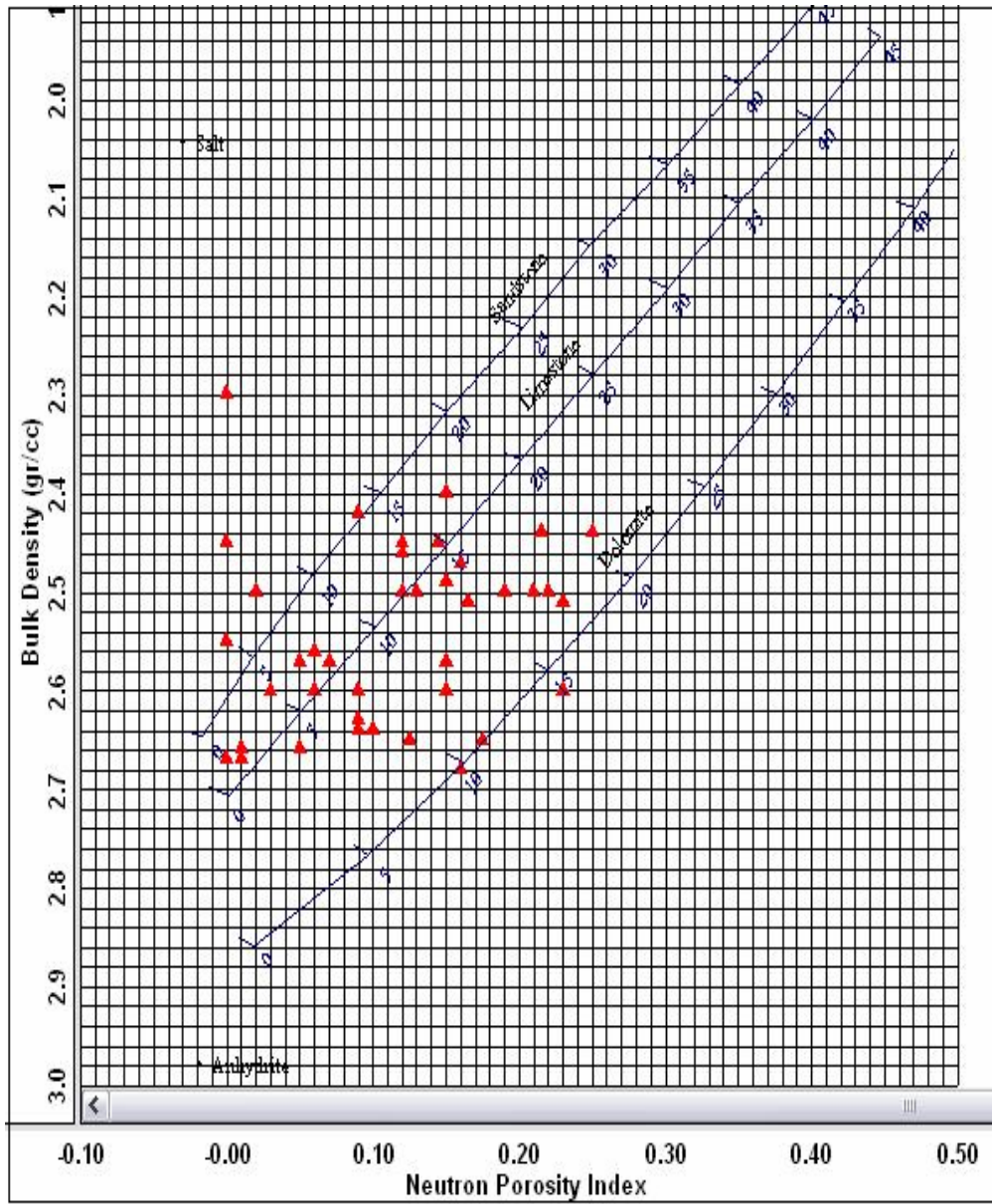


Figure 6. 4 Density-Neutron Crossplot - Well C

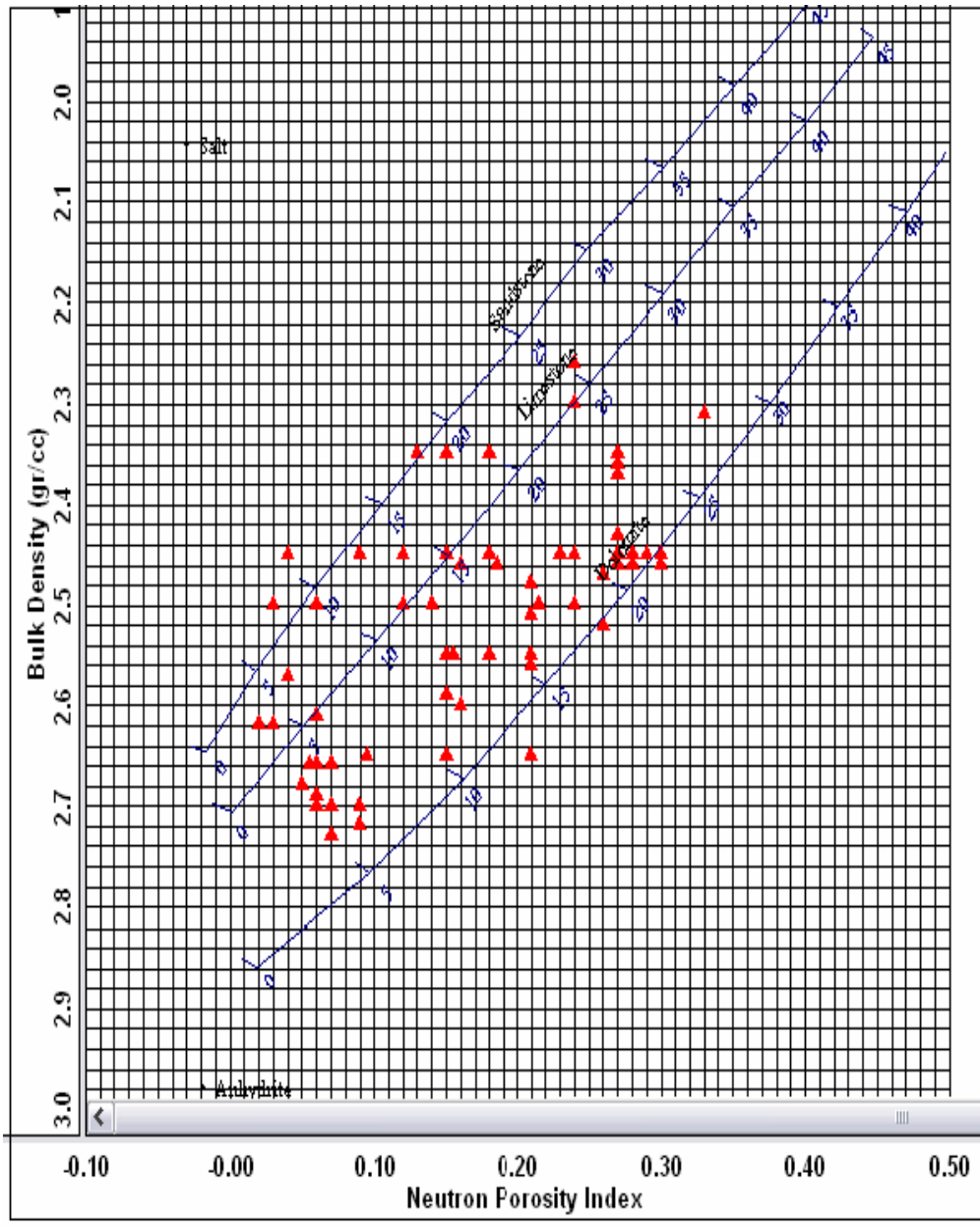


Figure 6. 5 Density-Neutron Crossplot - Well D

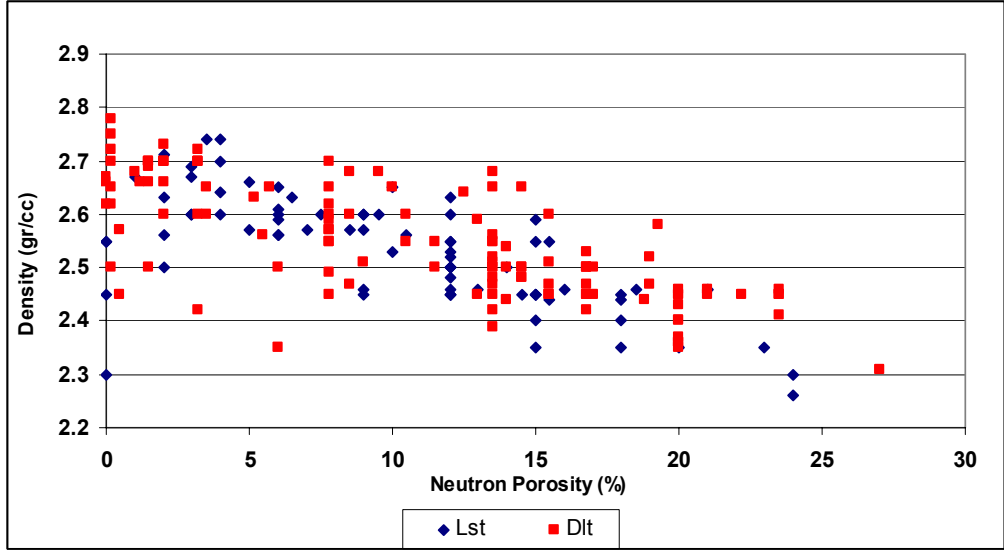


Figure 6. 6 Density and Neutron Porosity Recordings Plot

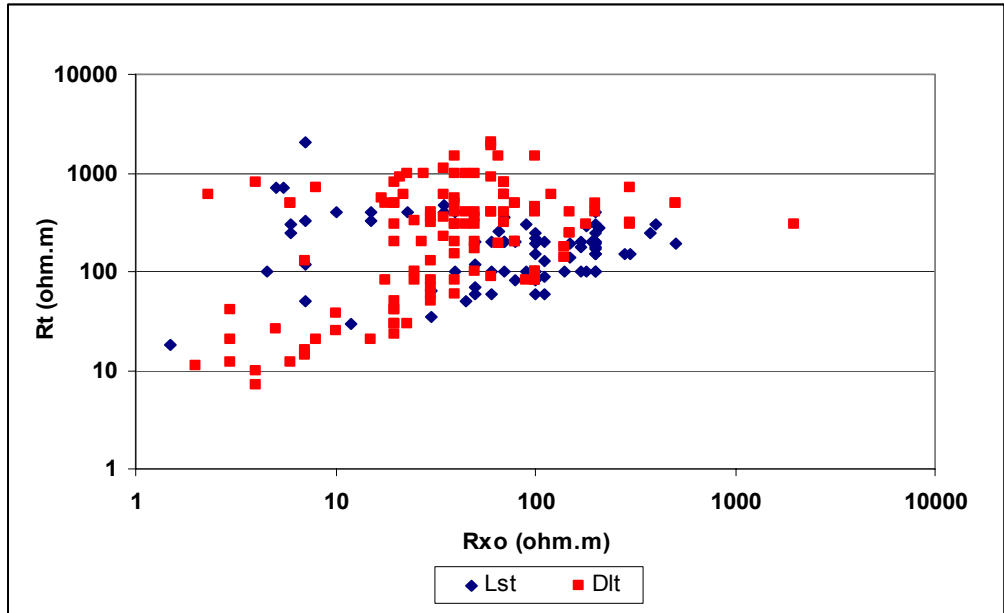


Figure 6. 7 Rt vs. Rxo plot

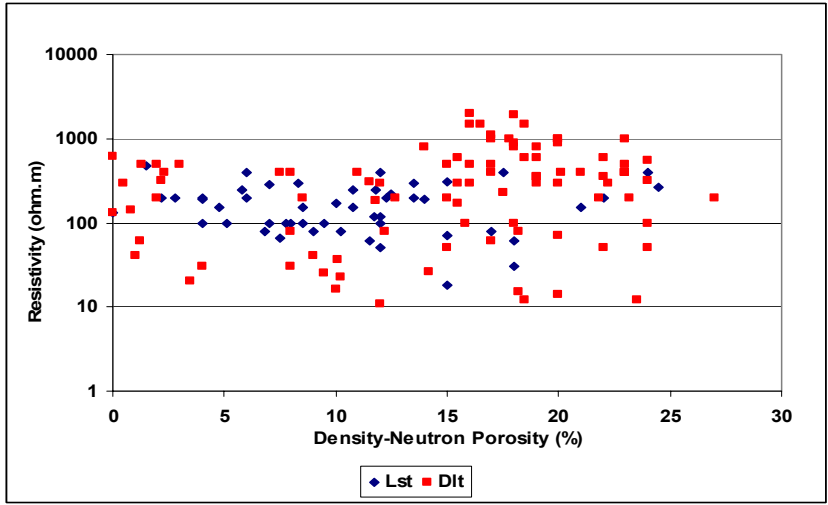


Figure 6. 8 Rt vs. Density-Neutron porosity

The low  $R_t$  – high  $\varnothing_{D-N}$  region can be related to sections with high  $S_w$ . The high  $R_t$  – high  $\varnothing_{D-N}$  region can be represented by oil saturations the other regions may count for impermeable zones.

The change in water saturation with depth in the formation should also be analysed.

The results are plotted as seen in Figures 6.9, 6.10, 6.11, and 6.12 for each well.

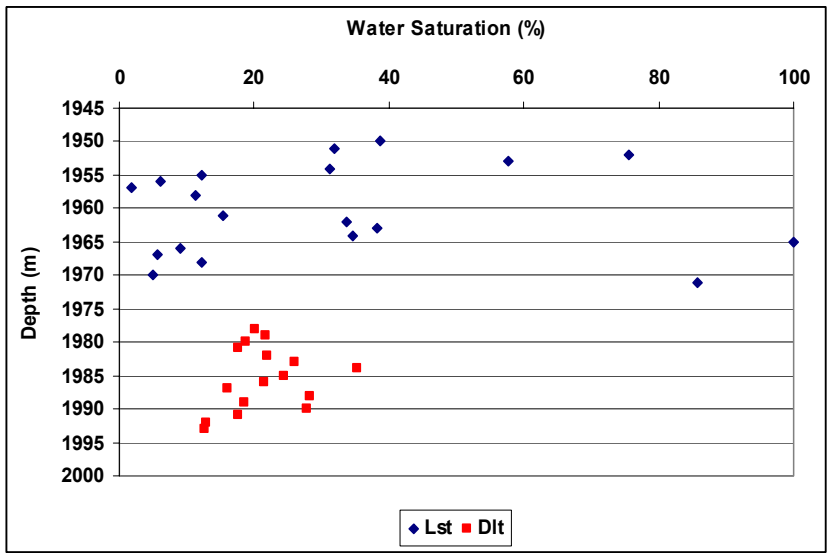


Figure 6. 9 Depth vs.  $S_w$  – Well A

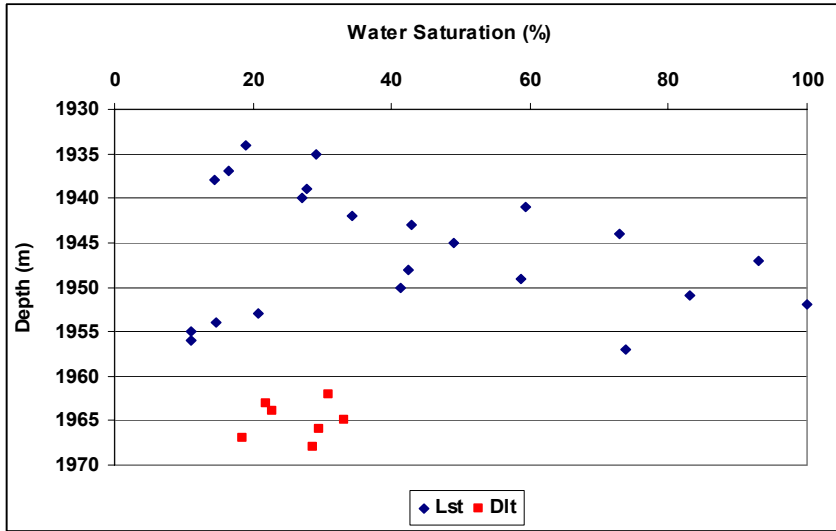


Figure 6. 10 Depth vs. Sw – Well B

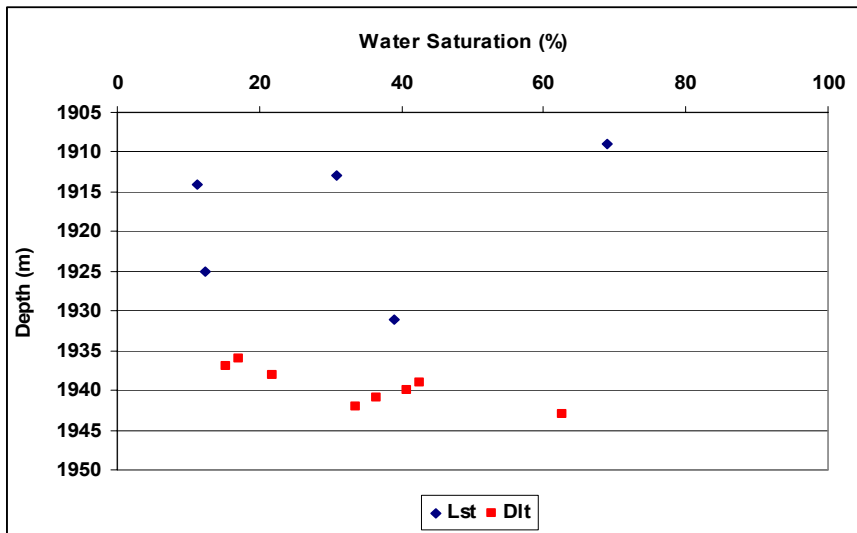


Figure 6. 11 Depth vs. Sw – Well C

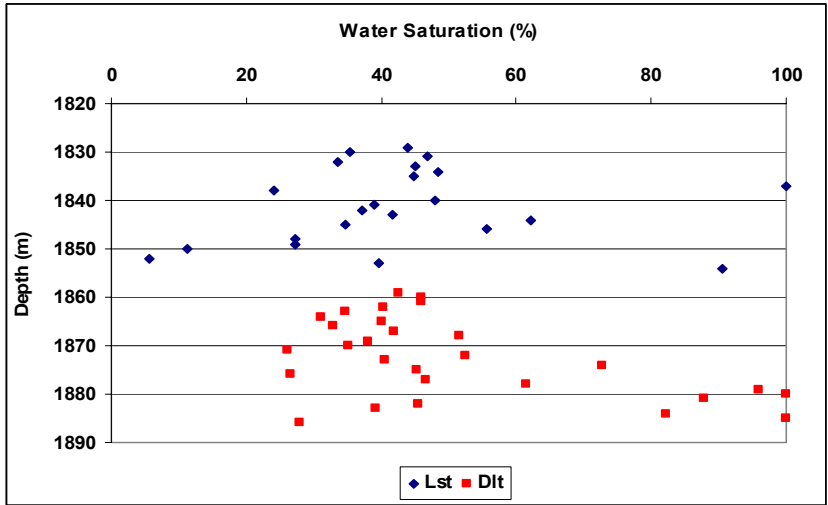


Figure 6. 12 Depth vs. Sw – Well D

$S_w$  can also be plotted against  $\emptyset_{D-N}$ . The plot is given in Figure 6.13.

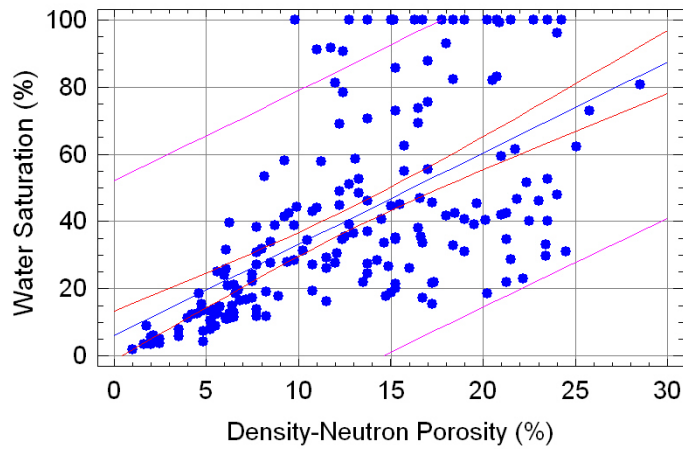


Figure 6. 13 Sw vs. Density-Neutron Porosity

The expected curve should be different than the one obtained, because due to irreducible water saturation, as porosity decreases, water saturation should increase.

But Figure 6.13 is for the whole data set and the scattering of data is reasonable because of flow unit zonations and the existence of 100% water saturation due to bound water in dolomitic shale intervals.

With the help of  $S_w$  calculations, the saturation profile of the formation can be described easily.

Another way of representing the  $S_w$  profile is done by  $R_o$  and  $R_t$  analysis. The obtained  $R_o$  values can be plotted with  $R_t$  values. The intersection points of these curves are the sections bearing 100% water. The sections where  $R_t > R_o$  can be oil bearing zones.

An example correlation between Well A and Well B for  $R_o$ - $R_t$  method is shown in Figure 6.14. The intersections of  $R_t$  and  $R_o$  are the intervals with dolomitic shales.

Another concept related to resistivity analysis is MOS and ROS. The terms are very important for oil production.

For Derdere Formation, MOS and ROS values were also calculated and given in Appendix D.5.

For MOS and ROS analysis, Well A can be chosen.

For the limestone section,  $S_w$  values are generally high but there are some values which are comparatively low, that we may expect oil saturations.

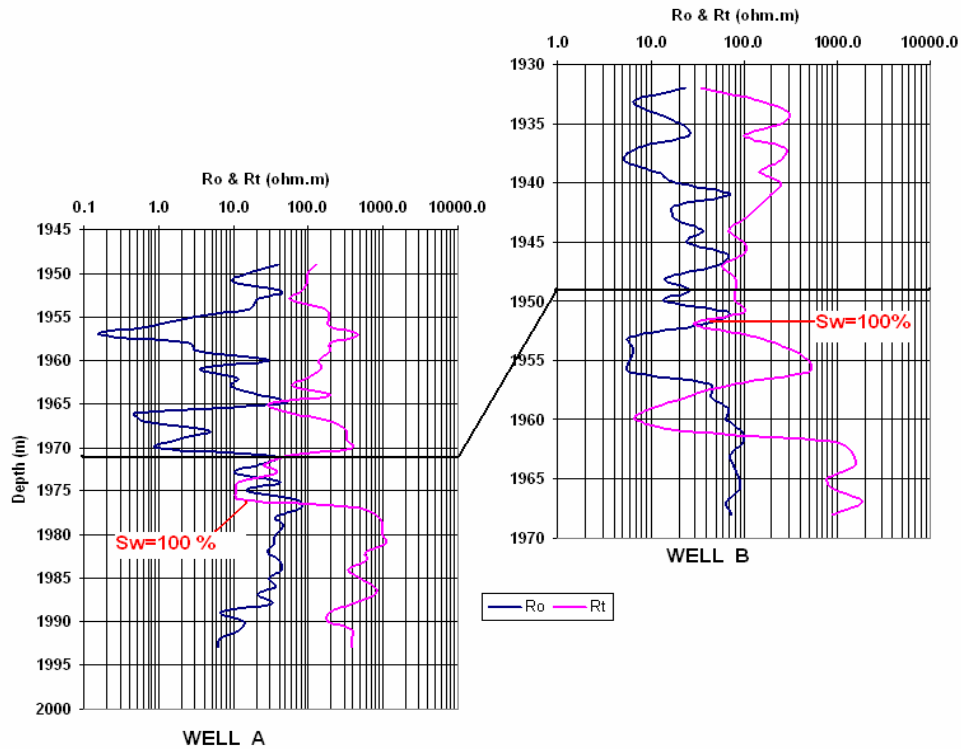


Figure 6. 14  $R_o$ - $R_t$  curves for 100 %  $S_w$

But, if we look at MOS values, the range is about 5 %-20 %, which means that, the oil is not movable, so there exists a ROS of 80 %-90%. But for dolomites, the case changes. For the low  $S_w$  values, MOS increases dramatically and ROS decreases as well. This trend is seen in the middle of dolomites, where the producing reservoir is present. The top and bottom sections are generally represented by low MOS. The derived ROS and MOS values are given in Appendix D.4.

## 6.2. Core Plug Data Interpretation

A basic geologic framework of the formation was described by log interpretation. A more detailed and a consistent geologic framework is succeeded by core data analysis, since a main idea about the petrophysics of the formation can be derived.

### 6.2.1. Porosity-Permeability Relations

As for every petrophysical study, the main driving starting point is to construct a relationship between core plug porosity and permeability.

In literature, most of the researchers agreed on that the most successful models can be characterized by a linear relationship between log permeability and porosity coordinate system, with the following equation;

$$\log(k) = a \log \phi + b \quad (6.1)$$

where  $a$  and  $b$  are the calibration parameters.

This equation works properly for the sandstone reservoirs, but there is a big problem for carbonate reservoirs. The equation fails with increasing heterogeneity and non-uniformity that characterize the carbonate rocks (Altunbay, et.al., 1997).

The core plug porosity measurements are plotted against logarithm of core plug air permeability. The plot is given in Figure. 6.15.

A linear regression analysis was run between the two data. The results are given in Table 6.2.

The resulting regression equation is given as;

$$\log_{10}(k_a) = -1.81 + 0.15\phi_{core} \quad (6.2)$$

The  $R^2$  is obtained as a high value (81.73 %), meaning that there exists a good correlation between the measured permeabilities and porosities of the core data set. This is a good theory for the derived regression equations in the following sections.

An increase in porosity is followed by an increase of permeability in some regions, but the amount of increase in porosity is not directly proportional to permeability, due to isolated pores which do not contribute to permeability.

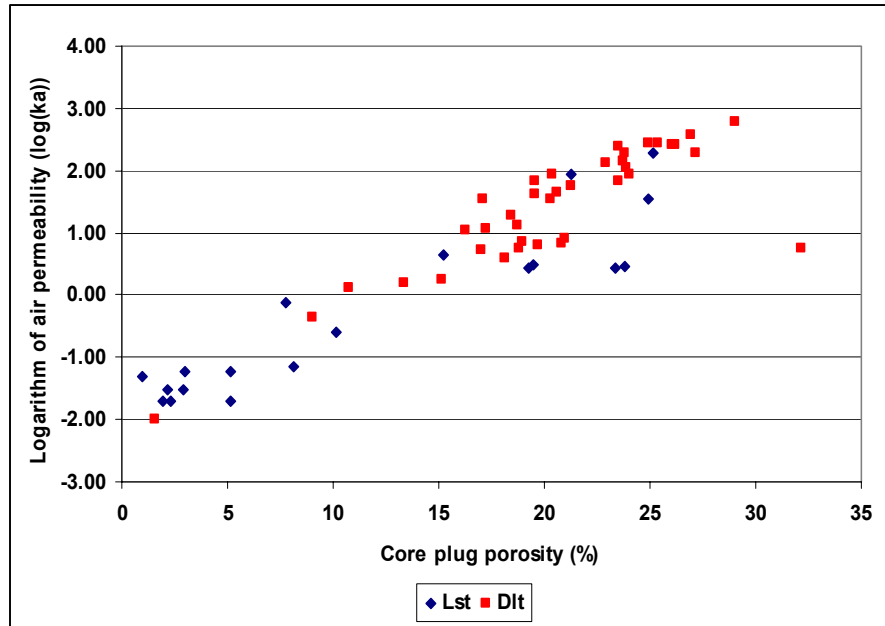


Figure 6. 15 Core plug porosity vs. logarithm of air permeability for all data set

Table 6. 2 Linear regression results for core plug porosity and logarithm of air permeability-whole data set

Intercept	Slope	F-ratio	r	R <sup>2</sup> (%)
-1.81	0.15	250.64	0.90	81.73

The distinctive units are also seen in the plot. Limestones differ in another trend and the dolomites have two zones of clustering. There are some over-estimated or under-estimated values but these are very few and can be negligible. The distinctive unit analysis will be mentioned in the following parts.

### 6.2.2. Rock-Fabric Classification

The goal of reservoir characterization is to describe the spatial distribution of petrophysical parameters, such as porosity, permeability, and saturation. Studies that relate rock-fabric to pore-size distribution, and thus to petrophysical properties, are key to quantification of geologic models (Lucia, F.J. 1999).

Geologic models are mainly based on visual observations if available. In the subsurface, well logs, and seismic data are the main sources of reinforcing these observations. The petrophysically-based study is constructed on wireline logs and core analyses.

This part will try to define some important geologic parameters that will lead to petrophysical properties of the Derdere Formation. A relationship between carbonate rock fabrics and petrophysical properties are introduced.

In 1952, Archie made the first attempt to relate rock-fabrics to petrophysical rock properties in carbonate rocks. Pore space is divided into matrix and visible porosity. Visible pore space is described according to pore spaces. A for no visible pore space and B,C, D for increasing pore sizes from pinpoint to larger than cutting size. Porosity / permeability trends are related to these textures.

Archie's method is difficult to relate with geologic models because the descriptions can not be defined in depositional and diagenetic terms.

Lucia F.J. (1983), presented a petrophysical classification of carbonate porosity. He showed that the most useful division of pore types are between pore space located between grains or crystals, called *interparticle porosity*, and all other pore space, called *vuggy porosity*.

The comparison between the two classifications is shown in Figure 6.16.

The foundation of the classification is the concept that pore-size distribution controls permeability and saturation, and that pore-size distribution is related to rock-fabric. In order to relate carbonate carbonate rock fabrics to pore size distribution, it is important to determine if the pore space belongs one of the major pore-type classes, interparticle, separate vug, or touching-vug. The most efficient and easy way to understand this is to conduct capillary pressure test with mercury injection.

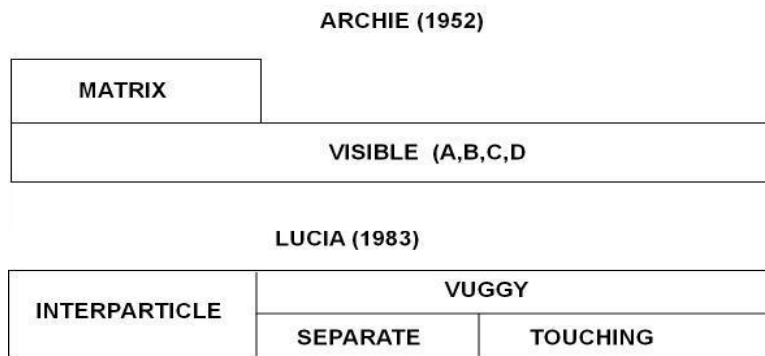


Figure 6. 16 Comparison between Archie & Lucia classifications

For the data samples of cores, no capillary pressure test is available, therefore, a pore-size distribution profile can not be constructed. But, Lucia stated that, pore-size distribution in carbonates can be described in terms of particle size, sorting, and interparticle porosity. He suggested three permeability fields that can be defined by using particle size boundaries of 100  $\mu\text{m}$  and 20  $\mu\text{m}$ , and the relation is limited by 500  $\mu\text{m}$ . He combined data from limestones and dolomites in one porosity-permeability cross plot, defining 3 classes of, Class 1, Class 2, and Class 3.

Class 1 ; (>100  $\mu\text{m}$  permeability field )

- (1) limestones and dolomitized grainstones
- (2) large crystalline grain-dominated dolopackstones and mud-dominated dolostones

Class 2; (100 – 20  $\mu\text{m}$  permeability field)

- (1) grain-dominated packstones
- (2) fine-to medium crystalline grain-dominated dolopackstones
- (3) medium crystalline mud-dominated dolostones

Class 3; (<20  $\mu\text{m}$  permeability field )

- (1) mud-dominated fabrics

The available core plug porosity and permeability data were tried to be put in one of the classes. The cross plot is given in Figure 6.17. The lines represent permeability fields.

Most of the points are between the 20-100  $\mu\text{m}$  field, which is the Class 2. This states that the the carbonates of the formation is mainly fine to medium grain-dominated. There exist distinctions in limestones. One group is clustered at the left-hand side bottom of the plot. The data scattered here comes from Well B, where the porosity and permeability values are very low. These low values are also reinforced by the log responses. This section of the limestones are the *tight limestones* showing very coarse reservoir characteristics. The distinctions in dolomites are also visible in this plot, but mainly the data for dolomites is clustered for high porosity and permeability values indicating a good reservoir section.

Due to differences in the dolomite particle size, sorting and crystal size, there are 4 different clustering within the Class 2.

This is because the region is represented by both grain-dominated dolopackstones and mud-dominated dolostones. The low porosity and permeability values may result from the presence of mud as matrix.

Lucia also derived permeability equations for each class.

Class 1 ;

$$k = (45.35 \times 10^8) \times \phi_{ip}^{8.537} \quad (r=0.71) \quad (6.3)$$

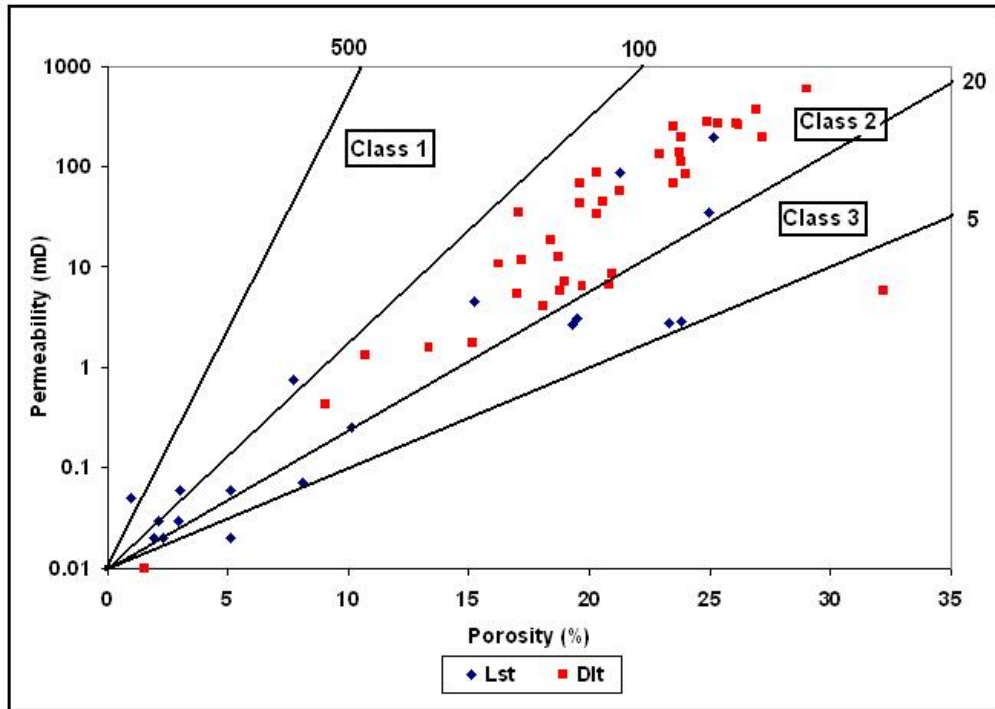


Figure 6. 17 Porosity-permeability cross plot of Lucia classification

Class 2;

$$k = (1.595 \times 10^5) \times \phi_{ip}^{5.184} \quad (r= 0.80) \quad (6.4)$$

(or recommended Class 2 equation)

$$k = (2.040 \times 10^6) \times \phi_{ip}^{6.38} \quad (6.5)$$

Class 3;

$$k = (2.884 \times 10^3) \times \phi_{ip}^{4.275} \quad (r=0.81) \quad (6.6)$$

where  $\phi_{ip}$  is the interparticle porosity in (%)

### 6.2.3. Reservoir Quality

A quality of reservoir is controlled by hydrocarbon storage and flow capacity. These help to define intervals of similar and predictable flow characteristics, which are the flow units. The hydrocarbon storage is a function of porosity, and flow capacity is a function of permeability. Flow units can be identified from an interrelated series of petrophysical crossplots and from the calculation of pore-throat radii ( $R_{35}$ , pore-size) at the 35 % pore volume using Winland Equation.

The Winland Equation is;

$$\log R_{35} = 0.732 + 0.88 \log k_a - 0.864 \log \phi \quad (6.7)$$

where,  $R_{35}$  is in microns,  $k_a$  is the air permeability in mD, and  $\phi$  is the porosity in percent. Another way of determining the reservoir quality is to analyze  $k/\phi$  ratio which is called the *reservoir process speed*. When carbonates are deposited, they tend to have a correlation of particle size to parameters related to porosity and permeability (Hartmann, D.J., 1999).  $R_{35}$  and  $k/\phi$  are a function of porosity and permeability and can be correlated with pore type and reservoir quality.

The  $R_{35}$  of a given rock type both reflects its depositional and diagenetic fabric and influences fluid flow and reservoir performance (Hartmann, D.J., 1980).  $R_{35}$  determines the effective pore type which dominates over the fluid flow in the rock. Estimating  $R_{35}$  from cores and logs using the Winland Equation, or directly from capillary pressure data (in this study, this data is not available), provides the basis for a zonation that can be used by geologists and reservoir engineers (Martin, A.J., et al, 1997). Therefore,  $R_{35}$  values within the Derdere formation can be used to determine reservoir quality and identify the flow units. But it must be kept in mind that, the calculated values are based on empirical data.

$R_{35}$  values are utilized to define petrophysical units as follows;

*Mega*port; units with  $R_{35}$  values greater than 10  $\mu$ .

*Macro*port; units with  $R_{35}$  values between 2 and 10  $\mu$ .

*Meso*port; units with  $R_{35}$  values between 0.5 and 2  $\mu$ .

*Micro*port; units with  $R_{35}$  values between 0.1 and 0.5  $\mu$ .

*Nano*port; units with  $R_{35}$  values smaller than 0.1  $\mu$ .

Winland  $R_{35}$  plot for the Derdere Formation is given in Figure 6.18.

Figure 6.18 is a very good crossplot for determining the possible flow units. The diagonal lines represent equal pore-throat sizes (pore-size). Points along the contours represent rocks with similar flow characteristics which are the flow units. Megaports, macroports, mesoports, and microports are present in the formation.

Limestones are represented by micro and mesoports. The dolomites have intense megaports which are related to good porosity and permeability measurements from cores. These megaports combination forms one flow unit, which is the reservoir unit.

Mesoport type is the second dominant type in dolomites. These are represented by lower values, and the data samples are clustered in two groups within the interval of mesoport ( 0.5– 2  $\mu$ ). These groups form distinctive units. The porosity-permeability cross plot for  $k/\phi$  (reservoir process speed) is given in Figure 6.19.

$R_{35}$  values are generally plotted with  $k/\phi$  to visualize the reservoir zonations. Higher reservoir quality zones, have higher  $k/\phi$  ratios. The calculated  $R_{35}$  and  $k/\phi$  values are given in Appendix E.

By looking at the both plots for  $R_{35}$  and  $k/\emptyset$ , we can conclude that, for the formation in question, reservoir quality is increasing with increasing pore-throat sizes. The proof is that, the dolomites with megaports and macroports count for the reservoir section, whereas the limestones with microports and nanoports are responsible for no flow units.

There is a general agreement that the  $R_{35}$  and  $k/\emptyset$  methods are powerful petrophysical techniques for characterizing the quality of a reservoir with interparticle (intergranular or intercrystalline) porosity as the principal pore type. For Derdere case, it was seen that the data points for reservoir sections are grouped in the grain-dominated dolostones, in which the porosity is interparticle. The  $R_{35}$  and  $k/\emptyset$  crossplots are the final results that show us there exists 4 types of units in the formation, two of them are in the limestones, the other two are in dolomites.

### 6.3. Flow Unit Determination & Permeability Prediction

The interpretations of the well log attributes and the summary statistics analyses including the histograms of the core plug data show that there exists separations in the Derdere Formation. In fact one of the separated unit is the limestones by themselves. Compared to dolomites, they show less porosity and permeability distributions which make them to be a worse reservoir rock in the formation. The limestone section is subdivided into two units. The first unit is the limestones with good porosities and the other unit is underlying the first one. This second part can be described as “*tight limestones*” because, in the log sections they can be detected with lower neutron porosities and higher bulk densities. For simplicity, the upper limestone unit that has flow characteristics with good porosity and permeability will be named as *L-1* and the tight limestone unit will be named as *L-2*. The cores taken from *L-2* come from Well A, Well B and Well X and they show very poor reservoir characteristics. Porosity range can be described as 0-8 %, and permeability range is 0-0.7 md), The porosities are very low and permeabilities are near 0, which means that “*no flow*” is expected within this unit. The cores for unit *L-1* come from Well A, and Well X.

Dolomites can be subdivided into two units, basically based on their porosity and permeability distributions.

The first unit is the reservoir section that has a porosity range of 17–30 % and permeability range of 34 – 595 md. The porosity values are higher and permeability values are much more than the other defined units of limestones. The second unit is just at the bottom of the reservoir section with lowering porosities and permeability range of 0-30 mD. For simplicity, the first unit will be named as *D-1*, the second one will be named as *D-2*.

The core plug analysis, pore-size study, and the  $k/\emptyset$  analysis showed that the data samples clustered around these different units and the defined units have unique properties within each other.

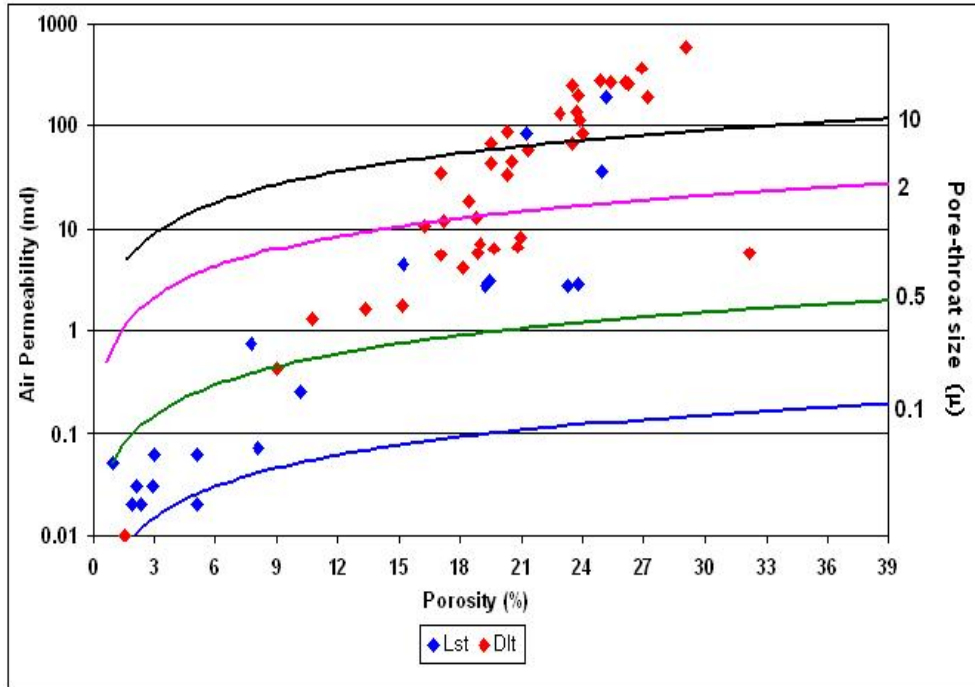


Figure 6. 18 Winland R35 Plot for Derdere Formation  
 ( The diagonal curves represent equal port-sizes)

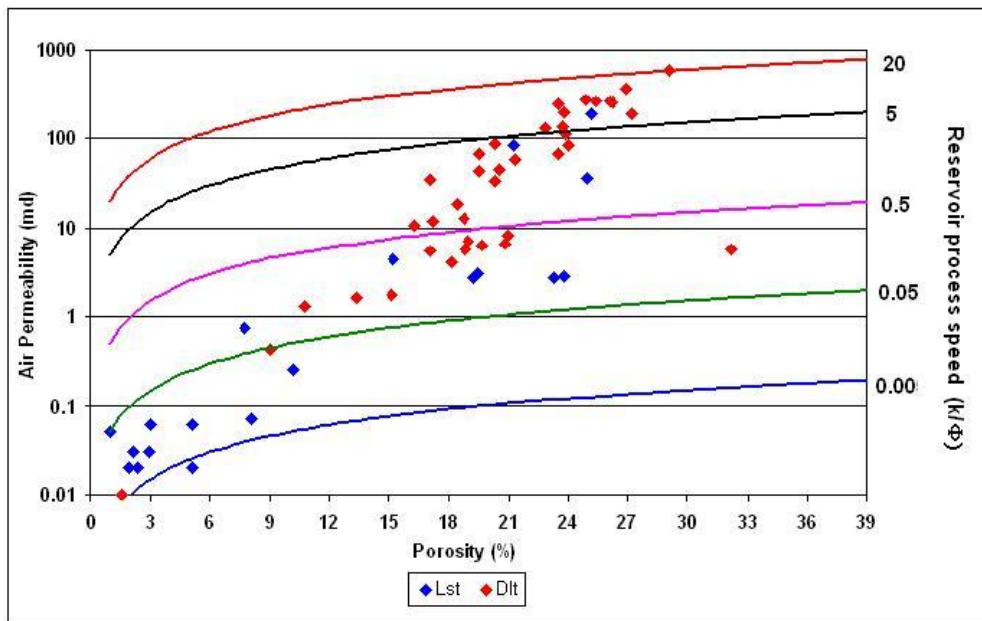


Figure 6. 19 Porosity-Permeability plot of  $k/\phi$  for Derdere Formation

Limestones have high porosity values, whereas the permeabilities are low (the limestone unit in consideration is the *L-1* U unit where one can expect flow, and this unit can be studied detailedly in one well, because only Well X has more core plugs than Well A which we can depend on through these limestones) so it is not easy to talk about on the limestones much at this point, due to lack of data. But, because of high porosity, and low permeability, we can say that the limestones can have vuggy-moldic porosity, with isolated pores, preventing the fluid flow. The tight limestones are the unit in this formation where we can not expect a hydraulic flow, due to low properties of reservoir parameters. Dolomites display two distinctive trends, *D-1*; have moderately high porosities, and high permeabilities, show good reservoir characteristics. The pores are interconnected as seen in the high permeability values. The dominant porosity in this unit is microporosity with intercrystalline porosity type. The dolomitization has great effects on this porosity. The size and the shape of the dolomite crystals contribute to the porosity and as a result permeability also increases. Also the microfractures and fissures may act as conduits for fluid flow.

The third unit, *D-2*, is observed in every well, at the bottom of the dolomite reservoir unit. Its thickness is very thin within the continuous profile. Porosities are moderately high but lower than the *D-1* unit, but permeability values lower, maybe indicating for vuggy-moldic porosity types. In such type dominant formations, even if the porosity increases with more vugs and molds, permeability does not increase as much as porosity increases, because molds and vugs are isolated. Fractures and fissures may help permeability increases in these reservoirs.

The distinctive units within the studied core plug data is illustrated in Figure 6.20. The core plug data for unit *L-1* is scattered within the other limestone data points labeled in blue.

While studying with  $R_{35}$  and  $k/\phi$  methods, it will always be helpful to plot stratigraphic flow profile obtained by the core data. One profile is prepared for Well X, bearing limestone units of *L-1* and *L-2*, and dolomite units of *D-1*, *D-2*, as seen in Figure 6.21. It must also be kept in mind that there exists a dolomitic shale interval just at the bottom of *L-1* unit, as passing to the *D-1* unit.

Well B, compared to Well X, has limited data, there are no cores for other units are available. All the units are seen in the well logs, but there are limited data for the cores. The flow profile of Well B is given in Figure 6.22.

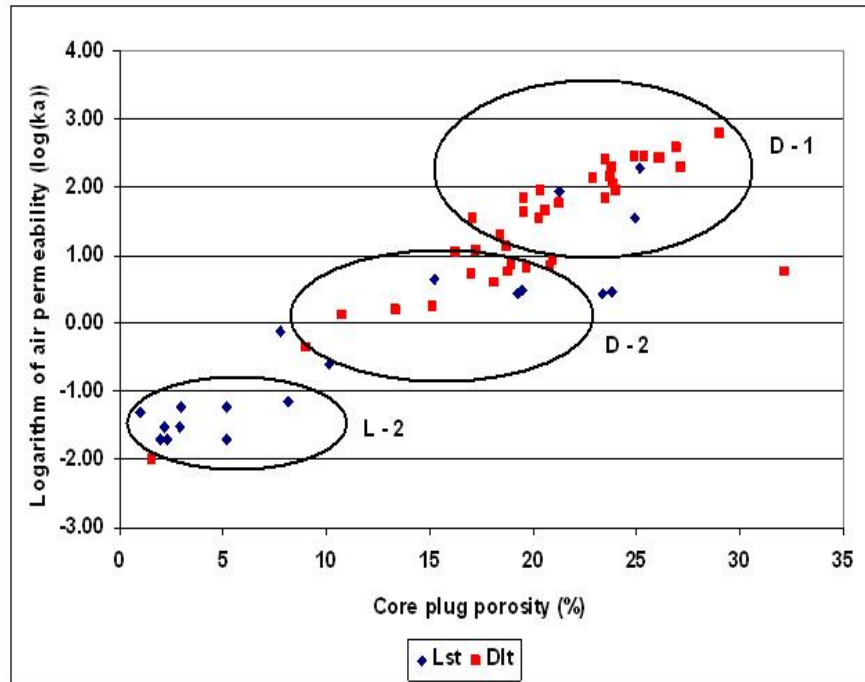


Figure 6. 20 Distinctive units in Derdere Formation

The petrophysical parameters derived from well loggings were already plotted against each other to see the discriminations of units. In this part, geostatistical models will be applied to understand the mathematical change of these derived parameters among each other. The whole log data set will be the starting point.

The correlation coefficients for the regressed parameters of well log derived values are shown in Table 6.3.

According to the regression results, for all of the porosity values, porosity is decreasing with increasing depth. The best correlation between porosity and depth can be observed for the  $\varnothing_D$  values. All porosity values are also well correlated with each other indicating the good estimates of porosity from logs. All porosity values positively correlate with water saturation which may indicate that, as porosity increases, the water saturation increases. This may be rather strange behaviour, because most of the high porosity values represent oil saturations higher than water saturations, but due to some water bearing big pores causing high porosity, this trend may be seen.

Table 6. 3 Correlation coefficients for well log parameters

	Depth (m)	$\varnothing_s$ (%)	RHOB (g/cc)	$\varnothing_D$ (%)	$\varnothing_N$ (%)	$\varnothing_{D-N}$ (%)	Rt ( $\Omega.m$ )	Rxo ( $\Omega.m$ )	Sw (%)
Depth	1	-0.06	0.22	-0.20	-0.10	-0.13	0.16	0.07	-0.12
$\varnothing_s$		1	-0.50	0.65	0.81	0.77	-0.04	-0.22	0.63
RHOB			1	-0.83	-0.61	-0.79	-0.10	0.26	-0.25
$\varnothing_D$				1	0.76	0.87	0.20	-0.28	0.30
$\varnothing_N$					1	0.93	0.09	-0.27	0.46
$\varnothing_{D-N}$						1	0.12	-0.27	0.45
Rt							1	-0.03	-0.34
Rxo								1	-0.19
Sw									1
$V_{sh}$									

There exists a low correlation between  $R_t$  and  $R_{xo}$ , indicating the probable fractures and fissures also tracked with a separation between these logs in wells.

This correlation coefficient table was prepared on the basis of whole data set including the four different units, but for a better estimates of other parameters and future studies, the geostatistical methods should be applied separately for each unit. This will lead the studies for better flow unit delineations, and permeability predictions.

The major petrophysical data obtained from the units of Derdere formation were averaged arithmetically. The results are given in Table 6.4.

Table 6. 4 Average values for each unit

Units	Average $\varnothing$ (%)	Average ka (mD)	Range of $\varnothing$ (%)	Range of ka (mD)	$R^2$ (%) between $\varnothing$ -ka	Port-size type
L - 1	20.58	7	10.13-25.16	0.26-35	85.25	micro-meso
L - 2	3.60	0.11	0.97-7.73	0.02-0.7	40.74	nanno-micro
D - 1	24.70	171.90	17.07-27.2	34-369	72.66	mega-macro
D - 2	17.94	8.09	9-20	0-30	33.83	meso

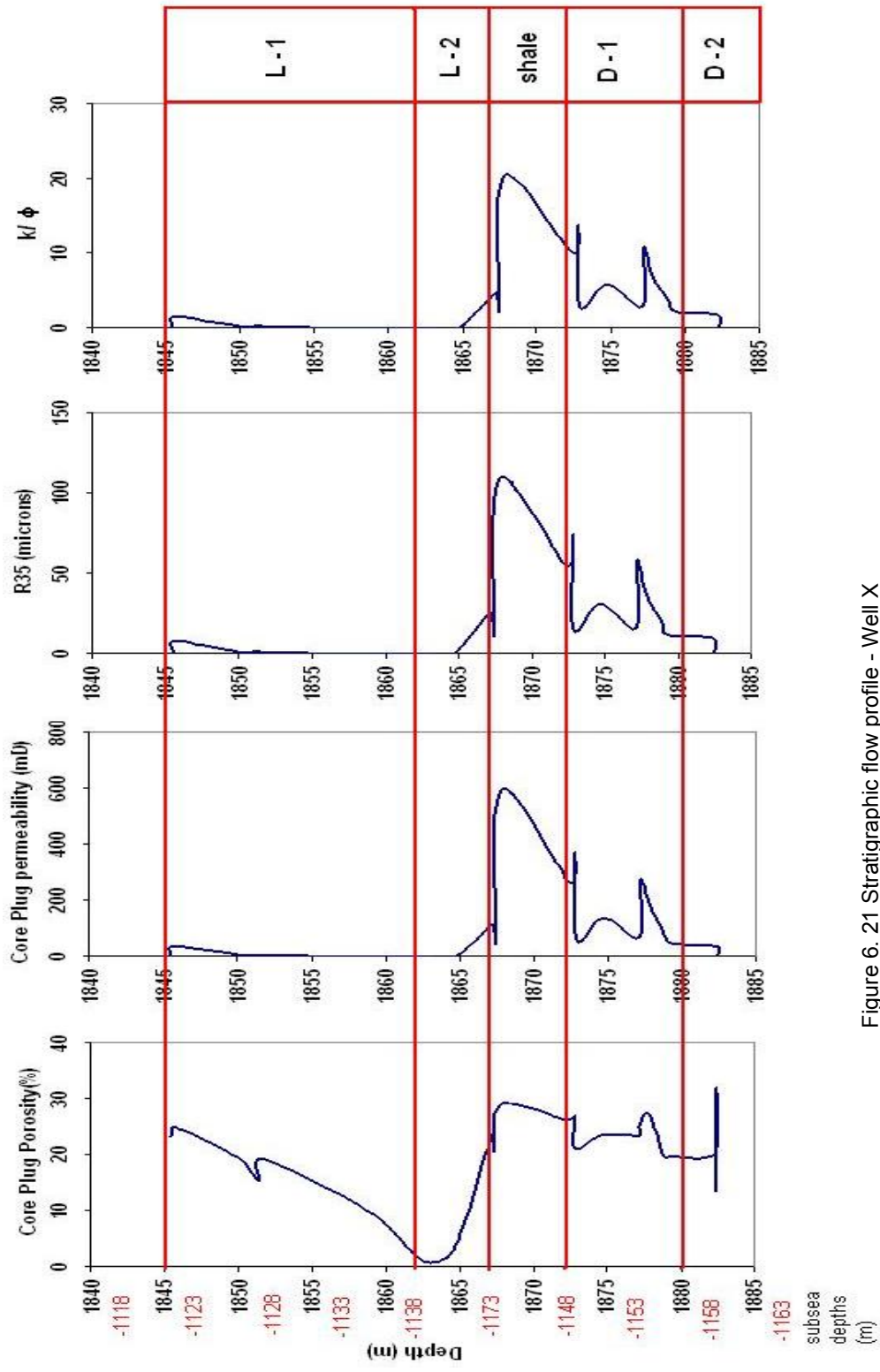


Figure 6. 21 Stratigraphic flow profile - Well X

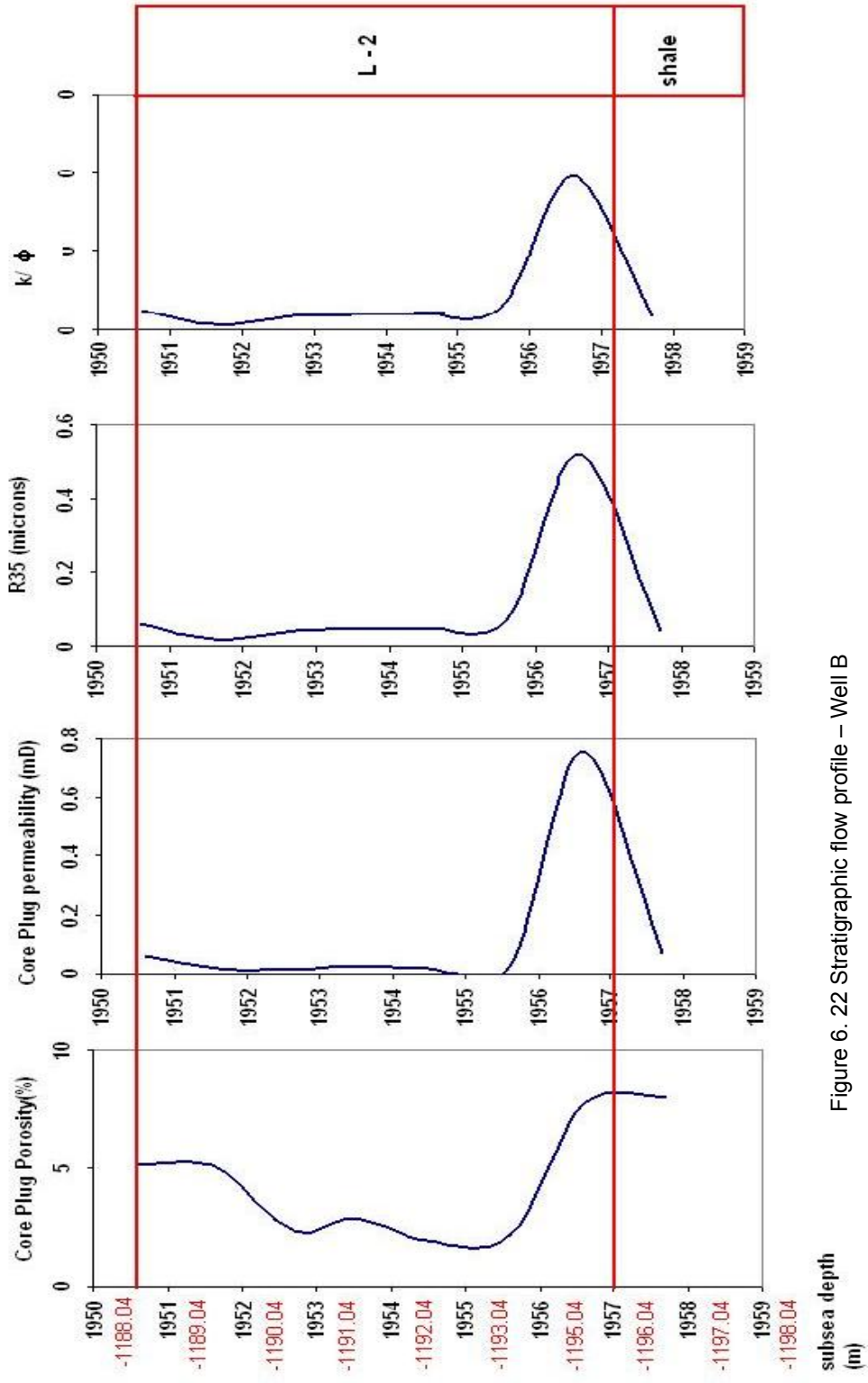


Figure 6. 22 Stratigraphic flow profile – Well B

### 6.3.1 Limestone L - 1 Unit Analysis

The analysis was performed for the whole limestone data set of core plugs, and there different porosity-permeability trends in this data set. For this reason any prediction of permeability would be insufficient without the study of the units; *L-1* and *L-2* separately.

The regression analysis plot of core plug porosity and logarithm of air permeability is for the whole data set is given in Figure 6.23. For the whole data set  $R^2$  is 83.14%.

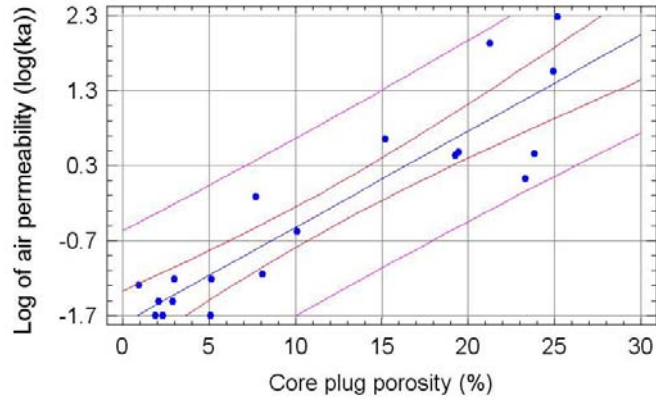


Figure 6. 23 Linear regression between whole limestone data set

A linear regression is done for the data set of core plug porosity and air permeability from *L-1* unit. The resulting plot is seen in Figure 6.24. The results for the regression is listed in Table 6.5.

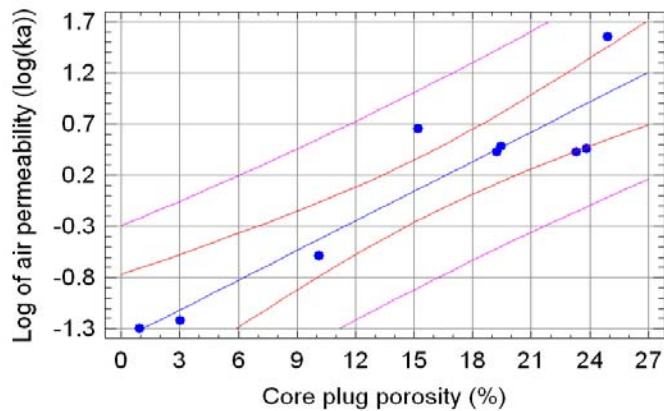


Figure 6. 24 Linear regression for core plug porosity and logarithm of air permeability for L-1

Table 6. 5 Linear regression results for core plug porosity and logarithm of air permeability for L-1

Intercept	Slope	F-ratio	r	R <sup>2</sup> (%)
-1.41	0.10	40.44	0.92	85.25

Thus the results yield an regression equation of ;

$$\text{Log}_{10}(k_a) = -1.41 + 0.1\phi_{CPP} \quad (6.8)$$

where,  $k_a$  is the core plug air permeability, and  $\phi_{CPP}$  is the core plug porosity.

Only 8 limestone core plugs are available for this unit; from Well X. Therefore; the calculations must be based on the data set from Well X, where GR and sonic log sets are available only. For this reason, only sonic porosity values are present for comparison between core plug porosity and well log derived porosity.

The results for regression analysis between core plug porosity and sonic porosity are listed in Table 6.6.

As seen in the table, there is a slightly strong relationship between two porosities. In order to go on with permeability prediction, core plug air permeability should be tested with the sonic porosity. The resulting regression is given in Table 6.7.

Table 6. 6 Linear regression results for core plug porosity and sonic porosity for L-1

Intercept	Slope	F-ratio	r	R <sup>2</sup> (%)
8.25	0.40	2.39	0.50	25.46

Table 6. 7 Linear regression results for permeability and sonic porosity for L-1

Intercept	Slope	F-ratio	r	R <sup>2</sup> (%)
-1.03	0.08	3.69	0.59	34.55

The regression equation for this analysis can be given as;

$$\log_{10}(k_a) = -1.03 + 0.08\phi_s$$

In order to model permeability for the limestones, sonic porosity may not be adequate, and for sake of using all the available data GR recordings can be added to the regression.

For this purpose, stepwise multiple regression analysis should be applied. The results for the multiple regression is given in Table 6.8.

Table 6. 8 Multiple regression results for logarithm of air permeability

Independent variable	Coefficient	Significance level
Constant	-1.66	0.01
$\phi_s$ (%)	0.09	0.02
GR (API)	0.01	0.02

The multiple regression of logarithm of air permeability with sonic porosity and GR reading yields a  $R^2$  of 65.52 %. In fact this value is not as high as it was expected but compared to the linear regression of logarithm of air permeability with sonic porosity (in this case  $R^2 = 34.55$  %), it may give better results.

The resulting multiple regression equation can be given as;

$$\log_{10}(k_a) = -1.66 + 0.01GR + 0.09\phi_s \quad (6.9)$$

The relation between the core plug calculated permeabilities and the predicted permeabilities from the MRA analysis by means of the above equation is seen in Figure 6.25.

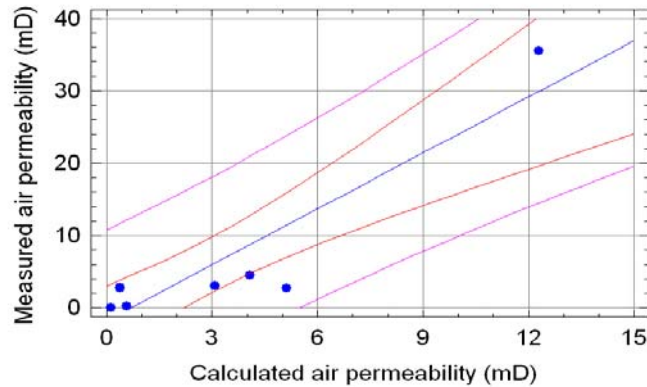


Figure 6. 25 Relation between calculated permeability & measured permeability for L-1

The  $R^2$  for the results is 83.68 % which counts for a relatively strong correlation between the MRA calculated permeabilities and measured ones from the cores for limestones.

The obtained MRA equation can be used for the permeability prediction of  $L-1$  unit for the uncored section of Well C.

The  $L-1$  unit for Well C is between 1908 -1925 m. The predicted values of  $k_a$  can be seen in Table 6.9.

Of course the values seem very low, but this is in fact due to the lack of independent variables used in MRA analysis. Only Well X has limestone core data, and the whole model should be based on this.

As it is obvious,  $\varnothing_s$  and GR are not alone sufficient for permeability predictions. Also, the lack of porosity and resistivity logs for Well X limited the correlations between core data and well logging attributes.

As a result, the obtained MRA equation should be relied on. After all, the values are low, but if we look at the measured values of permeability in Well X, at the top of the L - 1 unit, the values are high, and through bottom, values get lower. This is also observed in the predicted values, which may be the indicator for good correlation.

Table 6. 9 Predicted  $k_a$  values for Well C, L - 1 Unit

Depth (m)	Predicted $k_a$ (mD)	Depth (m)	Predicted $k_a$ (mD)
1908	3.74	1917	0.38
1909	1.66	1918	0.14
1910	0.44	1919	0.06
1911	0.17	1920	0.09
1912	0.68	1921	0.18
1913	0.60	1922	0.51
1914	0.10	1923	0.07
1915	0.10	1924	0.05
1916	0.11		

### 6.3.2. Limestone L - 2 Unit Analysis

A linear regression is done between the core plug porosity and air permeability data set for the cores belonging to L - 2 unit. The resulting  $R^2 = 54.92\%$ . The plot is given in Figure 6.26.

In well logs, L - 2 unit is observed, which is just over the main reservoir unit of D -1. It can be tracked at the bottom of limestones. This unit can be tracked very easily on logs because these are the *tight limestones* with lowering porosities on porosity logs, and high  $R_t$  values in resistivity logs. From all these wells, Well B and Well X has total 10 core plug data belonging to L - 2 unit. Both the porosity and the air permeability values are very low.

A linear regression analysis was applied to the core plug porosity and well log derived porosities of  $\varnothing_s$ ,  $\varnothing_D$ ,  $\varnothing_N$ , and  $\varnothing_{D-N}$  for unit L - 2. The relationship between the porosities is shown in Figure 6.27. The linear regression results are given in Table 6.10.

As seen in the table, the porosities are not well correlated with one another, only sonic and neutron porosities seem to have moderately strong relations. These porosities can be used in permeability modeling.

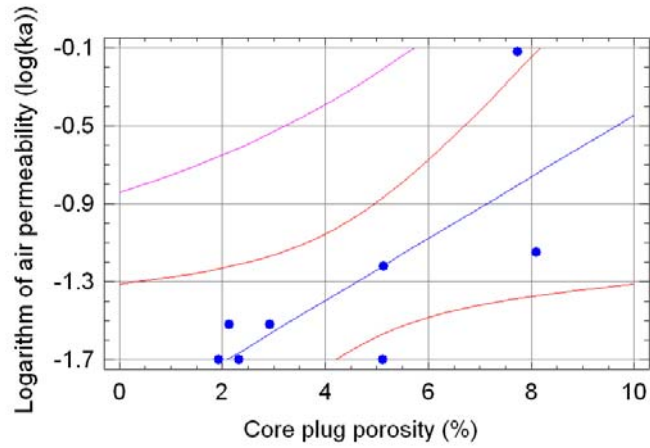


Figure 6. 26 Linear regression for core plug porosity and logarithm of air permeability for L-2

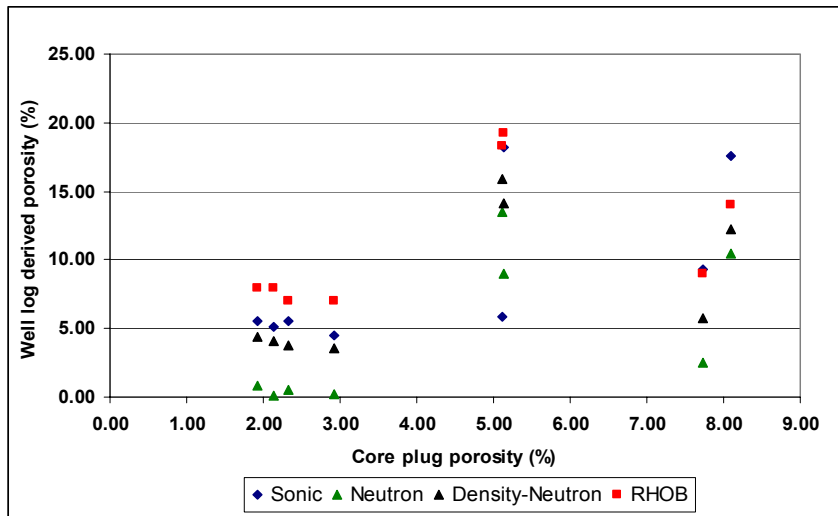


Figure 6. 27 Relation of core plug porosity and well log derived porosities for L-2

Table 6. 10 Linear regression results for core plug porosity and well log derived porosities for L-2

Porosity Type	Intercept	Slope	F-ratio	r	R <sup>2</sup> (%)
Ø <sub>S</sub> (%)	1.74	0.30	5.35	0.69	47.13
Ø <sub>pb</sub> (%)	1.70	0.24	1.94	0.50	24.42
Ø <sub>N</sub> (%)	3.11	0.28	3.74	0.62	38.38
Ø <sub>D-N</sub> (%)	2.25	0.27	2.87	0.57	32.36

A MRA was applied to the logarithm of permeability using ρ<sub>b</sub> recordings, Ø<sub>S</sub>, Ø<sub>D</sub>, Ø<sub>N</sub>, and Ø<sub>D-N</sub> porosities, R<sub>t</sub>, R<sub>xo</sub> and S<sub>w</sub> values corresponding to related core plug data as read from the logs.

The MRA resulted in a 61.54 % of R<sup>2</sup>, which is not a good correlation. Then, each parameter was linearly regressed with logarithm of air permeability. The parameters showing the highest correlation coefficients were selected for another MRA.

Only Ø<sub>D-N</sub> porosity values are eliminated for the new MRA, because of having correlation coefficient of 0.014.

The results are given in Table 6.11.

Table 6. 11 MRA coefficients between logarithm of air permeability and log derived parameters

Independent variable	Coefficient
Constant	2158.6
Ø <sub>N</sub> (%)	0.74
ρ <sub>b</sub> (g/cc)	751.34
Ø <sub>D</sub> (%)	-14.76
R <sub>t</sub> (Ω.m)	0.0018
R <sub>xo</sub> (Ω.m)	0.0085
Ø <sub>S</sub> (%)	-0.039
S <sub>w</sub> (%)	0.007

The yielded MRA equation is ;

$$\log_{10}(k_a) = 2158.7 + 0.74\phi_N - 751.34\rho_{b_{records}} - 14.76\phi_D + 0.0018R_t + 0.0085R_{xo} - 0.039\phi_S + 0.007S_w$$

(6.10)

The resulting  $R^2$  is 98.38 % which is a very good correlation between the independent variables and dependent variable (logarithm of  $k_a$ ) of the MRA.

By using the derived MRA equation, permeabilities are re-calculated. The relationship between the calculated values of permeability and core plug measured permeability is given in Figure 6.28.

This MRA equation is then can be used safely for permeability predictions in wells where there are no cores for the unit L - 2.

The predicted  $k_a$  values for the uncored section of L - 2 unit in Well C are listed in Table 6.12.

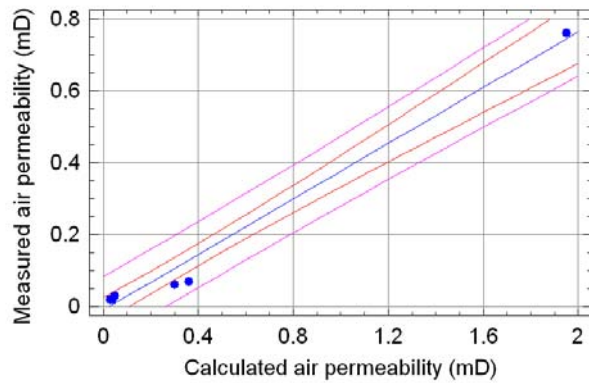


Figure 6. 28 Relation between calculated values of permeability and core plug permeability for L-2

Table 6. 12 The predicted  $k_a$  values for of L - 2 unit in Well C

Depth (m)	Predicted $k_a$ (mD)
1925	0.01
1926	0.01
1927	0.07
1928	0.07
1929	1.58
1930	1.00

### 6.3.3. Dolomite D – 1 Unit

The regression analysis plot core plug porosity and logarithm of air permeability for whole dolomite data set is given in Figure 6.29.

The results for the regression is listed in Table 6.13.

As it is expected, the logarithm of air permeability is increasing with porosity linearly, and the  $R^2$  is 86.92 % which is higher than expected.

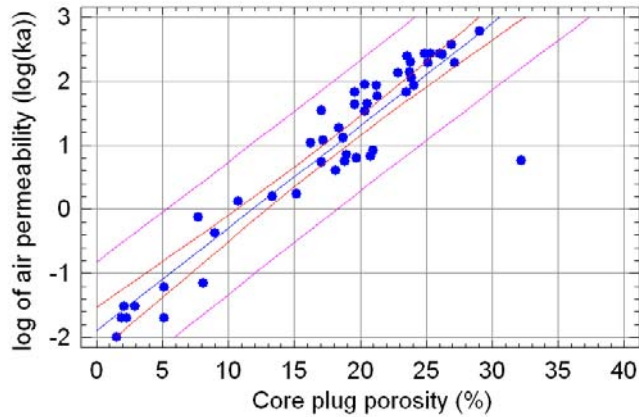


Figure 6. 29 Linear regression for core plug porosity and logarithm of air permeability for dolomites

Table 6. 13 Linear regression results for core plug porosity and logarithm of air permeability for dolomites

Intercept	Slope	F-ratio	r	$R^2$ (%)
-1.90	0.16	305.67	0.93	86.92

The core data for the  $D - 1$  unit is available for Well D, and Well X, and since Well X has only GR and sonic log data, the derived equations will be mainly based on Well D data.

The  $D - 1$  unit is mainly composed of extreme values of porosity and permeability. The porosity range is between 17-30%, and the permeability range is between 34-369 mD. There are some extremes values of permeability, that maybe resulted from fractures , and if necessary, these data may be excluded during calculations.

The relations between the log derived porosities and core plug porosity is firstly established. The relation is seen in Figure 6.30, and the linear regression results are given in Table 6.14.

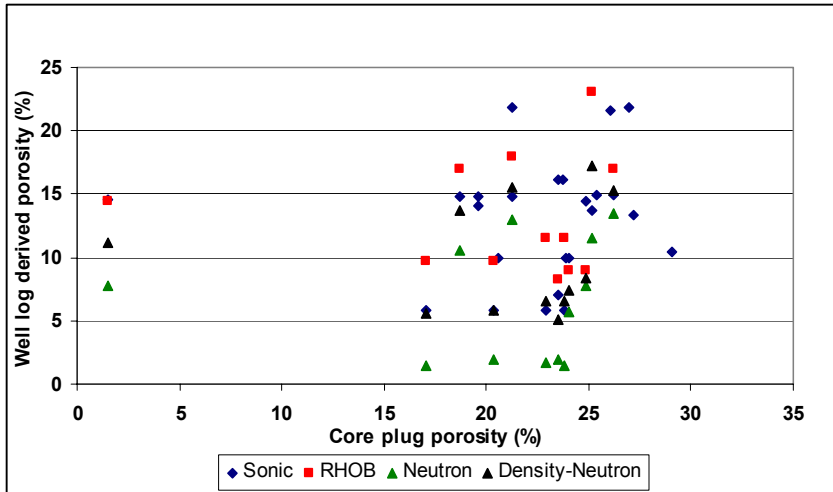


Figure 6. 30 Relation between log derived porosities and core plug porosity for D-1

There are two data from Well D with extreme low values of porosity and permeability. For a simplification, these data are excluded. The porosity values do not show good correlations with each other. The only porosity type which is near to the calculated one is the  $\varnothing_N$ . A linear regression is applied to the core plug porosity and logarithm of air permeability for  $D - 1$  unit. The corresponding plot is given in Figure 6.31.

The results are given in Table 6.15

Table 6. 14 Linear regression results of log derived porosities and core plug porosity for D-1 unit

Porosity Type	Intercept	Slope	F-ratio	r	R <sup>2</sup> (%)
$\varnothing_S$ (%)	21.22	0.17	2	0.0	9.1
$\varnothing_{pb}$ (%)	20.72	0.17	0.9	0.32	10.15
$\varnothing_N$ (%)	21.40	0.25	2.37	0.48	22.88
$\varnothing_{D-N}$ (%)	20.66	0.24	1.75	0.42	17.97

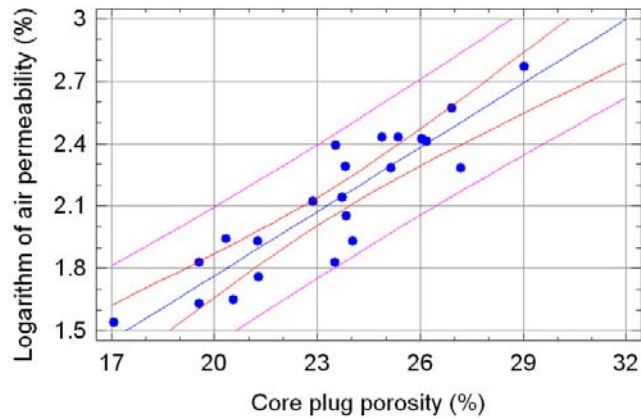


Figure 6. 31 Linear regression for core plug porosity and logarithm of air permeability for D-1

Table 6. 15 Linear regression results of core plug porosity and logarithm of air permeability for D-1

Intercept	Slope	F-ratio	r	R <sup>2</sup> (%)
-0.30	0.10	83.75	0.90	80.72

There is a strong relation between the core plug porosity and permeability values of unit D-1. But since the well log derived porosities can not be used instead of the core plug porosity due to low correlation coefficients, permeability must somehow effected by other petrophysical parameters.

Logarithm of air permeability was tried to relate with the core derived porosities, the correlation coefficients obtained are seen in Table 6.16.

Table 6. 16 Correlation coefficient between logarithm of air permeability and log derived porosity, D-1

Porosity type	r	R <sup>2</sup> (%)
$\varnothing_s$ (%)	0.38	14.4
$\varnothing_{pb}$ (%)	0.18	3.22
$\varnothing_N$ (%)	0.29	8.41
$\varnothing_{D-N}$ (%)	0.25	6.24

After these trial of fitting well log derived porosity to permeability, it can be said that the reservoir characteristics of the  $D - 1$  unit is mainly influenced by the permeability, the correlations are low, but only the directly measurements from the core data porosity gives good correlations with permeability.

Each of the well log derived petrophysical properties are correlated to permeability for better understanding of the relations. The results are listed in Table 6.17.

Table 6. 17 Correlation coefficients between logarithm of permeability and log derived parameters

Variable	r	R <sup>2</sup> (%)
Rt (Ω.m)	-0.08	0.67
∅ <sub>N</sub> (%)	0.29	8.41
∅ <sub>D-N</sub> (%)	0.25	6.24
Sw (%)	0.25	6.14
∅ <sub>D</sub> (%)	0.18	3.22
Rxo (Ω.m)	0.01	0.01
GR (API)	0.40	15.4
∅ <sub>S</sub> (%)	0.38	14.4
ρb records (g/cc)	-0.19	3.63

For a first trial of MRA, 8 independent variables of containing ∅<sub>N</sub>, ∅<sub>D-N</sub>, ρ<sub>b</sub> recordings, R<sub>t</sub>, R<sub>xo</sub>, S<sub>w</sub>, GR recordings and ∅<sub>S</sub> are used as input to relate with logarithm of air permeability.

The variables are put in to the regression starting from the highest correlation coefficients. Then one by one the variables with smaller correlation coefficients are excluded from the model. The resulting R<sup>2</sup> values for the tried MRA analysis with changing number of variables are listed in Table 6.18.

Having 8, 7 and 6 variables do not affect the quality of the correlation as seen in the table. But when the correlation is done with 5 variables, as excluded from ρ<sub>b</sub> recordings, the R<sup>2</sup> changes dramatically.

Table 6. 18 The change in R<sup>2</sup> with the number of parameters in the MRA equation

Number of independent variables	R <sup>2</sup> (%)
8 (all variables included)	100
7 (Rxo extracted)	96.97
6 (Rxo+Rt extracted)	96.54
5 (Rxo+Rt+ρb records extracted)	57.76

3 different MRA equations are obtained. These equations are used to re-calculate the core plug air permeabilities. The predicted values are plotted against the measured values as given in Figure 6.32.

For the 8-variable equation, the values are extremely under-estimated. The  $R^2$  is 14.22 %.

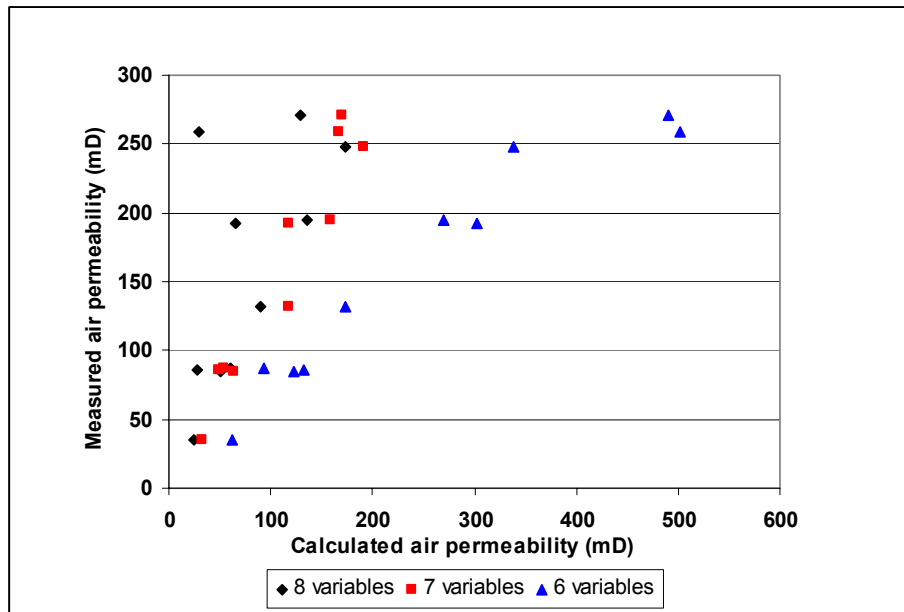


Figure 6. 32 Relation between calculated permeability and measured permeability

For the 6-variable equation, the values are slightly over-estimated. The  $R^2$  is 85.76 %.

For the 7- variable equation, the values are well correlated and the yielding  $R^2$  is 84.55 %. This equation is chosen for permeability prediction since it gives closer values to measured values.

The 7-variable equation is obtained as;

$$\log_{10}(k_a) = 116.65 - 0.06GR + 0.39\phi_S + 1.17\phi_N - 0.87\phi_{D-N} - 0.17Sw - 40.69\rho b_{records} - 0.0009Rt \quad (6.11)$$

This equation differs from the other derived equations as it contains GR recording. The GR recordings must be included in the equation since they give high correlation with permeability.

The reason for that can be the homogeneous GR recordings as observed within the cored interval.

The derived equation can be used to predict uncored section of *D - 1* unit of Well C.

The predicted values of permeability for the *D - 1* unit in Well C are listed in Table 6.19.

Table 6. 19 The predicted  $k_a$  values for of *D-1* unit in Well C

Depth (m)	Predicted $k_a$ (mD)
1934	163.78
1935	148.82
1936	176.86
1937	131.54
1938	130.55
1939	141.36
1940	149.03

The values predicted are ideal permeability values for a reservoir section. They may reflect as high values, but this may cause from the high  $R_t$  reaching 2000  $\Omega.m$  readings for the uncored sections.

#### 6.3.4. Dolomite *D - 2* Unit

The unit *D - 2* has core data from Well X and Well D. The unit is very thin, as observed at the bottom of the reservoir section.

A linear regression analysis was applied to the core plug porosity and well log derived porosities of  $\varnothing_s$ ,  $\varnothing_D$ ,  $\varnothing_N$ , and  $\varnothing_{D-N}$  for unit *D - 2*.

The relationship between the porosities is shown in Figure 6.33. The linear regression results are given in Table 6.20.

The porosities are not well correlated with one another, only  $\varnothing_N$  and  $\varnothing_{D-N}$  porosities seem to have moderately strong relations. These porosities can be used in permeability modeling.

The regression analysis plot of core plug porosity and logarithm of air permeability for *D -2* unit is given in Figure 6.34.

The linear regression results for the core plug porosity and air permeability of unit *D - 2* is listed in Table 6.21.

The reason for having such a a low correlation is that, the defined *D - 2* unit is mainly composed of permeability range 1 -7 mD, and porosity range of 9-30 %. The calculated  $R_{35}$  values showed that the dominant pore-size is the mesopore with a range of 1-5  $\mu$ .

This is the general trend of the unit, but there are 4 values that do not represent the unit characteristics.

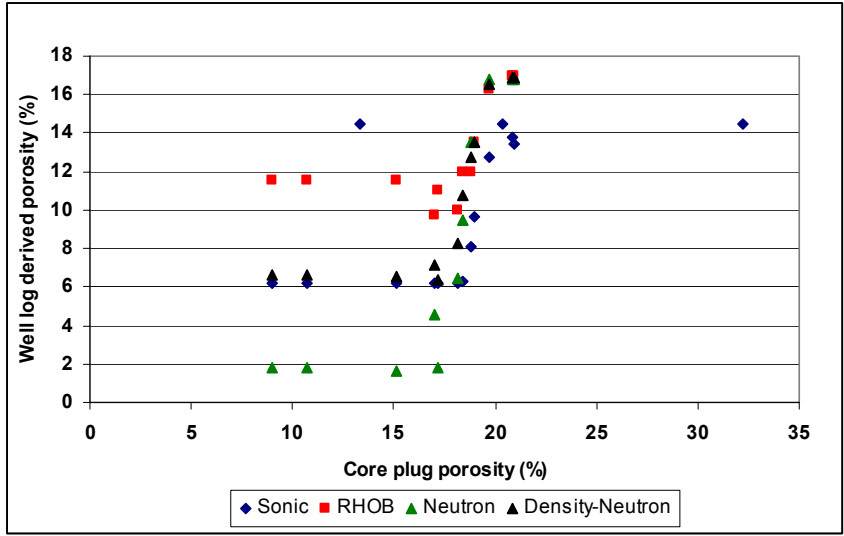


Figure 6. 33 Relation between core plug porosity and well log derived porosities

Table 6. 20 Linear regression results of core plug porosity and log derived porosities for D-2

Porosity Type	Intercept	Slope	F-ratio	r	R <sup>2</sup> (%)
$\phi_s$ (%)	2.12	0.40	6.36	0.56	31.24
$\phi_{pb}$ (%)	6.22	0.38	4.62	0.54	29.60
$\phi_N$ (%)	13.51	0.43	16.49	0.77	59.98
$\phi_{D-N}$ (%)	10.62	0.61	13.22	0.74	54.60

These values have extreme permeabilities, which are mostly likely caused by the fractures present in the data sample. They are classified as macroport with the calculated  $R_{35}$  values. For better results, these values can be excluded for permeability predictions.

With the new data set, a linear regression was applied between the logarithm of air permeability and core plug porosity. The outcoming  $R^2 = 56.45\%$  is higher than the first regression, resulting in a linear regression equation as;

$$\log_{10}(k_a) = -0.37 + 0.05\phi_{CPP} \quad (6.12)$$

The permeability prediction then can be based on the new data set.

Logarithm of air permeability was tried to relate with the core derived porosities, the correlation coefficients were obtained as seen in Table 6.22.

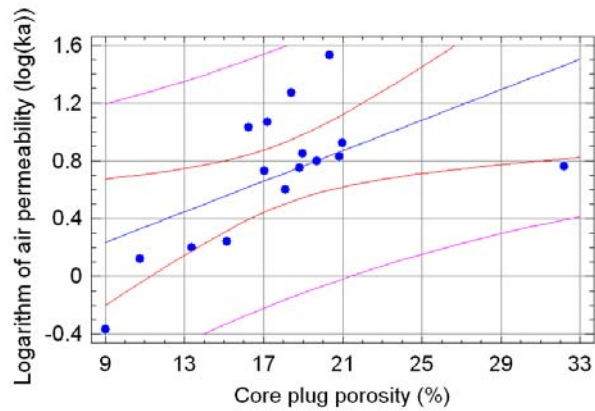


Figure 6. 34 Linear regression for core plug porosity and logarithm of air permeability for D-2

Table 6. 21 Linear regression results for core plug porosity and logarithm of air permeability for D-2

Intercept	Slope	F-ratio	r	R <sup>2</sup> (%)
-0.24	0.05	7.02	0.58	33.83

As it was also seen in the relation between the core plug porosity and the log derived porosity,  $\emptyset_N$  and  $\emptyset_{D-N}$  give better correlation coefficients with the permeability.

For the first MRA application, 7 independent variables were put into the model. These are chosen as their highest correlation coefficient with the logarithm of permeability. The independent variables are,  $R_t$ ,  $\emptyset_N$ ,  $\emptyset_{D-N}$ ,  $S_w$ ,  $\rho_b$  recordings,  $R_{xo}$ , and GR recordings. The correlation coefficients of the variables with the logarithm of permeability are listed in Table 6.23.

Table 6. 22 Correlation between logarithm of air permeability and log derived porosities for D-2

Porosity type	r	R <sup>2</sup> (%)
$\emptyset_S$ (%)	0.45	20.70
$\emptyset_{pb}$ (%)	0.48	23.60
$\emptyset_N$ (%)	0.81	65.20
$\emptyset_{D-N}$ (%)	0.74	54.66

The 7 variables was put in a MRA , and the resulting  $R^2= 92.77\%$ , which represents a very high correlation. In order to see how the  $R^2$  changes with the decreasing number of independent variables, the variables with the lowest values of correlation coefficient are extracted from the model one by one. The results are shown in Table 6.24.

If GR recordings and  $R_{xo}$  values are extracted from the regression model, the yielding  $R^2$  is still in a safe range, but it dramatically decreases.

Table 6. 23 Correlation coefficients of logarithm of permeability and log derived parameters for D-2

Variable	r	$R^2$ (%)
Rt ( $\Omega.m$ )	-0.82	67.70
$\emptyset_N$ (%)	0.81	65.20
$\emptyset_{D-N}$ (%)	0.74	54.66
Sw (%)	0.68	46.56
pb (g/cc)	-0.51	26.10
Rxo ( $\Omega.m$ )	-0.44	19.60
GR (API)	-0.3	8.68

Table 6. 24 The change in  $R^2$  with the number of parameters in the MRA equation

Number of independent variables	$R^2$ (%)
7 (all variables included)	92.77
6 (GR extracted)	84.88
5 (GR+Rxo extracted)	80.84

The MRA equation containing 7 variables are used in order to re-calculate the core derived permeabilities, but the results are over-estimated. Such a model can not be used for permeability prediction. Then, the model was tried with 6 variables, again the values are over estimated. The trial is made until 4 independent variables are present in the equation. The variation of  $R^2$  between the predicted permeability and core measured permeability, with decreasing number of independent variables is given in Table 6.25.

Table 6. 25 The change in  $R^2$  between predicted and calculated values of air permeability with decreasing number of variables

Number of independent variables	$R^2$ (%)
7 (all variables included)	4.00
6 (GR extracted)	43.00
5 (GR+Rxo extracted)	60.00
4 (GR+Rxo+pb extracted)	76.65

As a result, the MRA equation with 4 independent variables containing  $Rt$ ,  $\phi_N$ ,  $\phi_{D-N}$ ,  $S_w$  is decided to use for permeability predictions.

The resulting MRA equation is given as;

$$\log_{10}(k_a) = 4.05 + 0.07\phi_N - 0.32\phi_{D-N} - 0.005Rt + 0.011S_w \quad (6.13)$$

The above equation can be used for permeability predictions in uncored sections of D-2 units of Well C.

The predicted values are given in Table 6.26.

Table 6. 26 The predicted  $k_a$  values for of D-2 unit in Well C

Depth (m)	Predicted $k_a$ (mD)
1941	0.52
1942	0.06
1943	1.00

The resulting stratigraphic flow profile for Well C can be plotted. The derived values of air permeabilities are utilized, and since the core plug porosity values are lacking, the density-neutron porosity values can be used for  $k/\phi$  and  $R_{35}$  calculations.

The flow profile is given in Figure 6.35.

The averaging values are listed as seen in Table 6.27.

Table 6. 27 Average values for each unit – Well C

Units	Average $\phi_{D-N}$ (%)	Average $k_a$ (mD)	Range of $\phi_{D-N}$ (%)	Range of $k_a$ (mD)	$R^2$ (%) (from MRA)	Port-size type
L - 1	7.93	0.28	4-12	0-1.6	83.68	micro-meso
L - 2	6.00	2.87	0-6	0-6	98.38	nanno-micro
D - 1	14.5	150.9	8-20	130-176	84.55	mega
D - 2	13.3	0.36	11-14	0-1	76.65	meso

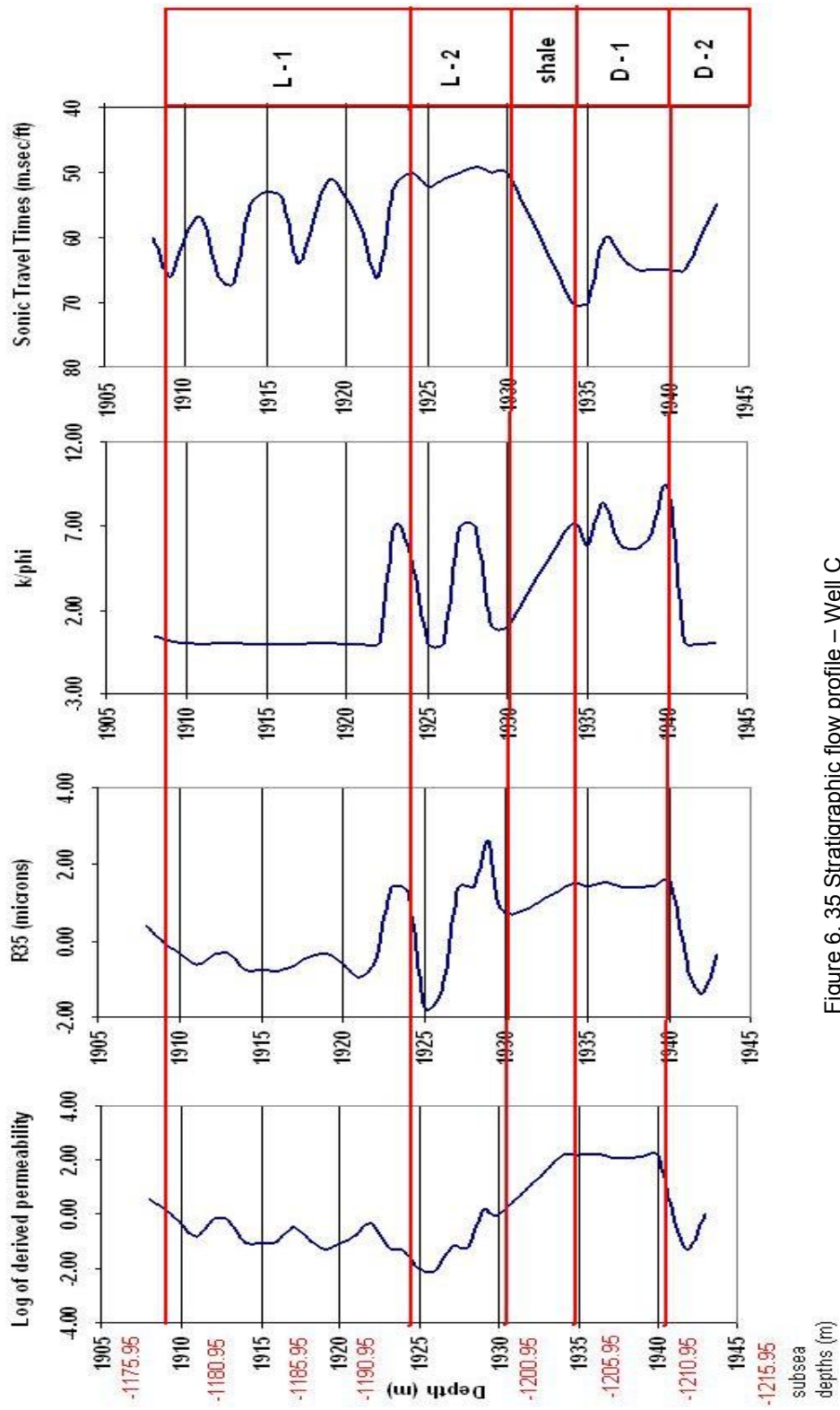


Figure 6. 35 Stratigraphic flow profile – Well C

## CHAPTER 6

### CONCLUSIONS

The significant conclusions from this research can be listed as;

- 4 different units were identified within the Derdere Formation.
- The first unit is the *L – 1* unit of limestones. To be compared with the dolomites, the limestones are characterized by low porosity values as recorded by the logs. The permeability values are very low to be characterized as a reservoir, but there are also high values. The unit can be defined as a “flow unit” with relatively good reservoir quality. The study on limestones would go further is more core plug data were available, but the data samples were exhaustive.
- The second limestone unit is the *L – 2* unit. It can be easily tracked in well logs with lowering neutron porosity recordings and denser values in density recordings. Also increases in true resistivity recordings are the best indicators. The unit is composed of tight limestones, in composition with minor dolomites. The porosity and permeability values are very low, in where one can not expect any hydraulic flow within the unit.
- The dolomites have 2 units, named as *D - 1*, and *D - 2* from top to bottom.
- The unit *D - 1* is the reservoir unit of the Derdere dolomites. It is tracked in all the logs. These dolomites fall in Class 2 of Lucia’s classification, in which the grain-dominated dolostones are dominant. Dolomites have better porosity and permeability values compared to limestones. This may be resulted from secondary porosity generation due to dolomitization. The texture is described as intercrystalline porosity type dominant dolosparites by previous studies. But the core data showed that there exist fractures and may be touching-vugs in the unit, because of extreme permeabilities as 300 millidarcy. The derived equation of permeability prediction is based on gamma ray recordings, sonic, neutron, density-neutron porosities,  $R_t$ ,  $S_w$  and density recordings. The unit is a certain flow unit detected in the Derdere Formation.
- The unit *D -2* is placed at the bottom of the each reservoir unit. The thickness is very small in the logs. Porosities are lower than *D -1* units, but permeability values are not as low as expected. By looking at the permeability values, and the saturation derived from this unit, one can define the as a flow unit, but having poorer characteristics than the main dolomite unit.

- Since the methodology of study is based on well logs and core data, the resulting units are generally matrix-based, and may not reflect the influence of fractures on fluid flow. Only general statements can be done as looking at the extreme permeability values. The study can be proceeded and combined with a study that characterizes the fracture framework.
- The petrophysical study could be more efficient with visual measurements of cores, well cuttings and thin section analysis.

## REFERENCES

- Abbaszadeh, M., Fujii, H., Fujimoto, F., " Permeability Prediction by Hydraulic Flow Units- Theory and Applications " , paper SPE 30158 prepared for presentation at the SPE Petrovietnam Conference held in Hochiminh, Vietnam, 1-3 March, 1995.
- Aguilera, R., Aguilera, M.S., " The Integration of Capillary Pressures and Pickett Plots for Determination of Flow Units and Reservoir Containers ", paper SPE 71725 prepared for presentation at the 2001 SPE Annual and Technical Conference and Exhibition held in New Orleans, Louisiana, 30 September- 3 October, 2001.
- Akatsuka, K., " 3D Geological Modeling of a Carbonate Reservoir, Utilizing Open-Hole Log Response-Porosity & Permeability-Lithofacies Relationship ", paper SPE 87239 prepared for presentation at the 9<sup>th</sup> Abu Dhabi International Petroleum Exhibition and Conference held in Abu Dhabi, U.A.E., 15-18 October, 2000.
- Al-Ajmi, F., Holditch, S.A., " Permeability Estimation Using Hydraulic Flow Units in a Central Arabia Reservoir ", paper SPE 63254 prepared for presentation at the 2000 SPE Annual Technical Conference and Exhibition held in Dallas, Texas, 1-4 October, 2000
- Ala, M.A., Moss, B.J., " Comparative Petroleum Geology of Southeast Turkey and Northeast Syria ", Journal of Petroleum Geology, v.1, p.3-27, 1979.
- Alaygut, D., " Saddle Dolomites in the Derdere Formation and Their Importance in Oil Generation", Proceedings of 9<sup>th</sup> Petroleum Congress of Turkey, p.113-120, 1992
- Altunbay, M., Georgi, D., Takezaki, H.M., " Permeability Prediction for Carbonates: Still a Challenge?", paper SPE 37753 prepared for presentation at the 1997 Middle East Oil Show and Conference held in Manarba, Bahrain, 15-18 March, 1997.
- Ang, A.H., Tang, W.H., " Probability Concepts in Engineering Planning and Design ", John Wiley & Sons, 409 p., 1975.
- Amaefule, J.O., Altunbay M., Taib, D., Kersey, D.G., Keelan, D.K., "Enhanced Reservoir Description: Using Core and Log Data to Identify Hydraulic (Flow) Units and Predict Permeability in Uncored Intervals/Wells ", paper SPE 26436 prepared for presentation at the 68<sup>th</sup> Annual Technical Conference and Exhibiton of SPE held in Houston, Texas, 3-6 October, 1993.
- Amyx, J., Bass, D., Whiting, R., " Petroleum Reservoir Engineering ", McGraw - Hill Book Company, 610 p., 1960.

- Antelo, R., Aguirre, O., " Permeability Calculations From Clustering Electrofacies Technique for the Petrophysical Evaluation in La Pena and Tundy Oil Fields ", paper SPE 69400 prepared for presentation at the SPE Latin American and Caribbean Petroleum Engineering Conference held in Buenos Aires, Argentina, 25-28 March, 2001.
- Archie, G.E., " The Electrical Resistivity Log as an Aid in Determining Some Reservoir Characteristics ", Trans. AIME, v.146, p. 54-67,1942.
- Archie, G.E., " Introduction to Petrophysics of Reservoir Rocks", AAPG Bulletin, v.34, n.5, p. 943-961, 1950.
- Archie, G.E., " Classification of Carbonate Reservoir Rocks and Petrophysical Consideration ", AAPG Bulletin, v.36, n.2, p. 278-298, 1952.
- Asquith, G.B., " Handbook of Log Evaluation Techniques for Carbonate Reservoirs ", AAPG Methods in Exploration Series 5, Tulsa, Oklahoma, p. 3-18, 1985.
- Aufricht, W.R., Koepf, E.H., " The Interpretation of Capillary Pressure Data From Carbonate Reservoirs ", Trans. AIME, v. 210, p. 402-405, 1957.
- Babadađlı, T., Al-Salmi, S., " Improvement of Permeability Prediction for Carbonate Reservoirs Using Well Log Data ", paper SPE 77889 prepared for presentation at the SPE Asia Pacific Oil and Gas Conference and Exhibition held in Melbourne, Australia, 8-10 October, 2002.
- Babadađlı, T., Al-Salmi, S., " A Review of Permeability-Prediction Methods for Carbonate Reservoirs Using Well-Log Data ", paper SPE 87824 prepared for presentation at the 2002 SPE Asia Pacific Oil and Gas Conference and Exhibition held in Melbourne, Australia, 8-10 October, 2002.
- Balan, B., Mohaghegh, S., Ameri, S., " State-Of-The-Art in Permeability Determination From Well Log Data: Part 1-A Comparative Study, Model Development ", paper SPE 30988 prepared for presentation at SPE Eastern Regional Conference & Exhibition held in Morgantown, West Virginia, U.S.A., 17-21 September, 1995.
- Barman, I., Sharma, A.K., Walker, R.F., Datta-Gupta, A., " Permeability Predictions in Carbonate Reservoirs Using Optimal Non-Parametric Transformations: An Application at the Salt Creek Field Unit, Kent Country, TX ", paper SPE 39667 prepared for presentation at the 1998 SPE/DOE Improved Oil Recovery held in Tulsa, Oklahoma, 19-22 April, 1998.
- Bassiouni, Z., " Theory, Measurement, and Interpretation of Well Logs ", Society of Petroleum Engineers, Richardson, Texas, 372 p., 1994.
- Bertrand, M.A, Prikel, K., Kyte, J.R., " Porosity and Lithology From Logs in Carbonate Reservoirs ", paper SPE 1867 prepared for the 24<sup>th</sup> Annual Fall Meeting of SPE of AIME held in Houston, Texas, 1-4 October, 1967.
- Bjorlykke, K., " Sedimentology and Petroleum Geology ", Springer Books, 363 p., 1989.

- Cater, J.M.L., Tunbridge, I.P., " Palaeozoic Tectonic History of SE Turkey ", Journal of Petroleum Geology, v.15, no.1, p. 35-50, 1992.
- Chilingarian, G.V., Mazzullo, S.J., Rieke, H.H., " Carbonate Reservoir Characterization: A geologic engineering analysis ", Elsevier Science Publishers, 1992.
- Choquette, P.W., Pray, L.C., " Geologic Nomenclature and Classification of Porosity in Sedimentary Carbonates ", AAPG Bulletin, v.54, p. 207-250, 1970.
- Cordey, W.G., Demirmen, F., " The Mardin Formation in Southeast Turkey ", Proceedings of 1<sup>st</sup> Petroleum Congress of Turkey, p. 51-71, 1971.
- CRC Enterprises, " Carbonate Reserach Consulting, Inc. ", <http://www.crienterprises.com>, accessed in 29 May, 2005.
- Çelikdemir, E., Dülger, S., Görür, N., Wagner C., Uygur, K., " Stratigraphy, Sedimentology, and Hydrocarbon Potential of Mardin Group, SE Turkey ", Special Publication of European Association of Petroleum Geologists , no.1, p. 439-454, 1991.
- Davies, D.K., Vessell, R.K., " Flow Unit Characterization of a Shallow Shelf Carbonate Reservoir: North Robinson Unit, West Texas ", paper SPE/DOE 35433 prepared for presentation at the SPE/DOE 10<sup>th</sup> Symposium on Improved Oil Recovery held in Tulsa OK, 21-24 April, 1996.
- Davies, D.K., Vessell, R.K., Auman, J.B., " Improved Prediction of Reservoir Behavior Through Integration of Quantitative Geological and Petrophysical Data ", paper SPE 38914 prepared for presentation at the 1997 SPE Annual Technical Conference and Exhibition held in San Antonio, Texas, 5-8 October, 1997.
- Davis, J.C., " Statistics and Data Analysis in Geology ", 2<sup>nd</sup> Edition, John Wiley & Sons, Toronto, Canada, 1986.
- Demirel, İ.H., Yurtsever, T.S., Güneri, S., " Petroleum Systems of Adiyaman Region, Southeastern Anatolia, Turkey ", Marine and Petroleum Geology, v.18, p. 391-410, 2001.
- Dewan, J., " Essentials of Modern Open-Hole log Interpretation ", PennWell Books, Tulsa, Oklahoma, 361 p, 1983.
- Dunham, R.J., " Classification of Carbonate Rocks According to Depositional Texture ", AAPG Memoir, no.1, p. 108-121, 1962.
- Duran, O., " Mardin Grubu Karbonatlarının, Şaryaj Önü ve Altındaki Mikrofasiyes ve Diyajenez İncelemesi ", TPAO Research Center, Report No: 323, 22 p. 1981.
- Duran, O., Aras, M., " Sedimentary Facies and Reservoir Characteristics of the Mardin Group Carbonates in Yeniköy Field, Southeast Anatolia ", Proceedings of 8<sup>th</sup> Petroleum Congress of Turkey, p. 272-280, 1990.
- Duran, O., Alaygut, D., " Adiyaman Dolayı Rezervuar Kayalarında (GD Türkiye) Porozite ve Permeabiliteyi Denetleyen Mekanizmalar ", Proceedings of 9<sup>th</sup> Petroleum Congress of Turkey, p. 390-406, 1992.

- Ebanks, W.J., Scheihing, M.H., Atkinson, C.D., " Flow Units for Reservoir Characterization ", AAPG Bulletin, p. 282-289, 1984.
- Folk, R.L., " Practical Petrographic Classification of Limestones ", AAPG Bulletin, v. 43, p.1-38, 1959.
- Garfield, T.R., Hurley, N.F., Budd, D.A., " Little Sand Draw Field, Big Horn Basin, Wyoming: A Hybrid Dual-Porosity and Single Porosity Reservoir in the Phosphoria Formation ", AAPG Bulletin, v.76, no.3, p. 371-391, March, 1992.
- Görür, N. Çelikdemir, E., Dülger, S., " Carbonate Platforms Developed on Passive Continental Margins: Cretaceous Mardin Carbonates in Southeast Anatolia as an example ", Bulletin of Technical University İstanbul, v.44, p. 301-324, 1991.
- Gunter, G.W., Finneran, J.M., Hartmann, D.J., Miller, J.D., " Early Determination of Reservoir Flow Units Using an Integrated Petrophysical Method ", paper SPE 38679 prepared for presentation at the 1997 SPE Annual Technical Conference and Exhibition held in San Antonio, Texas, 5-8 October, 1997.
- Haro, F.C., " The Perfect Permeability Transform Using Logs and Cores " paper Spe 89516 prepared for presentation at the SPE Annual Technical Conference and Exhibition held in Houston, Texas, 26-29 September, 20004
- Hearn, C.L., Ebanks, W.J., Tye, R.S., Ranganathan, V., " Geological Factors Influencing Reservoir Performance of Hartzog Draw Field, Wyoming ", JPT, v.36, no.9, p. 1335-1344, 1984.
- Helander, D.P., " Fundamentals of Formation Evaluation ", Oil & Gas Consultants International Co. Publications, Tulsa, Oklahoma, 123 p., 1983.
- İşbilir, M., Kirici, S., Yılmaz, Z., " Güneydoğu Anadolu Platform Bölgesinde (X. Petrol Bölgesi) Üst Kretase Yaşlı Karbonat Rezervuarlarının Değerlendirimi ", Proceedings of 9<sup>th</sup> Petroleum Congress of Turkey, p. 436-443, 1992.
- Jennings, J.W., Lucia F.J., " Predicting Permeability From Well Logs in Carbonates With a Link to Geology for Interwell Permeability Mapping ", paper SPE 71336 prepared for presentation at the 2001 SPE Annual Technical Conference and Exhibition held in New Orleans, Louisiana, 30 September-3 October, 2001
- Johnson, W.W., " Permeability Determination From Well Logs and Core Data ", paper SPE 27647 prepared for presentation at the 1994 SPE Permian Basin Oil and Gas Recovery Conference held in Midland, Texas, 16-18 March, 1994.
- Khalaf, A.S., " Prediction of Flow Units of the Khuff Formation ", paper SPE 37739 prepared for presentation at the 1997 Middle East Oil Show held in Bahrain, 15-18 March, 1997
- Klimentos, T., " Petrophysics and Seismic Wave technology: Applications in Exploration, Formation Evaluation, and Reservoir Characterization ", paper SPE prepared for presentation at the SPE Middle East Oil Show held in Bahrain, 11-14 March, 1995.

- Karabulut, A., Köylüoğlu, M., Sayılı, A., “ Güneydoğu Anadolu Platform Bölgesinde (X. Petrol Bölgesi) Mardin Grubu ve Karaboğaz Formasyonu Rezervuarlarının Değerlendirimi “, Proceedings 9<sup>th</sup> Petroleum Congress of Turkey, p. 471-478, 1992.
- Karadavut, A., “ Petrophysical-Based Method for Flow-Unit Determination in the Phosphoria Formation, Little Sand Draw Field, Wyoming ”, Master Thesis in Geology, Colorado School of Mines, 190 p., November 2000.
- Katz, A.J., Thompson, A.H., “ Quantitative Prediction of Permeability in Porous Rocks ”, Physical Review B, v.34, no.11, p.8179-8181, December 1986.
- Kerans, C., “ Integrated Characterization of Carbonate Ramp Reservoirs Using Permian San Andres Formation Outcrop Analogs ”, AAPG Bulletin, v.78, n.2, p.181, 1994.
- Lee, S.H., Datta-Gupta, A., “ Electrofacies Characterization and Permeability Predictions in Carbonate Reservoirs: Role of Multivariate Analysis and Nonparametric Regression ”, paper SPE 56658 prepared for presentation at the 1999 SPE Annual Technical Conference and Exhibition held in Houston, Texas, 3-6 October, 1999.
- LESA, “ Log Evaluation System Analysis – Evaluation Version 4.2 “, 2004.
- Lucia, F.J., “ Petrophysical Parameters Estimated From Visual Descriptions of Carbonate Rocks: A Field Classification of Carbonate Pore Space ”, Paper JPT prepared for presentation at the 1981 SPE Annual Technical Conference and Exhibition held in San Antonio, 5-7 October, 1983.
- Lucia, F.J., Kerans, C., Senger, R.K., “ Defining Flow Units in Dolomitized Carbonate-Ramp Reservoirs ”, paper SPE 24702 prepared for presentation at the 67<sup>th</sup> Annual Technical Conference and Exhibition of SPE held in Washington, D.C., 4-7 October, 1992.
- Lucia, F.J., “ Rock-Fabric/Petrophysical Classification of Carbonate Pore Space for Reservoir Characterization ”, AAPG Bulletin, v.79, no.9, p. 1275-1300, September 1995.
- Lucia, F.J., Ruppel, S.C., “ Characterization of Diagenetically Altered Reservoirs, South Cowden Grayburg Reservoir, West Texas ”, paper SPE 36650 prepared for presentation at the 1996 SPE Annual Technical Conference and Exhibition held in Denver, Colorado, U.S.A., 5-9 October, 1996.
- Lucia, F.J., Kerans C., Jennings, J.W., “ Carbonate Reservoir Characterization “, paper SPE 82071 prepared for Technology Today Series, p. 70-72, June, 2003.
- Martin, A.J., Solomon, S.T., Hartmann, D.J., “ Characterization of Petrophysical Flow Units in Carbonate Reservoirs “, AAPG Bulletin, v.81, no.5, p. 734-759, May 1997.
- Mathisen, T., Lee, S.H., Datta-Gupta, A., “ Improved Permeability Estimates in Carbonate Reservoirs Using Electrofacies Characterization: A Case Study of the North Robinson Units, West Texas “, paper SPE 70034 prepared for presentation at the SPE Permian Oil and Gas Recovery Conference held in Midland, Texas, 15-16 May, 2001.

- Mohaghegh, S., Balan, B., Ameri, S., " State-Of-The-Art in Permeability Determination From Well Log Data: Part 2- Verifiable, Accurate Permeability Predictions, the Touch-Stone of All Models ", paper SPE 30988 prepared for presentation at SPE Eastern Regional Conference & Exhibition held in Morgantown, West Virginia, U.S.A., 17-21 September, 1995.
- Montgomery, S.L., Davies, D.K., Vessell, R.K., Kamis, J.E., Dixon, W.H., " Permian Clear Fork Group, North Robinson Unit: Integrated Reservoir Management and Characterization for Infill Drilling, Part II-Petrophysical and Engineering Data ", AAPG Bulletin, v.82, no.11, p. 1985-2002, November, 1998.
- Murray, R.C., " Origin of Porosity in Carbonate Rocks ", Journal of Sedimentary Petrology, v. 30, no.1, p. 59-84, 1971.
- Pittman, E.D., " Microporosity in Carbonate Rocks ", AAPG Bulletin, v. 61, no. 7, p. 982-1009, 1971.
- Pittman, E.D., " Relationship of Porosity and Permeability to Various Parametes Derived From Mercury Injection-Capillary Pressure Curves for Sandstone ", AAPG Bulletin, v. 76, no. 2, p. 191-198, February, 1992.
- Porras, J.C., Barbato, R., Khazen, L., " Reservoir Flow Units: A Comparison Between Three Models in the Santa Barbara and Pirital Fileds, North Monagas Area, Eastern Venezuela Basin ", paper SPE 53671 prepared for presentation at the 1999 SPE Latin American and Caribbean Petroleum Engineering Conference held in Caracas, Venezuela, 21-23 April, 1999.
- Ratchkovski, A., Ogbe, D.O., Lawal, A.S., " Application of Geostatistics and Conventional Methods to derive Hydraulic Flow Units for Improved Reservoir Description: A Case Study of Endicott Field, Alaska ", paper SPE 54587 prepared for presentation at the 1999 SPE Western Regional Meeting held in Anchorage, Alaska, 26-27 May, 1999.
- Rigo de Righi, M. R., Cortesini, A., " Gravity tectonics in foothills structure belt of Southeast Turkey ", AAPG Bulletin, v. 48, p. 1915-1937, 1964.
- Rincones, J.G., Delgado, R., Ohen, H., Enwere, P.,Guerini,A., Marquez, P., " Effective Petrophysical Fracture Characterization Using the Flow Unit Concept-San Juan Reservoir, Orocuai Fieldi Venezuela ", paper SPE prepared for presentation at the 2000 SPE Annual Technical Conference and Exhibition held in Dallas, Texas, 1-4 October, 2000
- Senger, R.K., Lucia, F.J., Kerans, C.,Ferris, M.A., " Dominant control of reservoir-flow behaviour in carbonate reservoirs as determined from outcrop studies ", Reservoir Characterization III, Tulsa,Oklahoma, PennWell Books, p.107-150, 1993.
- Saner, S., Kissami, M., Al Nufaili, S., " Estimation of Permeability From Well Logs Using Resisitivity and Saturation Data ", SPE Formation Evaluation, p. 27-31, March, 1997.

- Schlumberger Basic Log Interpretation, Schlumberger Educational Services, U.S.A, 1984.
- Schlumberger Log Interpretation Charts, Schlumberger Educational Services, U.S.A., 1988.
- Schlumberger, Log Interpretation Principles/Applications, Schlumberger Educational Services, Houston, Texas, 1989.
- Shedidi, S.A., Almehaideb, R.A, “ Enhanced Reservoir Description of Heterogeneous Carbonate Reservoirs ”, JCPT, v.42, no.7, p. 23-28, July 2003.
- Soto R., Torres, F., Arango, S., Cobaleda, G., “ Improved Reservoir permeability Models from Flow Units and Soft Computing Techniques: A Case Study, Suria and Reforma-Libertad Fields, Colombia “, paper SPE 69625 prepared for presentation at teh SPE Latin American and Caribbean Petroleum Engineering Conference held in Buenos Aires, 25-28 March, 2001.
- Sungurlu, O., “ VI. Bölge Kuzeyinin Jeolojisi ve Petrol İmkanları”, Proceedings of 2<sup>nd</sup> Petroleum Congress of Turkey, p. 85-107, 1974.
- Şengör, A.M.C., Yılmaz, Y., “ Tectonic Evolution of Turkey: A Plate Tectonic Approach “ , Tectonophysics, 75, p. 181-241, 1981.
- Şengüdüz, N., Aras, M., “ XI. ve XII. Bölgelerde Mardin Grubu Karbonatlarının ve Karaboğaz Formasyonunun Fasiyes Dağılımı, Diyajenetik Özellikleri ve Çökelme Modeli “, TPAO research Center, Report No: 2297, 51 p. , 1986.
- StatGraphics Plus 5.1., “ Evaluation Version “, 2005.
- Talabani, S., Boyd, d., Wazeer, F.E., Al-Arfi, S., “ Validity of Archie Equation in Carbonate Rocks ”, paper SPE 87301 prepared for presentation at the 9<sup>th</sup> Abu Dhabi International Petroleum Exhibition and Conference held in Abu Dhabi, U.A.E., 15-18 October, 2000.
- Tandircioğlu, A., “ Petrophysical characteristics and fluid flow in the Derdere Formation around Beşikli-Tokaris fields, SE Turkey “A Ph.D Thesis in Geological Engineering Department of METU, 131 p. , 2002.
- The University of Texas at Austin, The School of Geosciences, “ Bureau of Economic Geology “ <http://www.beg.utexas.edu>, accessed in 29 May, 2005.
- Timur, A., “ Open-Hole Well Logging”, paper SPE 10037 prepared for presentation at the International Exposition and Technical Conference, Beijing, 19-22 March, 1982.
- Tuna, D., “ Explanatory Report on LithostratigraphicUnits in the VI. Petroleum District “, Proceedings of 2<sup>nd</sup> Petroleum Congress of Turkey, p. 83-192, 1974.
- Ulu, M., “ Description and Characterization of a Carbonate Reservoir in Karababa-C Member, South Karakuş Field: Southeast Turkey ”, A Master Thesis in Geological Engineering Department of METU, 131 p. , September 1996.
- Ulu, M., Karahanoğlu, N., “ Characterization of the Karababa-C Reservoir in the South Karakuş Oilfield, Southeast Turkey ”, Marine and Petroleum Geology, v.15, p. 803-820, June 1998.

- Yao, C.Y., Holditch, S.A., " Reservoir Permeability Estimation from Time-Lapse Log Data ", paper SPE 25513 prepared for presentation at the Production Operations Symposium held in Oklahoma City, OK, U.S.A., 21-23 March, 1993
- Yarborough, P.C., " A Review of Well Log Interpretation Techniques for Carbonate Reservoirs of South-East Asia ", Proceedings of 5<sup>th</sup> Offshore South East Asia Symposium, Session 6: logging, p. 1-19, 1984,
- Wagner, C., Soylu, C., Pehlivanli, M. " Oil Habitat of the Adiyaman Area, Southeast Turkey: A joint geological-geochemical study ", TPAO Research Center, Report No: 2139, 45 p., 1986.
- Wang, F.P., " Critical Scale, Upscaling, and Modeling of Shallow Water Carbonate Reservoirs ", paper SPE 27715 prepared for presentation at the 1994 SPE Permian Basin Oil and Gas Recovery Conference held in Midland, Texas, 16-18 March, 1994
- Wang, F.P., Lucai, F.J., Kerans, C., " Integrated Reservoir Characterization Study of a Carbonate Ramp Reservoir: Seminole San Andres Unit, Gaines Country, Texas ", paper SPE 36515 prepared for presentation at the 1996 SPE Annual Technical Conference and Exhibition held in Denver, 6-9 October, 1996.
- Wardlaw, N.C., " Pore Geometry of Carbonate Rocks as Revealed by Pore Casts and Capillary Pressure ", AAPG Bulletin, v.60, pp. 245-257, 1976.
- Zimmerle, W., " Petroleum Sedimentology ", Kluwer Academic Publishers, 413 p., 1995.

## APPENDIX A

### CARBONATE ROCKS CLASSIFICATION SCHEMES

#### A.1. CLASSIFICATION BASED ON ROCK TEXTURE

##### DUNHAM CLASSIFICATION (1962)

Dunham, R.J., (1962) proposed a carbonate rock classification system utilizing some of the same principles used by Folk, R.L., (1959). In Dunham's nomenclature, textural considerations are the main discriminators of a rock including whether texture was recognizable in the rock. Another important parameter is the bound between sedimentary materials as a part of depositional process. Once the basic textural categories were assigned, relative proportion of mud in the sample should be investigated. (e.g. If the rock has no mud and it is dominated by coarse-grained sediments, then it is called as *grainstone*).

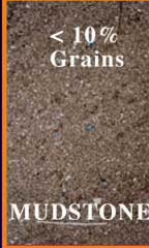
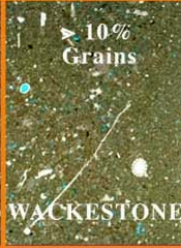
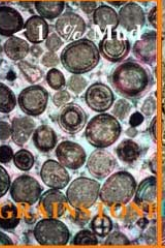
Depositional Texture Recognized				Not Recognizable
Not Bound at Deposition		Bound at Deposition		CRYSTALLINE CARBONATE
Mud-supported	Grain-supported			
<p>&lt; 10% Grains</p>  <p>MUDSTONE</p>	<p>&gt; 10% Grains</p>  <p>WACKESTONE</p>	<p>&gt; 1% Mud</p>  <p>PACKSTONE</p>	<p>&lt; 1% Mud</p>  <p>GRAINSTONE</p>	 <p>BOUNDSTONE</p>

Figure A. 1 Dunham Classification according to depositional texture

(after Dunham 1962, modified by Embry & Klovan , Carbonate Reserach Consulting, 2003, taken from [www.crienterprises.com](http://www.crienterprises.com) )

## A.2. CLASSIFICATION BASED ON POROSITY AND PORE SYSTEMS

### CHOQUETTE & PRAY CLASSIFICATION (1970)

This classification is utilized to categorize carbonate pore space for questions on how the pore systems evolved.

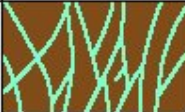
Fabric-selective		Not fabric-selective		Fabric-selective or not	
	Interparticle		Fracture		Breccia
	Intraparticle				
	Intercrystal		Channel		Boring
	Moldic		Vug		Burrow
	Fenestral				
	Shelter		Cavern*		Shrinkage
	Growth-framework	*Cavern applies to man-sized or larger pores of channel or vug shapes			

Figure A. 2 Geological classification of pores and pore systems in carbonate rocks (after Choquette and Pray, 1970)

### LUCIA CLASSIFICATION (1999)

This classification describes the relationships between carbonate rock fabrics and petrophysical properties. Vuggy porosity is pore space that is within grains or crystals or that is significantly larger than grains or crystals. In the absence of vuggy porosity, pore-size distribution in carbonate rocks can be described in terms of particle size, sorting, and interparticle porosity.

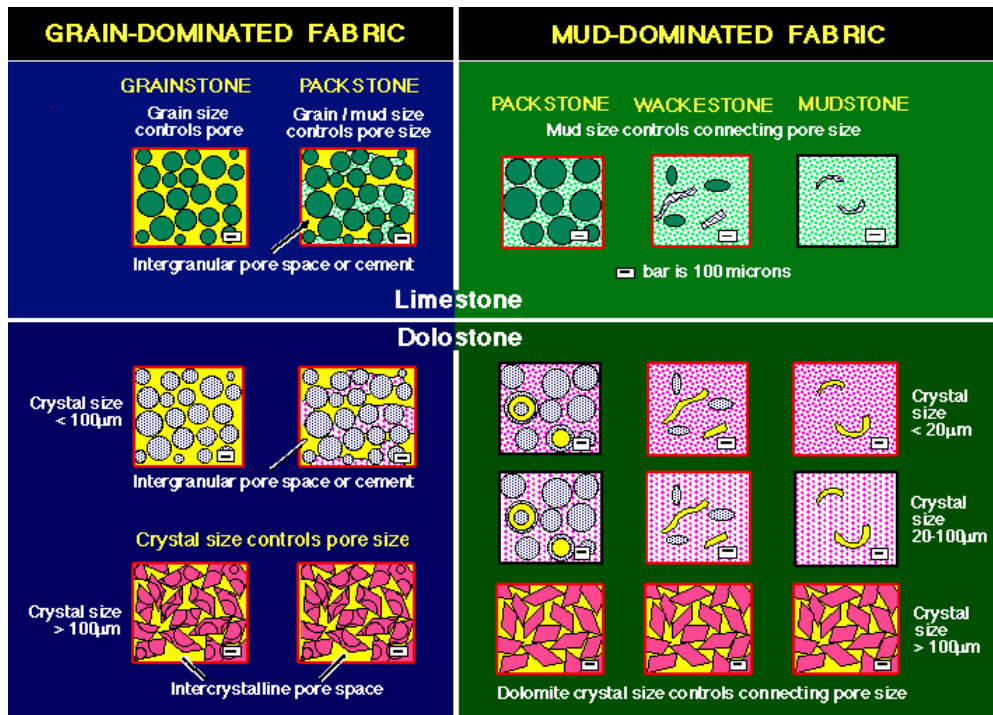


Figure A. 3 Classification of carbonates by interparticle pore space (Lucia, 1995)  
(taken from <http://www.beg.utexas.edu> )

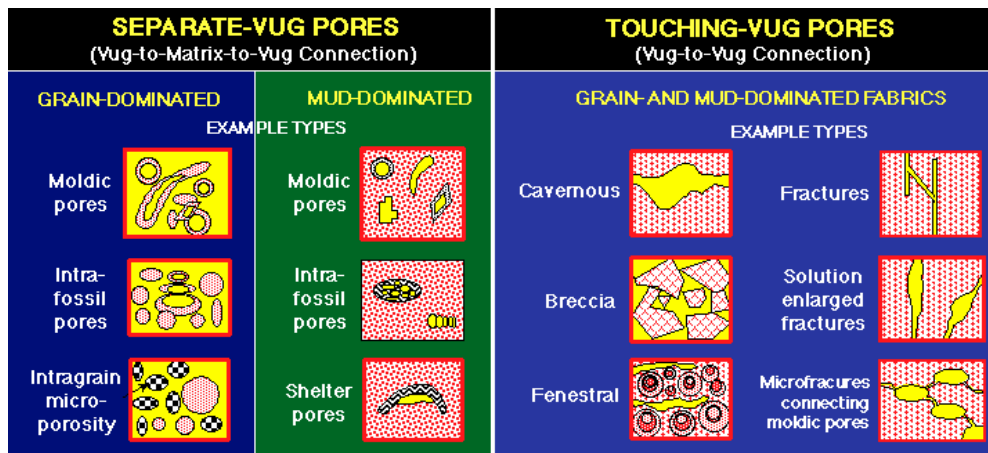


Figure A. 4 Classification of carbonates by vuggy pore space (Lucia, 1995)  
(taken from <http://www.beg.utexas.edu> )

## APPENDIX B

### WELL LOGGING DATA

#### B.1. WELL A

Table B. 1 Well Log Data -Well A

Depth (m)	GR (API)	$\Delta t$ ( $\mu\text{s}/\text{ft}$ )	$\rho_b$ (g/cc)	PHIN (%)	MSFL ( $\Omega\cdot\text{m}$ )	LLS ( $\Omega\cdot\text{m}$ )	LLD ( $\Omega\cdot\text{m}$ )	Lithology
1946	70	60	2.64	12	120	120	120	Sayindere (Marn)
1947	190	60	2.59	13	90	150	150	
1948	30	64	2.52	12	150	150	140	
1949	20	65	2.44	15.5	110	160	130	
1950	19	60	2.56	10.5	170	130	100	
1951	43	60.5	2.6	9.5	200	150	100	Derdere Limestone
1952	35	65	2.44	18	100	90	80	
1953	19	65.5	2.53	12	110	80	60	
1954	29	60	2.53	10	200	190	170	
1955	28	55.5	2.64	4	500	200	190	
1956	45	53	2.69	3	110	250	200	
1957	30	52	2.71	2	35	470	470	
1958	24	51	2.67	3	70	200	200	
1959	15	53	2.6	4	50	200	200	
1960	15	59	2.46	13	150	140	140	
1961	16	53	2.65	6	300	170	150	
1962	23	57	2.63	12	40	100	100	
1963	25	61	2.6	9	30	65	65	
1964	16	60	2.55	15	70	200	200	
1965	39	67	2.46	21	12	30	30	
1966	33	55	2.74	3.5	60	60	60	
1967	40	52	2.74	4	60	160	200	
1968	43	50	2.56	2	15	250	320	
1969	50	49	2.63	2	7	250	320	
1970	35	50	2.7	4	10	300	400	
1971	38	56	2.45	15	7	40	50	

Table B.1, (cont'd)

Depth (m)	GR (API)	$\Delta t$ ( $\mu\text{s}/\text{ft}$ )	$\rho_b$ (g/cc)	PHIN (%)	MSFL ( $\Omega\cdot\text{m}$ )	LLS ( $\Omega\cdot\text{m}$ )	LLD ( $\Omega\cdot\text{m}$ )	Lithology
1972	36	65	2.55	19	5	20	26	Dolomitic Shale
1973	41	62	2.62	15	10	28	37	
1974	100	69	2.42	21	3	9	12	
1975	70	68	2.64	20	2	9	11	
1976	41	72	2.41	30	6	10	12	
1977	21	70	2.4	27	18	400	500	Derdere Dolomite
1978	19	65	2.48	22	21	600	900	
1979	18	67	2.45	24.5	23	700	1000	
1980	20	65	2.47	21	28	700	1000	
1981	21	64	2.5	22	35	800	1100	
1982	22	68	2.54	21.5	70	500	600	
1983	21	69	2.5	24.5	22	400	600	
1984	20	65	2.47	24	35	300	350	
1985	32	68	2.52	21	20	400	500	
1986	25	65	2.48	22	70	600	800	
1987	24	63	2.59	20.5	20	600	800	
1988	25	63.5	2.5	21	60	300	400	
1989	22	60	2.63	12	80	200	200	
1990	21	56	2.57	15	140	180	180	
1991	22	59	2.59	15	70	310	400	
1992		58	2.6	9.5	100	310	400	
1993		58	2.6	9	200	310	400	
1994		58	2.65	3	270			

## B.2. WELL B

Table B. 2 Well Log Data - Well B

Depth (m)	GR (API)	$\Delta t$ ( $\mu s/ft$ )	$\rho_b$ (g/cc)	PHIN (%)	MSFL ( $\Omega.m$ )	LLS ( $\Omega.m$ )	LLD ( $\Omega.m$ )	Lithology
1927	30	56.5	2.57	7	120	170	170	Sayindere (Marn)
1928	31	60	2.58	7	210	200	200	
1929	41	63	2.55	7	110	200	300	
1930	80	66	2.53	6	100	150	200	
1931	170	65	2.45	9	20	50	50	
1932	140	55.5	2.46	9	30	35	35	
1933	65	55	2.59	6	200	110	150	Derdere Limestone
1934	40	56	2.57	8.5	200	300	300	
1935	120	62	2.52	12	100	260	250	
1936	45	55	2.48	12	140	130	100	
1937	40	55	2.6	7.5	210	310	280	
1938	40	58	2.63	6.5	380	300	250	
1939	30	55	2.57	9	280	290	150	
1940	16	68	2.55	12	200	280	250	
1941	23	60	2.35	23	170	200	200	
1942	20	55	2.55	12	100	150	150	
1943	20	60	2.65	10	60	100	100	
1944	20	57	2.45	15	50	70	70	
1945	15	70	2.5	12	100	100	100	
1946	14	71	2.35	20	70	90	100	
1947	21	60	2.4	18	50	50	60	
1948	20	61	2.6	12	80	70	80	
1949	18	53	2.56	12	100	80	80	
1950	20	65	2.6	7	90	80	80	
1951	25	55	2.45	21	50	100	100	
1952	20	51	2.7	15	23	30	30	
1953	20	50	2.78	3	140	140	140	
1954	19	50	2.75	3	2000	200	300	
1955	20	51	2.7	3	40	300	500	
1956	28	55	2.72	3	20	300	500	
1957	32	65	2.6	18	30	70	80	Dolomitic Shale
1958	58	70	2.68	17	10	20	25	
1959	60	73.5	2.68	21	4	7	10	
1960	20	70	2.65	22	4	6	7	
1961	20	65	2.58	26.5	15	20	20	Derdere Dolomite
1962	20	62	2.4	27	40	600	1000	
1963	18	60	2.47	23	40	800	1500	
1964	17	63	2.53	24	100	900	1500	
1965	25	65	2.45	24	70	600	800	
1966		58	2.42	24	50	800	1000	
1967		60	2.45	20.5	60	1300	1900	
1968		65	2.39	21	60	700	900	

### B.3. WELL C

Table B. 3 Well Log Data - Well C

Depth (m)	GR (API)	$\Delta t$ ( $\mu s/ft$ )	$\rho_b$ (g/cc)	PHIN (%)	MSFL ( $\Omega.m$ )	LLS ( $\Omega.m$ )	LLD ( $\Omega.m$ )	Lithology
1905	32	64	2.64	10	27	27	27	Sayindere (Marn)
1906	32	63	2.63	9	20	26	25	
1907	34	65	2.64	9	15	20	20	
1908	60	60	2.6	9	50	70	70	
1909	70	66	2.5	12	45	50	50	Derdere Limestone
1910	50	60	2.57	7	200	190	150	
1911	30	57	2.56	6	400	350	300	
1912	31	66	2.46	12	200	140	100	
1913	20	67	2.6	9	180	150	100	
1914	19	55	2.66	5	200	200	200	
1915	31	53	2.57	5	150	190	190	
1916	30	54	2.56	6	200	180	180	
1917	19	64	2.45	14.5	170	180	180	
1918	20	57	2.6	3	190	200	200	
1919	20	51	2.67	1	70	350	350	
1920	21	54	2.6	3	200	190	190	
1921	18	59	2.4	15	110	90	90	
1922	19	66	2.45	12	100	70	60	
1923	20	52	2.3	0	6	300	300	
1924	20	50	2.55	0	7	2000	2000	
1925	25	52	2.6	6	23	400	400	
1926	22	51	2.5	2	180	290	290	
1927	23	50	2.45	0	5	600	700	
1928	25	49	2.55	0	5.5	600	700	
1929	28	50	2.67	0	8	600	700	
1930	30	50	2.66	1	40	450	550	
1931	35	56	2.65	12.5	18	70	80	Dolomitic Shale
1932	65	60	2.68	16	20	30	40	
1933	60	61	2.65	17.5	20	20	23	
1934	40	70	2.6	23	8	17	20	
1935	31	70	2.44	25	30	60	70	
1936	15	60	2.5	21	65	1000	1500	Derdere Dolomite
1937	12	63	2.5	22	60	1500	2000	
1938	15	65	2.51	23	45	900	1000	
1939	15	65	2.44	21.5	45	230	300	
1940	15	65	2.47	16	80	200	200	
1941	15	65	2.5	13	20	200	200	
1942	10	60	2.57	15	180	200	300	
1943		55	2.5	19	100	100	100	
1944		62	2.6	15	100			
1945		62	2.49	15	4			
1946			2.51	16.5	4			
1947			2.42	9	2.5			

## B.4. WELL D

Table B. 4 Well Log Data - Well D

Depth (m)	GR (API)	$\Delta t$ ( $\mu s/ft$ )	$\rho_b$ (g/cc)	PHIN (%)	MSFL ( $\Omega.m$ )	LLS ( $\Omega.m$ )	LLD ( $\Omega.m$ )	Lithology
1825	31	65	2.54	15.5	40	50	55	Sayindere (Marn)
1826	30	64.5	2.57	15	50	70	70	
1827	30	64.5	2.55	15.5	45	50	50	
1828	30	63.5	2.57	15.5	90	90	90	
1829	40	61	2.59	15	90	100	100	Derdere Limestone
1830	120	61.5	2.55	15.5	200	200	200	
1831	31	65	2.45	18	80	200	200	
1832	33	61	2.46	18.5	200	400	400	
1833	37	65	2.46	16	100	170	190	
1834	29	60	2.5	14	50	100	120	
1835	30	65	2.5	12	7	120	120	
1836	17	52	2.45	9	6	250	250	
1837	21	82	2.45	15	1.5	18	18	
1838	30	56	2.61	6	4.5	100	100	
1839	20	60	2.45	12	15	300	400	
1840	13	75	2.3	24	40	300	400	
1841	18	70	2.35	18	35	300	400	
1842	19	60	2.45	12	100	200	220	
1843	15	65	2.35	15	90	250	300	
1844	13	75	2.26	24	65	210	260	
1845	15	60	2.45	15	30	290	310	
1846	18	61	2.35	13	40	150	150	
1847	15	55	2.45	4	65	190	190	
1848	21	54	2.5	3	7	130	130	
1849	17	54	2.62	2	30	130	130	
1850	20	51	2.57	4	6	400	500	
1851	17	50	2.62	3	4	700	800	
1852	20	50	2.68	5	2.3	500	610	
1853	20	51	2.66	6	3	40	40	
1854	30	60	2.55	15	20	28	30	
1855	39	60	2.52	26	3	20	20	Dolomitic Shale
1856	48	62	2.65	21	7	15	16	
1857	46	65	2.5	24	7	14	15	
1858	35	74	2.46	30	7	14	14	
1859	11	69	2.31	33	50	150	200	Derdere Dolomite
1860	13	65	2.45	27	60	290	400	
1861	15	65	2.45	30	40	290	400	
1862	16	65	2.45	30	30	300	400	
1863	23	65	2.47	26	50	390	400	
1864	26	65	2.45	27	35	450	600	
1865	30	62	2.45	23	120	500	600	
1866	40	65	2.36	27	17	450	550	
1867	35	64	2.5	24	80	400	500	

Table B.4, (cont'd)

Depth (m)	GR (API)	$\Delta t$ ( $\mu s/ft$ )	$\rho_b$ (g/cc)	PHIN (%)	MSFL ( $\Omega.m$ )	LLS ( $\Omega.m$ )	LLD ( $\Omega.m$ )	Lithology
1868	31	64	2.46	27	45	320	400	Derdere Dolomite
1869	30	64.5	2.45	29	50	250	300	
1870	32	62	2.51	21	40	280	300	
1871	40	59	2.55	21	40	290	300	
1872	38	50	2.6	16	70	200	310	
1873	28	65	2.36	27	25	300	320	
1874	35	60	2.45	23	50	300	350	
1875	35	66	2.37	27	27	190	200	
1876	40	66	2.45	24	20	250	300	
1877	41	57	2.56	21	80	390	500	
1878	25	65	2.43	27	30	300	350	
1879	25	65	2.45	28	40	190	200	
1880	20	65	2.35	27	25	100	100	
1881	19	70	2.36	27	30	50	50	
1882	40	60	2.5	21.5	30	60	60	
1883	25	65	2.48	21	35	200	230	
1884	24	60	2.55	21	50	130	170	
1885	30	65	2.5	24	25	70	80	
1886	24	69	2.46	28	20	45	50	

## B.5. WELL X

Table B. 5 Well Log Data - Well X

Depth (m)	GR (API)	$\Delta t$ ( $\mu\text{s}/\text{ft}$ )	Lithology	
1842	130	65	Derdere Limestone	
1843	50	59		
1844	28	70		
1845	22	55		
1846	26	54		
1847	31	65		
1848	28	55		
1849	50	55		
1850	30	65		
1851	18	73		
1852	17	78		
1853	18	71		
1854	19	65		
1855	13	73		
1856	14	72		
1857	12	70		
1858	19	57		
1859	20	55		
1860	19	56		
1861	22	64		
1862	21	50		
1863	26	50		
1864	28	50		
1865	29	50		
1866	32	50		
1867	31	54		
1868	30	55	Dolomitic Shale	
1869	50	61		
1870	55	71		
1871	62	85	Derdere Dolomite	
1872	13	68		
1873	14	75		
1874	14	60		
1875	15	63		
1876	15	67		
1877	20	65		
1878	20	71		
1879	20	71		
1880	20	63		
1881	20	65		
1882	22	63		
1883	20	56		

## APPENDIX C

### CORE PLUG DATA

Table C. 1 Core plug data for the studied wells

Well	Year	Depth Interval (m)	Plug Depth (m)	Porosity (%)	k air (md)	k liq. (md)	Grain Density (g/cc)
A	1999	1970.5-1971.5	1971.95	25.16	192.34	179.32	2.82
A	1999	1970.5-1971.5	1971.30	21.26	85.62	76.04	2.83
B	1988	1950-1959	1950.60	5.14	0.06	0.03	2.80
B	1988	1950-1959	1951.60	5.12	0.02	0.01	2.78
B	1988	1950-1959	1952.70	2.33	0.02	0.01	2.75
B	1988	1950-1959	1953.50	2.93	0.03	0.02	2.75
B	1988	1950-1959	1954.50	1.93	0.02	0.01	2.71
B	1988	1950-1959	1955.60	2.13	0.03	0.02	2.74
B	1988	1950-1959	1956.60	7.73	0.76	0.51	2.79
B	1988	1950-1959	1957.70	8.10	0.07	0.04	2.77
D	1989	1887-1893	1887.10	26.20	258.95	238.95	2.83
D	1989	1887-1893	1890.60	18.72	12.88	10.21	2.84
D	1989	1887-1893	1891.45	1.53	0.01	0.01	2.67
D	1990	1887-1893	1887.20	24.89	270.41	250.41	2.81
D	1990	1887-1893	1887.35	24.04	84.87	75.33	2.82
D	1990	1887-1893	1887.65	23.54	247.67	227.67	2.82
D	1990	1887-1893	1887.05	20.34	87.35	77.67	2.81
D	1990	1887-1893	1888.35	17.07	34.86	29.33	2.82
D	1990	1887-1893	1888.50	22.88	132.35	120.65	2.82
D	1990	1887-1893	1888.60	23.82	195.17	175.17	2.82
D	1990	1887-1893	1889.10	16.24	10.83	8.50	2.82
D	1990	1887-1893	1889.45	17.21	11.82	9.32	2.82
D	1990	1887-1893	1890.05	10.75	1.32	0.91	2.82
D	1990	1887-1893	1890.50	9.02	0.43	0.28	2.83
D	1990	1887-1893	1890.75	15.16	1.73	1.22	2.80
D	1990	1887-1893	1890.85	17.04	5.41	4.10	2.81
D	1990	1887-1893	1891.40	18.12	4.02	2.97	2.82
D	1990	1887-1893	1891.60	18.41	18.53	15.01	2.83
D	1990	1887-1893	1891.90	18.81	5.63	4.25	2.83
D	1990	1887-1893	1892.05	18.97	7.03	5.37	2.80
D	1990	1887-1893	1892.50	19.69	6.31	4.79	2.81
D	1990	1887-1893	1892.60	20.97	8.33	6.43	2.79
D	1990	1887-1893	1892.80	20.82	6.69	5.10	2.79

Table C.1, (cont'd)

Well	Year	Depth	Plug Depth	Porosity	k air	k liq.	Grain Density
		Interval (m)	(m)	(%)	(md)	(md)	(g/cc)
X	1981	1845.25-1857	1845.40	21.60	1.69	1.19	2.74
X	1981	1845.25-1857	1845.40	25.06	3.75	2.76	2.80
X	1981	1845.25-1857	1845.50	23.82	2.87	2.08	2.76
X	1981	1845.25-1857	1845.60	24.94	35.53	29.93	2.72
X	1987	1848.25-1957	1851.55	19.45	3.02	2.19	2.75
X	1987	1848.25-1957	1849.95	15.22	4.45	3.31	2.70
X	1987	1848.25-1957	1851.45	19.25	2.70	1.95	2.72
X	1987	1857-1862	1858.60	10.13	0.26	0.16	2.77
X	1987	1862-1867	1862.60	0.97	0.05	0.03	2.71
X	1987	1862-1867	1864.65	3.01	0.06	0.03	2.72
X	1981	1867-1872	1867.20	23.86	112.96	102.00	2.84
X	1981	1867-1872	1867.39	20.56	45.16	38.60	2.85
X	1987	1867-1972	1867.80	29.03	595.56	565.56	2.81
X	1981	1872-1877	1872.34	26.05	264.64	244.64	2.82
X	1981	1872-1877	1872.85	26.93	369.13	339.13	2.84
X	1981	1877-1882	1877.22	21.29	57.64	49.99	2.83
X	1981	1877-1882	1877.15	23.74	137.51	125.64	2.83
X	1981	1877-1882	1877.80	23.51	67.83	59.40	2.70
X	1981	1882-1887	1882.28	25.36	269.13	249.13	2.85
X	1987	1872-1877	1874.70	27.19	192.09	172.09	2.81
X	1987	1872-1877	1872.90	19.57	67.88	59.45	2.76
X	1987	1877-1882	1878.85	19.57	42.72	36.39	2.82
X	1987	1877-1882	1879.25	20.33	34.02	28.59	2.82
X	1981	1882-1887	1882.37	32.19	5.79	4.37	2.42
X	1987	1882-1887	1882.40	13.36	1.60	1.12	2.71

## APPENDIX D

### WELL LOG DERIVED PARAMETERS

#### D.1. Lithology Fractions

Table D. 1 Lithology Fractions - Well A

Depth ( m )	Dolomite (%)	Limestone (%)	Lithology
1949			Derdere Limestone
1950	5	95	
1951	20	80	
1952	5	95	
1953	5	95	
1954	0	100	
1955	0	100	
1956	5	95	
1957	5	95	
1958	3	97	
1959			
1960			
1961	10	90	
1962	50	50	
1963	10	90	
1964	30	70	
1965	50	50	
1966	30	70	
1967	30	70	
1968	0	100	
1969			
1970	20	80	Dolomitic Shale
1971	0	100	
1972	50	50	
1973	60	40	
1974	40	60	
1975	100	0	
1976	95	5	
1977	60	40	

Table D.1, (cont'd)

Depth ( m )	Dolomite (%)	Limestone (%)	Lithology
1978	50	50	Derdere Dolomite
1979	60	40	
1980	50	50	
1981	60	40	
1982	70	30	
1983	70	30	
1984	60	40	
1985	60	40	
1986	50	50	
1987	90	10	
1988	50	50	
1989	50	50	
1990	50	50	
1991	50	50	
1992	10	90	
1993	10	90	
1994	0	100	

Table D. 2 Lithology Fractions - Well B

Depth ( m )	Dolomite (%)	Limestone (%)	Lithology
1932			Derdere Limestone
1933			
1934	0	100	
1935	3	97	
1936			
1937	3	97	
1938	10	90	
1939	3	97	
1940	15	85	
1941	10	90	
1942	15	85	
1943	30	70	
1944	0	100	
1945	0	100	
1946			
1947	0	100	
1948	30	70	
1949	20	80	

Table D.2, (cont'd)

Depth ( m )	Dolomite (%)	Limestone (%)	Lithology
1950	0	100	Derdere Limestone
1951	30	70	
1952	80	20	
1953	50	50	
1954	30	70	
1955	20	80	
1956	20	80	
1957	70	30	
1958	95	5	
1959			Dolomitic Shale
1960			
1961			
1962	70	30	Derdere Dolomite
1963	50	50	
1964	10	90	
1965	60	40	
1966	50	50	
1967	40	60	
1968	20	80	

Table D. 3 Lithology Fractions - Well C

Depth ( m )	Dolomite (%)	Limestone (%)	Lithology
1909	0	100	Derdere Limestone
1910			
1911			
1912			
1913	20	80	
1914	10	90	
1915			
1916			
1917			
1918			
1919			
1920			
1921			
1922			
1923			
1924			
1925	0	100	

Table D.3, (cont'd)

Depth ( m )	Dolomite (%)	Limestone (%)	Lithology
1926			
1927			
1928			
1929			
1930			
1931	50	50	
1932	10	90	Dolomitic Shale
1933	10	90	
1934			
1935	60	40	
1936	60	40	
1937	60	40	
1938	70	30	
1939	40	60	
1940	20	80	
1941	5	95	
1942	50	50	
1943	50	50	
1944	50	50	
1945	20	80	
1946	30	70	
1947			

Table D. 4 Lithology Fractions - Well D

Depth ( m )	Vsh(%)	Limestone (%)	Dolomite (%)	Lithology
1829	30	35	65	Derdere Limestone
1830	25	60	40	
1831	10	70	30	
1832	17	80	20	
1833	3	85	15	
1834	3	85	15	
1835	0	100	0	
1836				
1837	0	100	0	
1838	1	99	1	
1839				
1840	0	100	0	
1841	10	80	20	
1842	10	80	20	
1843	15	60	40	

Table D.4, (cont'd)

Depth ( m )	Vsh(%)	Limestone (%)	Dolomite (%)	Lithology
1844	5	90	10	Derdere Limestone
1845	0	100	0	
1846	5	95	5	
1847				
1848	13	80	20	
1849	10	70	30	
1850	11	70	30	
1851				
1852	13	70	17	
1853	10	80	10	
1854	45	40	15	
1855	60	0	40	Dolomitic Shale
1856	50			
1857	30			
1858	50			Derdere Dolomite
1859	40	16	44	
1860	30	5	65	
1861	30	0	100	
1862	30	0	100	
1863	30	5	95	
1864	30	5	95	
1865	3	47	53	
1866	0	50	50	
1867	11	25	75	
1868	15	5	95	
1869	20	3	97	
1870	10	20	80	
1871	10	20	80	
1872	5	25	75	
1873	0	50	50	
1874	3	47	53	
1875	4	48	52	
1876	10	20	80	
1877	21	10	90	
1878	20	10	90	
1879	20	10	90	
1880	0	50	50	
1881	0	50	50	
1882	10	20	80	
1883	0	50	50	
1884	20	10	90	
1885	25	25	75	
1886	40	5	95	

\* The gray-filled intervals are the readings affected by borehole.

## D.2. Well-Log Derived Porosities

Table D. 5 Porosities – Well A

Depth ( m )	$\emptyset_s$ (%)	$\emptyset_{ob}$ (%)	$\emptyset_{D-N}$ (%)	Lithology
1949				Derdere Limestone
1950	12.49	9.20	9.50	
1951	9.35	8.15	8.00	
1952	9.32	16.18	17.00	
1953	12.49	10.94	11.50	
1954	12.72	10.53	10.00	
1955	8.83	4.09	4.00	
1956	5.79	1.63	2.20	
1957	4.02	0.47	1.50	
1958	3.26	2.61	2.80	
1959				
1960				
1961	8.39	4.40	4.80	
1962	5.23	8.94	8.50	
1963	6.98	7.30	7.50	
1964	10.30	11.83	12.30	
1965	10.10	18.44	18.00	
1966	14.51	1.02	1.20	
1967	6.10	1.02	2.00	
1968	3.18	8.77	2.20	
1969				
1970	1.62	2.41	2.30	
1971	1.77	15.20	15.00	
1972	7.32	13.41	14.20	
1973	13.83	10.30	10.10	
1974	11.25	19.95	18.50	
1975	17.53	12.30	12.00	
1976	16.72	24.27	23.50	
1977	18.69	22.48	23.00	
1978	17.07	17.32	18.00	
1979	13.83	19.71	20.00	
1980	14.98	17.88	17.80	
1981	13.83	16.94	17.00	
1982	13.37	15.48	15.50	
1983	16.15	17.67	18.50	
1984	16.61	18.60	19.00	
1985	13.83	15.84	16.00	
1986	15.68	17.32	18.00	
1987	14.54	14.24	14.00	
1988	12.20	16.20	17.00	
1989	12.54	8.94	8.50	
1990	10.10	12.29	11.80	
1991	7.32	11.17	11.00	
1992	8.39	7.30	8.00	
1993	7.68	7.30	7.50	
1994	7.42	3.51	3.00	
				Dolomitic Shale
				Derdere Dolomite

Table D. 6 Porosities – Well B

Depth ( m )	$\emptyset_s$ (%)	$\emptyset_{pb}$ (%)	$\emptyset_{D-N}$ (%)	Lithology
1932				Derdere Limestone
1933				
1934	5.30	8.19	8.30	
1935	6.09	11.36	11.80	
1936				
1937	5.38	6.69	7.00	
1938	5.57	5.56	5.80	
1939	7.50	8.44	8.50	
1940	5.70	10.61	10.80	
1941	14.73	21.78	22.00	
1942	9.22	10.61	10.80	
1943	6.10	6.14	7.00	
1944	8.83	15.20	15.00	
1945	6.71	12.28	12.00	
1946				
1947	16.61	18.13	18.00	
1948	9.60	8.99	9.00	
1949	10.05	10.45	10.20	
1950	3.89	6.43	6.80	Derdere Limestone
1951	13.10	17.52	18.00	
1952	7.39	7.51	8.00	
1953	3.83	0.56	0.80	
1954	2.59	0.46	0.50	
1955	2.32	2.41	2.00	
1956	3.02	1.26	1.30	
1957	7.14	12.18	12.20	
1958	14.66	9.77	9.50	Dolomitic Shale
1959				
1960				
1961				
1962	14.07	23.16	23.00	Derdere Dolomite
1963	11.50	17.88	18.50	
1964	9.09	11.36	16.00	
1965	12.44	19.71	19.00	
1966	13.59	20.67	20.00	
1967	8.46	18.26	18.00	
1968	9.35	20.21	20.00	

Table D. 7 Porosities – Well C

Depth ( m )	$\emptyset_s$ (%)	$\emptyset_{pb}$ (%)	$\emptyset_{D-N}$ (%)	Lithology
1909	13.07	12.28	12	Derdere Limestone
1910				
1911				
1912				
1913	14.27	8.15	7.80	
1914	5.57	3.82	4.00	
1915				
1916				
1917				
1918				
1919				
1920				
1921				
1922				
1923				
1924				
1925	3.18	6.43	6.00	
1926				
1927				
1928				
1929				
1930				
1931	7.32	7.82	8.00	Dolomitic Shale
1932	9.09	2.67	9.00	
1933	9.80	4.40	10.20	
1934				
1935	17.30	20.27	20.00	Derdere Dolomite
1936	10.35	16.94	16.50	
1937	12.44	16.94	16.00	
1938	14.07	17.12	17.00	
1939	13.35	18.83	19.00	
1940	12.86	15.61	15.00	
1941	12.49	12.69	12.70	
1942	10.10	12.29	12.00	
1943	6.62	16.20	15.80	
1944	11.50	10.61	11.00	
1945	10.75	14.47	14.00	
1946			14.30	
1947				

Table D. 8 Porosities – Well D

Depth ( m )	$\emptyset_s$ (%)	$\emptyset_{pb}$ (%)	$\emptyset_{D-N}$ (%)	Lithology
1829	18.55	7.02	4.0	Derdere Limestone
1830	17.19	9.36	6.0	
1831	15.67	15.20	13.5	
1832	14.49	15.20	12.0	
1833	13.53	14.62	14.0	
1834	10.04	12.28	11.7	
1835	12.37	12.28	12.0	
1836				
1837	24.38	15.20	15.0	
1838	6.32	5.85	5.1	
1839				
1840	19.43	23.98	24.0	
1841	18.85	18.13	17.5	
1842	12.04	12.28	12.5	
1843	17.13	15.20	13.5	
1844	20.87	23.98	24.5	Derdere Limestone
1845	8.83	15.20	15.0	
1846	11.03	14.62	21.0	
1847				
1848	8.76	2.92	0.0	
1849	8.19	0.58	0.0	
1850	6.43	3.51	3.0	
1851				
1852	6.31	1.75	0.0	
1853	5.90	2.92	1.0	
1854	21.09	9.36	4.0	Dolomitic Shale
1855	24.83	18.72	3.5	
1856			10.0	
1857			18.2	
1858			20.0	Derdere Dolomite
1859	26.04	14.44	27.0	
1860	21.69	22.46	23.0	
1861	21.79	22.46	23.0	
1862	21.79	22.46	23.0	
1863	21.69	21.39	20.1	
1864	21.69	22.46	22.0	
1865	12.37	22.46	19.0	
1866	13.59	27.27	24.0	
1867	16.27	19.79	17.0	
1868	17.67	21.93	21.0	
1869	19.20	22.46	22.2	

Table D.8, (cont'd)

Depth ( m )	$\emptyset_s$ (%)	$\emptyset_{pb}$ (%)	$\emptyset_{D-N}$ (%)	Lithology
1870	14.79	19.25	16.0	Derdere Dolomite
1871	12.78	17.11	15.5	
1872	5.23	14.44	11.5	
1873	13.59	27.27	24.0	
1874	10.99	22.46	19.0	
1875	15.36	26.74	23.2	
1876	17.48	22.46	20.0	
1877	14.42	16.58	15.0	
1878	19.38	23.53	22.0	
1879	19.38	22.46	21.8	
1880	13.59	27.81	24.0	
1881	17.07	27.27	24.0	
1882	13.45	19.79	17.0	
1883	13.59	20.86	17.5	
1884	16.12	17.11	15.5	
1885	20.19	19.79	18.2	
1886	26.24	21.93	22.0	

### D.3. Depth vs. Porosity Plots

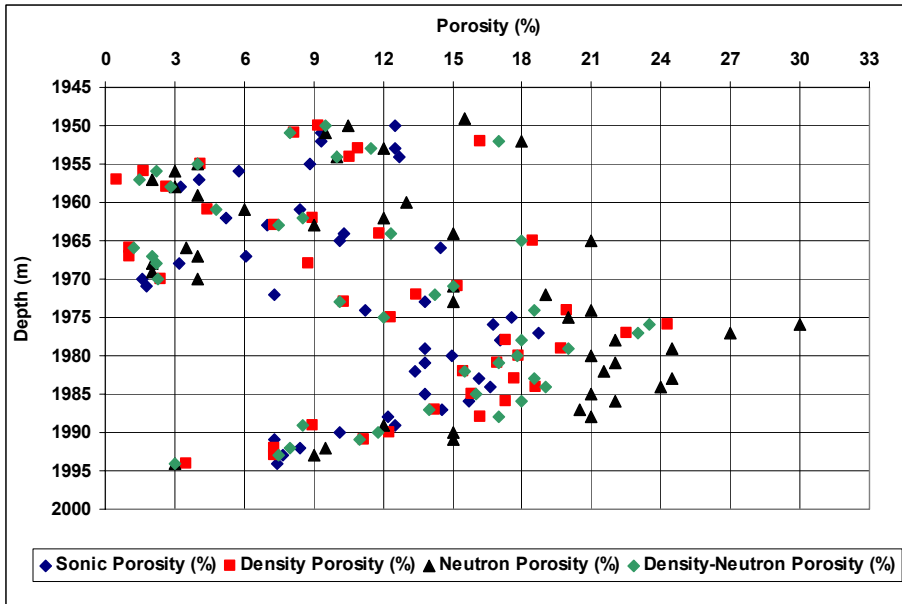


Figure D. 1 Depth vs. Well log derived porosities – Well A

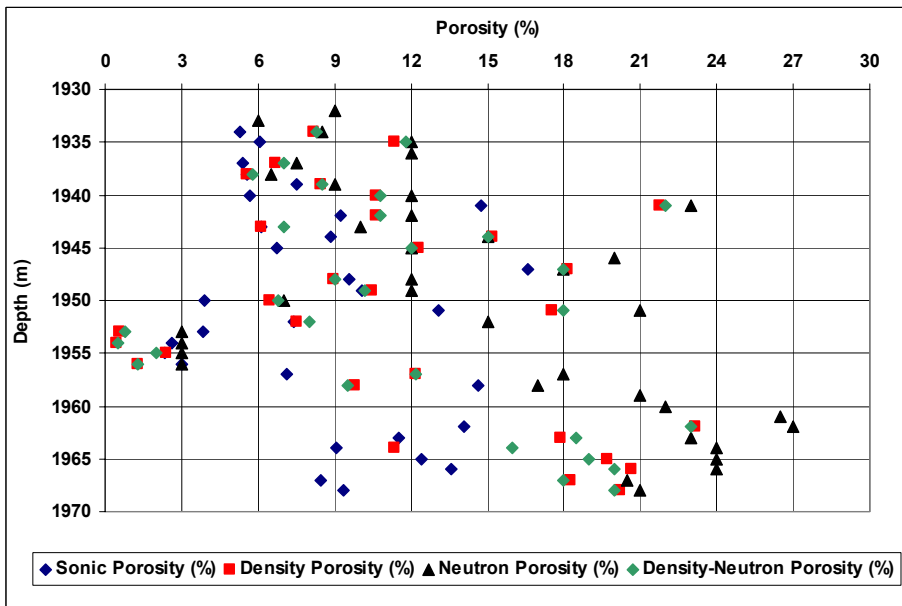


Figure D. 2 Depth vs. Well log derived porosities – Well B

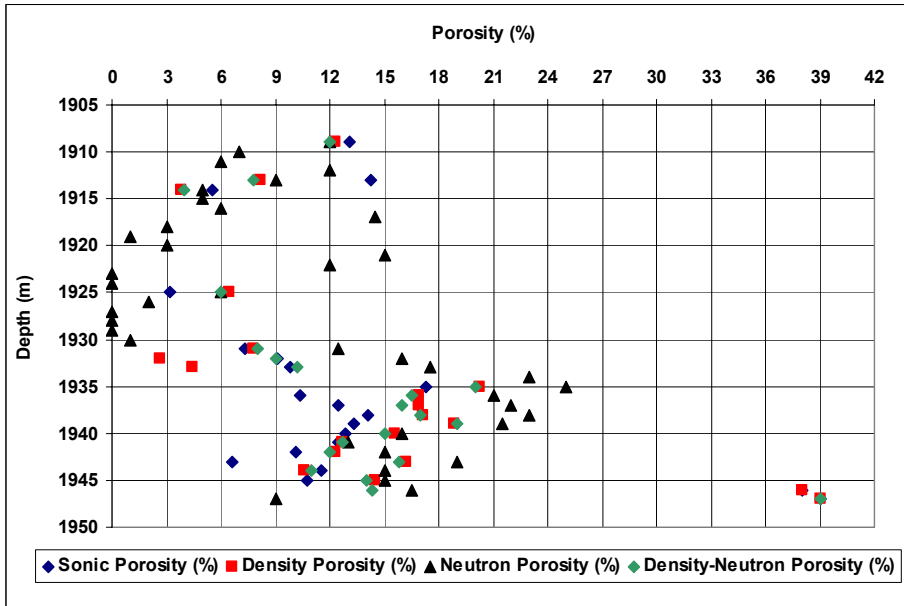


Figure D. 3 Depth vs. Well log derived porosities – Well C

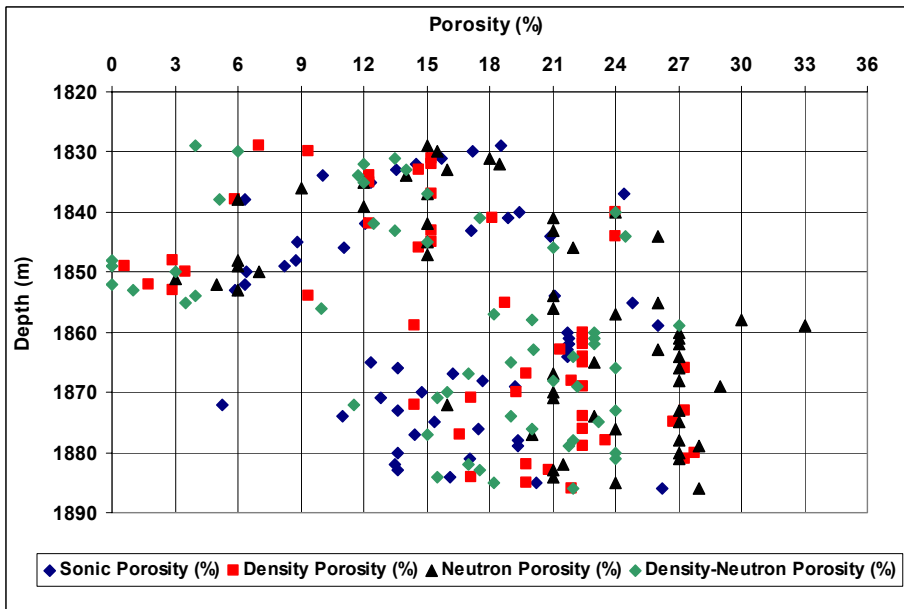


Figure D. 4 Depth vs. Well log derived porosities – Well D



## D.4. Saturations

Table D.9 Saturations - Well A

Depth ( m )	F	Sw (%)	Sxo (%)	ROS (%)	MOS (%)	Ro (Ω.m)	Lithology
1949							Derdere Limestone
1950	90.25	38.76	30.90	69.10	0.00	14.26	
1951	64.00	31.80	24.00	76.00	0.00	10.11	
1952	289.00	75.55	72.12	27.88	0.00	45.66	
1953	132.25	57.73	46.50	53.50	0.00	20.90	
1954	100.00	31.25	30.00	70.00	0.00	15.80	
1955	16.00	12.26	7.60	92.40	0.00	2.53	
1956	4.84	6.04	8.70	91.30	2.65	0.76	
1957	2.25	1.83	10.80	89.20	90.00	0.36	
1958	7.84	11.24	14.20	85.80	30.00	1.24	
1959							
1960							
1961	23.04	15.42	11.80	88.20	0.00	3.64	
1962	72.25	33.79	57.02	42.98	23.23	11.42	
1963	56.25	38.21	58.10	41.90	19.90	8.89	
1964	151.29	34.71	62.40	37.60	27.70	23.90	
1965	324.00	100.00	100.00	0.00	0.00	51.19	
1966	1.44	8.98	6.60	93.40	0.00	0.23	
1967	4.00	5.62	10.95	89.05	5.33	0.63	
1968	4.84	12.22	24.10	75.90	11.90	0.76	
1969							
1970	5.29	4.97	30.90	69.10	25.90	0.84	
1971	225.00	85.73	100.00	0.00	14.27	35.55	
1972	201.64	91.60	100.00	0.00	8.40	31.86	
1973	102.01	53.26	100.00	0.00	46.74	16.12	
1974	342.25	100.00	100.00	0.00	0.00	54.08	
1975	144.00	100.00	100.00	0.00	0.00	22.75	
1976	552.25	100.00	100.00	0.00	0.00	87.26	
1977	529.00	40.00	100.00	0.00	60.00	83.58	
1978	324.00	20.21	100.00	0.00	79.79	51.19	
1979	400.00	21.68	100.00	0.00	78.32	63.20	
1980	316.84	18.85	100.00	0.00	81.15	50.06	
1981	289.00	17.68	100.00	0.00	82.32	45.66	
1982	240.25	21.91	78.60	21.40	56.69	37.96	
1983	342.25	25.96	100.00	0.00	74.04	54.08	
1984	361.00	35.38	100.00	0.00	64.62	57.04	
1985	256.00	24.44	100.00	0.00	75.56	40.45	
1986	324.00	21.43	91.30	8.70	69.87	51.19	
1987	196.00	16.16	100.00	0.00	83.84	30.97	
1988	289.00	28.32	93.10	6.90	64.78	45.66	
1989	72.25	18.55	40.30	59.70	21.75	11.42	
1990	139.24	27.85	42.30	57.70	14.45	22.00	
1991	121.00	17.69	55.80	44.20	38.11	19.12	
1992	64.00	12.92	33.90	66.10	20.98	10.11	
1993	56.25	12.62	22.50	77.50	9.88	8.89	

Table D. 10 Saturations – Well B

Depth ( m )	F	Sw (%)	Sxo (%)	ROS (%)	MOS (%)	Ro (Ω.m)	Lithology
1932							Derdere Limestone
1933							
1934	68.89	19.05	31.10	68.90	12.00	11.02	
1935	139.24	29.09	62.40	37.60	33.30	22.28	
1936							
1937	49.00	16.37	26.50	73.50	10.10	7.84	
1938	33.64	14.55	15.70	84.30	1.20	5.38	
1939	72.25	27.76	26.88	73.12	0.00	11.56	
1940	116.64	27.20	40.40	59.60	13.20	18.66	
1941	484.00	59.40	89.30	10.70	29.90	77.44	
1942	116.64	34.29	57.10	42.90	22.80	18.66	
1943	49.00	43.00	47.80	52.20	4.80	7.84	
1944	225.00	72.91	100.00	0.00	27.10	36.00	
1945	144.00	49.00	63.50	36.50	14.50	23.04	
1946							
1947	324.00	92.95	100.00	0.00	7.00	51.84	
1948	81.00	42.49	53.20	46.80	10.70	12.96	
1949	104.04	58.58	54.00	46.00	0.00	16.65	
1950	46.24	41.37	37.90	62.10	0.00	7.40	
1951	324.00	83.00	100.00	0.00	17.00	51.84	
1952	64.00	100.00	88.30	11.70	0.00	10.24	
1953	0.64	20.79	3.60	96.40	0.00	0.10	
1954	0.25	14.78	0.60	99.40	0.00	0.04	
1955	4.00	11.00	16.70	83.30	5.70	0.64	
1956	1.69	11.00	15.40	84.60	4.40	0.27	
1957	148.84	73.79	100.00	0.00	26.20	23.81	
1958	90.25	100.00	100.00	0.00	0.00	14.44	
1959						Dolomitic Shale	
1960							
1961							
1962	529.00	30.99	100.00	0.00	69.01	84.64	
1963	342.25	21.95	100.00	0.00	78.05	54.76	
1964	256.00	22.88	100.00	0.00	77.12	40.96	
1965	361.00	33.09	100.00	0.00	66.91	57.76	
1966	400.00	29.60	100.00	0.00	70.40	64.00	
1967	324.00	18.58	100.00	0.00	81.42	51.84	
1968	400.00	28.67	100.00	0.00	71.33	64.00	

Table D. 11 Saturations – Well C

Depth ( m )	F	Sw (%)	Sxo (%)	ROS (%)	MOS (%)	Ro (Ω.m)	Lithology
1909	144.00	68.86	0.98	2.00	29.10	23.04	Derdere Limestone
1910							
1911							
1912							
1913	60.84	30.81	0.32	68.20	1.00	9.73	
1914	16.00	11.24	0.15	84.51	4.25	2.56	
1915							
1916							
1917							
1918							
1919							
1920							
1921							
1922							
1923							
1924							
1925	36.00	12.42	0.69	31.50	56.10	5.76	
1926							
1927							
1928							
1929							
1930							
1931	64.00	38.89	1.00	0.00	61.11	10.24	Dolomitic Shale
1932	81.00	58.14	1.00	0.00	41.86	12.96	
1933	104.04	91.17	1.00	0.00	8.83	16.65	
1934							
1935	400.00	99.29	1.00	0.00	0.71	64.00	Derdere Dolomite
1936	272.25	17.19	1.00	0.00	82.81	43.56	
1937	256.00	15.33	1.00	0.00	84.67	40.96	
1938	289.00	21.81	1.00	0.00	78.19	46.24	
1939	361.00	42.46	1.00	0.00	57.54	57.76	
1940	225.00	40.76	0.92	8.10	51.10	36.00	
1941	161.29	36.54	1.00	0.00	63.46	25.81	
1942	144.00	33.62	0.49	51.00	15.40	23.04	
1943	249.64	62.61	0.87	13.50	23.90	39.94	
1944	121.00					19.36	
1945	196.00					31.36	
1946	204.49					32.72	
1947							

Table D. 12 Saturations – Well D

Depth ( m )	F	Sw (%)	Sxo (%)	ROS (%)	MOS (%)	Ro (Ω.m)	Lithology
1829	16.00	44.00	100.00	0.00	56.00	2.56	Derdere Limestone
1830	36.00	35.36	100.00	0.00	64.64	5.76	
1831	182.25	46.95	100.00	0.00	53.05	29.16	
1832	144.00	33.50	100.00	0.00	66.50	23.04	
1833	196.00	44.98	100.00	0.00	55.02	31.36	
1834	136.89	48.38	100.00	0.00	51.62	21.90	
1835	144.00	44.73	100.00	0.00	55.27	23.04	
1836							
1837	225.00	100.00	100.00	0.00	0.00	36.00	
1838	26.01	24.00	100.00	0.00	76.00	4.16	
1839							
1840	576.00	48.00	100.00	0.00	52.00	92.16	
1841	306.25	39.00	100.00	0.00	61.00	49.00	
1842	156.25	37.08	100.00	0.00	62.92	25.00	
1843	182.25	41.57	100.00	0.00	58.43	29.16	
1844	600.25	62.14	100.00	0.00	37.86	96.04	
1845	225.00	34.65	100.00	0.00	65.35	36.00	
1846	441.00	55.52	100.00	0.00	44.48	70.56	
1847							
1848							
1849							
1850	9.00	11.18	100.00	0.00	88.82	1.44	
1851							
1852							
1853	1.00	39.53	100.00	0.00	60.47	0.16	
1854	16.00	90.56	100.00	0.00	9.44	2.56	
1855	12.25	100.00	100.00	0.00	0.00	1.96	
1856	100.00	100.00	100.00	0.00	0.00	16.00	
1857	331.24	100.00	100.00	0.00	0.00	53.00	
1858	400.00	100.00	100.00	0.00	0.00	64.00	
1859	729.00	80.61	100.00	0.00	19.39	116.64	
1860	529.00	42.50	100.00	0.00	57.50	84.64	
1861	529.00	46.00	100.00	0.00	54.00	84.64	
1862	529.00	46.00	100.00	0.00	54.00	84.64	
1863	404.01	40.30	100.00	0.00	59.70	64.64	
1864	484.00	34.70	100.00	0.00	65.30	77.44	
1865	361.00	31.03	71.51	28.49	40.49	57.76	
1866	576.00	40.08	100.00	0.00	59.92	92.16	
1867	289.00	32.91	84.82	15.18	51.90	46.24	
1868	441.00	42.00	100.00	0.00	58.00	70.56	
1869	492.84	51.62	100.00	0.00	48.38	78.85	

Table D.12, (cont'd)

Depth ( m )	F	Sw (%)	Sxo (%)	ROS (%)	MOS (%)	Ro (Ω.m)	Lithology
1870	256.00	38.11	100.00	0.00	61.89	40.96	Derdere Dolomite
1871	240.25	35.22	99.42	0.58	64.20	38.44	
1872	132.25	26.13	56.67	43.33	30.55	21.16	
1873	576.00	52.55	100.00	0.00	47.45	92.16	
1874	361.00	40.62	100.00	0.00	59.38	57.76	
1875	538.24	72.83	100.00	0.00	27.17	86.12	
1876	400.00	45.38	100.00	0.00	54.62	64.00	
1877	225.00	26.65	68.69	31.31	42.03	36.00	
1878	484.00	46.72	100.00	0.00	53.28	77.44	
1879	475.24	61.52	100.00	0.00	38.48	76.04	
1880	576.00	96.00	100.00	0.00	4.00	92.16	
1881	576.00	100.00	100.00	0.00	0.00	92.16	
1882	289.00	87.79	100.00	0.00	12.21	46.24	
1883	306.25	45.50	100.00	0.00	54.50	49.00	
1884	240.25	39.12	74.34	25.66	35.23	38.44	
1885	331.24	82.29	100.00	0.00	17.71	53.00	
1886	484.00	100.00	100.00	0.00	0.00	77.44	

## APPENDIX E

### R<sub>35</sub> AND K/Ø

Table E. 1 Calculated R<sub>35</sub> and k/Ø values from core data

Core Plug Depth (m)	Core Plug Porosity (%)	Core Plug Air Permeability (md)	R <sub>35</sub> (microns)	Port Type	Well	
1971.30	25.16	192.34	41.68	MEGA	A	
1971.95	21.26	85.62	21.88	MEGA		
1950.60	5.14	0.06	0.06	NANNO	B	
1951.60	5.12	0.02	0.02	NANNO		
1952.70	2.33	0.02	0.04	NANNO		
1953.50	2.93	0.03	0.05	NANNO		
1954.50	1.93	0.02	0.05	NANNO		
1955.60	2.13	0.03	0.07	NANNO		
1956.60	7.73	0.76	0.52	MICRO		
1957.70	8.10	0.07	0.04	NANNO		
1887.05	26.20	258.95	53.70	MEGA		D
1887.10	18.72	12.88	3.71	MACRO		
1887.20	1.53	0.01	0.03	NANNO		
1887.35	24.89	270.41	58.84	MEGA		
1887.65	24.04	84.87	19.05	MEGA		
1888.35	23.54	247.67	56.23	MEGA		
1888.50	20.34	87.35	22.91	MEGA		
1888.60	17.07	34.86	10.96	MEGA		
1889.10	22.88	132.35	30.90	MEGA		
1889.45	23.82	195.17	44.67	MEGA		
1890.05	16.24	10.83	3.63	MACRO		
1890.50	17.21	11.82	3.71	MACRO		
1890.60	10.75	1.32	0.66	MESO		
1890.75	9.02	0.43	0.26	MICRO		
1890.85	15.16	1.73	0.62	MESO		
1891.40	17.04	5.41	1.70	MESO		
1891.45	18.12	4.02	1.20	MESO		
1891.60	18.41	18.53	5.37	MACRO		
1891.90	18.81	5.63	1.62	MESO		
1892.05	18.97	7.03	1.99	MESO		
1892.50	19.69	6.31	1.74	MESO		
1892.60	20.97	8.33	2.14	MESO		
1892.80	20.82	6.69	1.74	MESO		

Table E.1, (cont'd)

Core Plug Depth (m)	Core Plug Porosity (%)	Core Plug Air Permeability (md)	R <sub>35</sub> (microns)	Port Type	Well
1845.40	23.33	2.72	0.63	MESO	X
1845.50	23.82	2.87	0.65	MESO	
1845.60	24.94	35.53	7.76	MACRO	
1849.95	19.45	3.02	0.83	MESO	
1851.45	15.22	4.45	1.58	MESO	
1851.55	19.25	2.70	0.76	MESO	
1858.60	10.13	0.26	0.14	MICRO	
1862.60	0.97	0.05	0.27	MICRO	
1864.65	3.01	0.06	0.11	MICRO	
1867.21	23.86	112.96	25.70	MEGA	
1867.39	20.56	45.16	11.75	MEGA	
1867.80	29.03	595.56	109.65	MEGA	
1872.34	26.05	264.64	54.95	MEGA	
1872.85	26.93	369.13	74.13	MEGA	
1872.90	21.29	57.64	14.45	MEGA	
1874.70	23.74	137.51	30.90	MEGA	
1877.15	23.51	67.83	15.49	MEGA	
1877.22	25.36	269.13	57.54	MEGA	
1877.80	27.19	192.09	38.02	MEGA	
1878.85	19.57	67.88	18.62	MEGA	
1879.25	19.57	42.72	11.75	MEGA	
1882.28	20.33	34.02	9.12	MACRO	
1882.37	32.19	5.79	0.98	MESO	
1882.40	13.36	1.60	0.65	MESO	